AFOSR FINAL SCIENTIFIC REPORT

AFOSR-TR-71-1968

Department of Mechanical Engineering

FUNDAMENTAL PROCESSES IN SOLID PROPELLANT IGNITION

by

R.K. Kumar and C.E. Hermance

GRANT AF-AFOSR-1274-67
Project-Task 9711-01

July 1971

University of Waterloo

Waterloo Ontario

Research Sponsored by:

Air Force Office of Scientific Research,
Office of Aerospace Research
United States Air Force

99

UNCLASSIFIED
Security Classification

DOCUMENT CONTROL DATA : R & D

(Security classification of title, body of abstract and indexing annotation must be entered when the overall report is classified)

1. ORIGINATING ACTIVITY *(Corporate author)*
University of Waterloo,
Department of Mechanical Engineering,
WATERLOO, Ontario, Canada.

2a. REPORT SECURITY CLASSIFICATION
UNCLASSIFIED

2b. GROUP

3 REPORT TITLE

FUNDAMENTAL PROCESSES IN SOLID PROPELLANT IGNITION

4 DESCRIPTIVE NOTES *(Type of report and inclusive dates)*
Scientific Final

5 AUTHOR(S) *(First name, middle initial, last name)*

R. KRISHNA KUMAR CLARKE E. HERMANCE

6 REPORT DATE	7a. TOTAL NO. OF PAGES	7b. NO. OF REFS
July 1971	101	20

8a. CONTRACT OR GRANT NO.
AF-AFOSR-1274-67

b. PROJECT NO.
9711-01

c.
61102F

d.
681308

9a. ORIGINATOR'S REPORT NUMBER(S)

9b. OTHER REPORT NO(S) *(Any other numbers that may be assigned this report)*
AFOSR-TR-71-1968

10. DISTRIBUTION STATEMENT

Approved for public release; distribution unlimited

11 SUPPLEMENTARY NOTES
TECH., OTHER

12. SPONSORING MILITARY ACTIVITY
AF Office of Scientific Research (NAE)
1400 Wilson Boulevard,
Arlington, Virginia 22209, U.S.A.

13. ABSTRACT

Analytically and numerically determined behaviour of the diffusion equations, with chemical reactions, describing a gas phase ignition process for homogeneous and composite solid propellants, suddenly exposed to an ignition stimulus, are reported. Stimuli considered are a high pressure and temperature, stagnant gas of specified oxidizer content, or a radiant heat flux impinging on a non-opaque propellant exposed to a low temperature gas phase of specified pressure and composition. The results, assuming a radiant stimulus, indicate that purely gas phase reaction processes play only a minor role in the overall ignition behaviour. Qualitative agreement with experiments is found for several flux and pressure levels. Most interesting are the results using a hot gas stimulus. In homogeneous propellants, ignition involves consecutive development of a primary flame between propellant pyrolysis products, and a secondary flame using unburned fuel from the primary flame and any ambient oxidizer present. A unique calculation of light emission during ignition development allowed direct theoretical/experimental comparison of results. Composite propellants ignite via pyrolysis of the propellant and reaction of fuel species with any ambient oxidizer present, followed by reaction with propellant produced oxidizer species. Matching of gas phase ignition processes produce ignition behaviour in excellent, quantitative agreement with experiments using a hot gas stimulus, regarding effects of ambient gas phase pressure and composition on the ignition delay.

DD FORM 1 NOV 68 1473

14. KEY WORDS	LINK A		LINK B		LINK C	
	ROLE	WT	ROLE	WT	ROLE	WT
IGNITION THEORY						
IGNITION OF SOLIDS						
COMPOSITE PROPELLANT IGNITION						
DOUBLE BASE PROPELLANT IGNITION						
SOLID PROPELLANT IGNITION MECHANISMS						
GAS PHASE IGNITION						
IGNITION CRITERIA						
IGNITION, PRESSURE EFFECTS						
IGNITION, GAS COMPOSITION EFFECTS						
NUMERICAL METHODS FOR DIFFUSION EQUATIONS						
ASYMPTOTIC MODELING TECHNIQUES						
TRANSIENT DIFFUSION WITH CHEMICAL REACTION						
FLAME, TWO STAGE						
RADIANT IGNITION						
HETEROGENEOUS IGNITION						
LIGHT EMISSION, THERMALLY STIMULATED, FROM CHEMICAL REACTIONS						

AFOSR FINAL SCIENTIFIC REPORT

AFOSR-TR-71-1968

FUNDAMENTAL PROCESSES IN SOLID PROPELLANT IGNITION

by

R.K. Kumar and C.E. Hermance

GRANT AF-AFOSR-1274-67
Project Task 9711-01

July 1971

Transmitted by:

Clarke E. Hermance
Principal Investigator

Department of Mechanical Engineering,
University of Waterloo, Waterloo. Ontario,
Canada.

CONTENTS

ACKNOWLEDGEMENT

This research was sponsored by the Air Force Office of Scientific Research, Office of Aerospace Research, United States Air Force, under grant AF-AFOSR-1274-67 from the period 1st February, 1967 to 31st July, 1971.

Technical Supervisor for this program was Dr. Bernard T. Wolfson, Energetics Division, Air Force Office of Scientific Research.

Much of this report was obtained from the Ph.D Thesis of R.K. Kumar, Department of Mechanical Engineering, University of Waterloo, Waterloo, Ontario, Canada.

CONDITIONS OF REPRODUCTION

ABSTRACT

The present work is a detailed, theoretical study of characteristic ignition behaviour of solids, which are capable of self sustained combustion, and ignite solely due to gas phase processes. The physical and mathematical situation in which ignition occurs is that of a solid exposed to a "tailored" reflexion of a shock wave from the proepllant surface. The primary object of the investigations of Part I is to analyse the structure of the gas phase adjacent to the surface of a homogeneous solid propellant during ignition, and the behaviour of the gas phase throughout the entire ignition process tc the establishment of steady state burning. It has been found -- through numerical computations -- that a long time after the propellant surface is exposed to the ignition stimulus, there exist two distinct reaction zones in the gas phase. An approximate theoretical criterion, chosen to represent some gas phase property within the secondary diffusion reaction zone, exhibits an approximately inverse square dependence of ignition times upon the external oxidizer mole fraction as has been observed experimentally. Asymptotic analyses have been carried out, where-ever possible, to check the results of numerical solutions. The agreement was found to be excellent.

To facilitate comparison of the theoretical results with experiments, and to explain the variations present in the experimental data, a new theoretical ignition criterion, based upon the time intensity of light emission, was developed. The results obtained with this criterion are in excellent agreement with those of experiments. It has been found that a low emission criterion corresponds to the development of a small temperature rise in the system -- dependent upon the development of the primary reaction zone -- and a high emission criterion corresponds to a long time criterion dependent upon the development of the secondary reaction zone. With the help of the new criterion, the type of data needed for experimental determiantion of the ignition mechanism of a given solid has been described. From numerical computations, as well as from asymptotic solutions, the marked influence of the total pressure of the gas phase upon the ignition behaviour of the solid has been described.

Since present day propellants may produce a highly reactive oxidizer upon decomposition, the case of a propellant producing an oxidizer much more reactive than the ambient oxidizer has been considered in Part II. The results show that the influence of the ambient oxidizer upon the ignition behaviour progressively decreases as the reactivity of the evolved oxidizer increases leading to the conclusion that either very little oxidizer is decomposed during the shock tube ignition of a typical solid propellant or that the kinetic properties of the evolved oxidizer are at best the same as those of the ambient oxidizer.

The ignition of a composite or heterogeneous propellant is dealt with in Part III. The model considers two dimensional diffusion and conduction in the gas phase and a solid consisting of an annulus of fuel surrounding a cylinder of solid oxidizer. Here also, the results obtained with short time temperature criterion and the emission criterion are in very good agreement with experiments. In particular, an approximately inverse square dependence of ignition times upon the oxidizer mole fraction with almost any realistic ignition criterion is found. The theory also indicates that the ignition behaviour of a heterogeneous solid propellant approached that of a homogeneous

propellant as the particle size is decreased.

Thus the present theoretical studies of decomposable solids leads to the conclusion that a purely gas phase mechanism alone can explain the experimentally observed ignition behaviour of both homogeneous and heterogeneous propellants under shock tube conditions.

In Part IV a brief discussion of radiant ignition is presented. Ignition of propellants by radiant energy has been widely employed to screen the propellants according to their ignitability. Gas phase model describing the ignition of propellants, including the effect of absorption of radiant energy by gret gases is considered. Numerical results agree with the approximate analysis of Waldman and Summerfield. However, the present treatment does not conclusively indicate the dominance of gas phase mechanism over heterogeneous surface reactions during ignition transients.

NOMENCLATURE

A	QR/nc_pEb, dimensionsless heat release parameter
B	pre-exponential factor of pyrolysis rate
b	dimensionless mass flux parameter
c_p	specific heat of the gas phase, 0.3 cal/g^oC
$\mathcal{D}$	local mass diffusivity, cm^2/sec
D	$=(\rho^2\mathcal{D}/\rho_g^2)$, effective mass diffusivity, cm^2/sec.
E_1, E_2, E	activation energy of gas phase reactions, cal/mole
E_p	activation energy of pyrolysis, cal/mole
g_{o1}, g_1, g_2	statistical weight of ground and excited states, cals
h_v	heat of pyrolysis, cal/g
I	intensity of electromagnetic radiation cm/sec
J	relative response
M_t	$\frac{E_u R}{kE}$, a dimensionless quantity
m	total mass flux issuing from the propellant surface, g/cm^2-sec
m_o	initial mass flux, g/cm^2-sec (at 400^{o}K)
n_1, n_2, n	molar stoichiometric ratio of gas phase reaction
Q_1, Q_2, Q	heat of combustion, cal/mole
R	universal gas constant, 1.986 cal/mole ^{o}K
r	radial distance
t	time, sec
t^*	ignition delay, millisec.
T, T_o	local initial gas phase temperature, ^{o}K
$T_s, T_{s,o}$	local initial solid phase temperature, ^{o}K
V	local velocity, cm/sec
x	linear distance, cm

y_f, y_{ox}'	respectively, mole fractions of fuel and evolved oxidizer
y_{ox}'', y_{ox}	gas phase supplied and total oxidizer mole fractions ($y_{ox} = y_{ox}' + y_{ox}''$)
y_{ox}^{∞}	initial oxidizer mole fraction in the gas phase
y_i	mole fraction of the inert gases
Z_1, Z_2, Z	pre-exponential factor of gas phase reactions
α	$\frac{m_f}{m}$, ratio of fuel mass flux to total mass flux
α_s	thermal diffusivity of solid phase, cm^2/sec
α_g	thermal diffusivity of gas phase, cm^2/sec
$\hat{\rho}$	$\frac{Rh_v}{c_p E}$, dimensionless heat of pyrolysis
ϵ	ignition criteria
ϵ_1, ϵ_2	energies of the excited states
$\eta_f, \eta_{ox}, \eta_{ox}$	dimensionless reactant concentration
η_i	inert gas concentration, dimensionless
θ	dimensionless gas phase temperature
θ_s	dimensionless solid phase temperature
θ_o	initial gasphase temperature, dimensionless
Λ	$\equiv(\lambda_s E_p / \lambda_g E)$, a dimensionless quantity
λ	stability parameter
λ_s, λ_g	thermal conductivities of solid and gas phase
μ	ratio of initial gas to solid phase densities
ξ	dimensionless distance in gas phase
ξ_s	dimensionless distance in solid
$\rho, \rho_g \rho_s$	local gas phase, initial gas phase and solid phase densities
ρ	dimensionless radial distance
ρ_2, ρ_1	dimensionless outer and inner radii

Σ	ratio of solid to gas phase thermal diffusivities
τ	dimensionless time
Γ	extinction coefficient for radiant transmissions cm^{-1}
k	Boltzman constant

Subscripts

s	solid
o	oxidizer
c	condensed phase
g	gas phase
i	initial
p	propellant
∞	at infinity
*	ignition condition

LIST OF TABLES

LIST OF FIGURES

INTRODUCTION

Ignition of solid propellants has been a topic of considerable interest in the development of operational motor systems for some time. In critical applications, such as missiles where a large amount of energy has to be released in a very short time, it is obvious that the ignition system has to operate repeatably and reliably. Design of such igniter system is eased by some knowledge of ignition mechanism.

Conceivably, to a certain degree, the ignition mechanism depends upon the ignition system employed. For example, if the ignition is achieved by the application of a hypergol, like chlorine trifluoride, the run-away reactions occur at the propellant surface and are termed as hetrogeneous reactions. There are several methods of igniting a solid propellant but the mechanism of ignition will fall into one of the following categories (1) solid phase reactions, (2) hetrogeneous reactions and (3) gas phase reactions. Determination of the exact mechanism by which a propellant ignities is extremely complex in any case.

However, in certain cases, like ignition in shock tubes, it is argued that ignition occurs by gas phase reactions. This is understandable because, the surface temperature reached in shock tube experiments are too low for any significant surface reactions to occur. In the case of hypergolic ignition, the run-away reactions are indisputably hetrogeneous. But in arc image ignition situations, the mechanism by which the ignition occurs is not obvious. In steady burning, solid phase reactions appear to be unimportant in the case of composite propellants. But it is not clear whether the ignition is due to hetrogeneous reactions or homogeneous gas phase reactions. Possibly, it is a combination of both. Theoretical models employing purely gas phase or purely heterogeneous reactions predict nearly the same behaviour, and no undisputably deterministic experiments have been performed. In the absence of proof for any particular mechanism controlling ignition, the only way out for an investigator is to examine theoretically the ignition behaviour assuming that the propellant ignition occurs by one of the above mentioned mechanisms.

The object of the present analysis is to establish the ignition behaviour based on the assumption that the run-away, thermo-chemical reactions leading to ignition, occur in the gas phase adjacent to the propellant surface.

The beginning of the history of ignition theories for solid propellants was marked by a simple solid phase ignition theory postulated by Hicks. In his theoretical model Hicks assumed that ignition was caused by run-away thermo-chemical reactions occurring in a thin region of the solid adjacent to the propellant burning surface. The entire ignition lag was composed of heat-up period; the time required to establish a gas phase flame was assumed small. The theoretical predictions of the ignition behaviour were in good agreement with the experimentally observed behaviour of the double base propellants employed at that time. However, it has been found, that in the case of modern

day composite propellants, the ignition behaviour depends considerably upon the properties of the adjacent gas phase; solid phase reactions are not important during rapid ignitions. Conclusive proof of this statement came from shock tube experiments on both double base and composite solid propellants[1]. In addition, experiments on steady burning of composite propellants have, in the past, indicated that vitally important heat release occurs in the gas phase. These and other considerations led to the study of models involving the participation of gas phase processes during ignition transients.

Studies made at Princeton University during the period from 1958 to 1963, on several double base and composite propellants, marks the beginning of intensive research in solid propellant ignition. Based on certain experimental observations, McAlevy and Summerfield [1] developed a gas phase ignition model in which a hot oxidizing gas reacts with fuel vapours issuing from the propellant surface due to decomposition of the solid. Importance was given to a special case of an environment containing an oxidizer, as the propellants tested would not ignite unless the environmental gas contained sufficient oxygen under the experimental conditions used. No analytical study encompassing a more general case of propellant decomposing into fuel and oxidizer vapours was made. Initial theoretical calculations using gas phase ignition theory for solid fueld showed qualitative agreement with the observed dependence of ignition of composite propellants upon the environmental gas.

Intensive research activity in the field of solid propellant ignition is perhaps better illustrated by a brief mention on the emergence of hypergolic, hetrogeneous ignition theory developed by Anderson and Brown [2] almost simultaneously to the development of gas phase theories. This theory was originally evolved from the studies on ignition of solids by chemical activation of the propellant surface by powerful oxidizers like fluorine and chlorine trifluoride. Accordingly, it was assumed in the hypergolic ignition model that ignition was initiated by heterogeneous surface reactions between the hypergol and the fuel surface. It was argued by Anderson and Brown that ignition under shock tube conditions might be due to surface reactions similar to hypergolic ignition reactions, since theory predicted a strong dependence of ignition behaviour upon the properties of the adjacent gas phase as was found from experiments.

Though the predictions of hypergolic model are in good agreement with experiments, it is somewhat dubious that surface reactions may have the strong hold in initiating ignition; the reported shock-tube generated, propellant surface temperatures were low, and oxygen is not active enough to cause vigorous surface reactions at these temperatures. Therefore further detailed study of gas phase processes of solid <u>propellants</u> (<u>not</u> pure fuels) -- discussed in the following sections -- was necessary before making further conclusions regarding the dominant ignition processes of solid propellants. The present investigation is an effort directed towards better understanding of the gas phase processes.

THEORY OF GAS PHASE IGNITION OF HOMOGENEOUS AND HETEROGENEOUS SOLID PROPELLANTS

CHAPTER I

1.1 Review of Previous Work:

Theoretical studies on ignition can be traced back to the early works of Semenov and Frank-Kamenetski who considered ignition as a thermal run-away in a system consisting of combustible, homogeneous mixture of a fuel and an oxidizer in the vapour phase. In this type of ignition it is assumed that exothermic chemical reactions are occurring everywhere in the system simultaneously; the gaseous mixture ignites after a short induction period undergoing a small temperature rise. A system in which the reactants are premixed is called a homogeneous system. Contrasted to the ignition of a homogeneous system is the ignition of heterogeneous systems in which the reactants are initially unmixed; the reactants may exist in different phases. A detailed discussion of homogeneous and hetergeneous reactions is given in reference (3). However, a few basic differences between homogeneous and heterogeneous ignitions may be worth mentioning: (1) thermal ignition of a homogeneous system depends entirely upon the thermo-chemical properties of the mixture whereas the ignition of a heterogeneous system depends upon the rate of consumption or the rate of supply of one or either of the reactants; (2) theoretical determination of the ignition of a homogeneous system does not depend upon the choice of ignition criteria whereas that of a heterogeneous system very strongly depends upon the choice of ignition criteria as discussed in later chapters. In what follows only heterogeneous systems in which both reactants exist in the same (gaseous) phase are considered.

The first attempt to describe mathematically and physically the ignition of heterogeneous systems was made by McAlevy and Summerfield. In their simplified version of the gas phase model, they assumed that the fuel vapours after decomposition at the proepllant surface diffused outwardly from the surface into the adjacent gas phase containing a hot oxidizer. Vigorous chemical reactions occur in the gas phase with the release of large amounts of heat leading to thermal ignition. Several simplifying assumptions were made in their theoretical analysis to solve the mathematical ignition model. The ignition event, according to McAlevy, was defined as the instant at which the heat generation at any location in the gas phase exceeds the heat losses at that location. Defining ignition in this manner was convenient for mathematical analysis, as well as being physically intelligible. The model was not an unequivocal success, however, though the predictions were in rough agreement with the observed behaviour of solid propellants under shock tube experiments. The theory indicated that $t_{ign} \sim (y_{ox}^{\infty})^{-2/3}$ whereas the experiments showed a much stronger dependence of ignition times upon the initial oxidizer mole fraction. But, before discarding the gas phase theory of ignition, it was necessary to

remove some of the restrictive assumptions of the McAlevy/Summerfield model. Later work by Hermance[3] included a more complete model in which simultaneous, transient, mass diffusion and chemical reactions occurred within the gas phase; both the solid surface temperature and the surface temperature dependent pyrolysis rates were assumed to be constant in time. The model demonstrated the strong effect of neglecting the consumption of the reactants (McAlevy's model neglected reactant consumption) and the dependence of ignition delay on the ignition criteria.

The mathematical criterion for defining the ignition event in Hermance's work was the first attainment of a maximum gas phase temperature which was 50% in excess of the initial gas phase temperature. It was found that McAlevy's criterion was inappropriate. Indeed it was shown by Hermance[3] that McAlevy's criterion was satisfied much too soon in the transient gas phase processes leading to ignition. The model gave results in better agreement with experiments on the ignition of pure fuels, but still could not explain the strong dependence of ignition delay upon the initial oxidizer mole fractions for propellants. The assumption of constant wall conditions was suspected to be responsible for this lack. Accordingly, self determining surface conditions (termed 'feed back' conditions) were introduced by Hermance[3] into the basic ignition model. This refinement established at least one interesting aspect: that even for fuels having low volatility, or low pyrolysis rates, at the interface temperatures initially established, the ignition occurred in a very short time (order of milliseconds) which was in agreement with experiments on some less volatile (e.g. epoxy) fuels. Surface temperature dependent pyrolysis rate of the form $m = \rho_s B e^{-E/RT_s}$ was assumed. The ignition criteria employed remained the same as before. Since the mathematical model included the ignition of pure fuels only, the work was considered incomplete. Further improvement -- the case of a solid which after decomposition produces both fuel and oxidizer vapours -- was imminent.

A gas phase model in which the propellant decomposed into fuel and oxidizer vapours was considered by Hermance and Kumar[4,5]. The model revealed two important things: (1) the propellant ignities in a neutral atmosphere utilizing its own oxidizer and (2) nearly steady bruning (or quasi-steady) conditions were established in the gas phase after a long time (order of few milliseconds). The model also indicated that $t_{ign} \sim (y_{ox}^{\infty})^{-n}$ where $n \leq 2/3$ depending upon the composition of the propellant (a high percentage of oxidizer in the solid showed a weaker dependence of ignition on the external oxidizer). The ignition criterion employed was the same as the one in references 3 and 4.

There were several obvious areas in which this model could be improved. These are (1) incorporating natural boundary conditions - i.e. - feedback, (2) development of an ignition criterion which closely corresponds to the experimental ignition criterion of light emission, (3) use of temperature dependent gas phase physical properties and (4) the effect of propellant inhomogeneuity. A detailed theoretical analysis of a gas phase ignition model with the introduction of the aforementioned aspects is presented in the succeeding chapters -- with interesting and significant results.

IGNITION OF HOMOGENEOUS SOLID PROPELLANTS UNDER SHOCK TUBE CONDITIONS

CHAPTER II

2.1 Physical Model:

The model considers one dimensional diffusion and simultaneous, gas phase chemical reaction of the gaseous species produced by the thermal decomposition of a homogeneous propellant under shock tube conditions. A schematic representation of the gas phase ignition model is shown in Figure 1. Ignition in a shock tube can be described as follows: A high intensity shock wave is made to propagate through a homogeneous mixture of an oxidizer and a neutral gas (generally nitrogen) in desired proportions, by the rupture of a diaphragm as described in reference 1. Upon reflection from the propellant surface (located flush with the end wall of the shock tube) the shock wave creates a high temperature and high pressure, stagnant gaseous atmosphere in the gas phase. Simultaneously, the propellant surface temperature jumps to a certain value determined by the thermal properties of the gas and the solid. The propellant surface starts to decompose at a rate which is dependent upon the mixture of fuel and oxidizer vapours, which in turn diffuse into, and chemically react with, the external oxidizer initially present in the gas phase. A major portion of the heat released by this chemical reaction is used up in raising the temperature of the gas phase; the remaining heat is fed back to the solid which in turn raises the surface temperature, providing a boot-strap effect. The following assumptions were made in formulating the present gas phase model:

1) The molecular weights of gas and solid are constant and equal.

2) The propellant is a homogeneous mixture of fuel and oxidizer and decompose according to the pyrolysis law $m = \rho_s B \exp(-E_p/RT_s)$ producing a homogeneous gaseous mixture of fuel and oxidizer.

3) The specific heat and thermal conductivities of gas and solid are constant and equal.

4) The Lewis number is unity and $\rho^2 D$ is a constant independent of temperature.

5) ρZ is a constant independent of temperature.

6) The chemical reaction between the reacting species is of global second order of the type

$$\left.\frac{\partial y_f}{\partial t}\right\}_{chem} = \frac{1}{n}\left.\frac{\partial y_{ox}}{\partial t}\right)_{chem} = -\frac{c_p}{Q}\left.\frac{\partial T}{\partial t}\right)_{chem} = -\rho Z\, y_f y_{ox} \exp(-E/RT)$$

with a constant molar stoichiometry of the form

$$|\text{fuel}| + n\,|\text{oxidizer}| \rightarrow (n+1)\,|\text{products}|$$

Assuming constant molar stoichiometry eliminates the necessity of considering Stephan flow in the gas phase; it is also a necessary consequence of assumption (1). It is interesting to note that assumptions (1),(3) and (4) are commonly employed in the combustion literature and are often justified. In so far as assumption (2) is concerned, it has been found that the surface dependent decomposition rate of several nitrate esters follow the Arhenius pyrolysis law. Assuming a constant $\rho^2 D$ in the gas phase is analogous to the assumption of constant $\rho\mu$ in gas dynamics problems, or the Chapman-Rubesin approximation. In the present case, coupled with the Howarth transformation, it reduces the problem of variable density into one of constant density. The jump temperature calculated using the modified equations is the correct "double jump" value. The jump temperature calculated without making this assumption is only one half of the experimentally measured value[6]. Detailed treatment of assumptions (4) and (5) are carried out in reference(19) where it is argued that the variation in $e^{-E/RT}$ is much greater than the variation of T alone and thus the assumption that ρZ is a constant is perhaps justified. Since normal gas phase reactions generally involve bimolecular collisions, assumption (6) also is proper. Equimolar stoichiometry may be true when a polymer decomposes into light weight gaseous hydrocarbons.

The present analysis is greatly simplified by assuming single step reaction kinetics. It can be said with great certainty that ignition reactions are not that simple, and single step kinetics perhaps is a gross simplification of the real physical situation. It, however, can be shown that some multiple step reactions can be simplified (mathematically) to single step kinetics and since in most of the cases the exact number of reaction steps are not known, the assumption of single step kinetics appears to be quite reasonable. Dissociation of the products should be taken into account, at high temperatures in reality, but for simplicity dissociation of the products is neglected in the present analysis.

2.2 Mathematical Formulation:

The time rate of change of concentration of any species within the control volume is equal to the algebraic sum of the rates at which the species is entering the control volume through diffusion and convection, and the rate at which the species is consumed or liberated due to chemical reactions. If we assume that the evolved oxidizer has the same physical and kinetic properties as the free stream oxidizer equations for the conservation of species and energy can be written as follows:

Let an operator K be defined as:

$$K \equiv \frac{\partial}{\partial t} + \frac{m}{\rho}\frac{\partial}{\partial x} - \frac{1}{\rho}\frac{\partial}{\partial x}\left(\rho D \frac{\partial}{\partial x}\right)$$

Then

$$K(y_f) = \frac{1}{\nu_i} K(y_{ox}) = -\frac{c_p}{Q} K(T) = -\rho Z y_f y_{ox} \exp(-E/RT) \qquad 2.1$$

$$K(y_i) = 0 \qquad 2.2$$

$$\frac{dT_s}{dt} + \frac{m}{\rho_s}\frac{dT_s}{dx} = \alpha_s \frac{d^2T_s}{dx^2} \qquad 2.3(a)$$

It was assumed in the above equations that $y_{ox} = y'_{ox} + y''_{ox}$ where y'_{ox} refers to evolved oxidizer mole fraction and y_{ox}'' refers to free stream oxidizer mole fraction.

The boundary and initial conditions for equations 2.1 and 2.3 are written as follows:

$$y_f(x,0) = y_f(\infty,t) = 0 \qquad m y_f(0,t) - \rho D \frac{dy_f(0,t)}{dx} = \alpha m$$

$$y_{ox}(x,0) = y_{ox}(\infty,t) = y_{ox}^{\infty} \qquad m y_{ox}(0,t) - \rho D \frac{dy_{ox}(0,t)}{dx} = (1-\alpha)m$$

$$y_i(x,0) = y_i(\infty,t) = y_i^{\infty} \qquad m y_i(0,t) - \rho D \frac{dy_i(0,t)}{dx} = 0$$

$$T(x,0) = T(\infty,t) = T_0 \qquad T(0,t) = T_s(0,t)$$

$$T_s(-x,0) = T_s(-\infty,t) = T_{s,0} \qquad m(t) = \rho_s B \exp(-E_p/RT_s)$$

$$-\lambda_s \frac{dT_s(0,t)}{dx} + m h_v = -\lambda_g \frac{dT(0,t)}{dx} \qquad 2.3(b)$$

Wherever needed, the mole fraction of products can be obtained from $y_p = 1 - (y_f + y_{ox} + y_i)$ which indeed satisfies the relationship

$$\frac{\partial y_p}{\partial t} + \frac{m}{\rho}\frac{dy_p}{dx} = \frac{1}{\rho}\frac{d}{dx}\left(\rho D \frac{dy_p}{dx}\right) + (n+1)\rho^2 Z y_f y_{ox} \exp(-E/RT) \qquad 2.4$$

Introducing Howarth length transformation of the form $\psi = \omega \int \frac{\rho(x,t)}{\rho_s} dx$ and assumptions (4) and (5) and defining dimensionless constants and variables as:

$$m_o = \rho_s B \exp(-E_p/400R) \qquad \theta = RT/E$$

$$\omega = \frac{m}{m_o} \qquad \theta_s = RT_s/E_p$$

$$\Sigma = \alpha_s/D \qquad \eta_f = nby_f$$

$$\Lambda = \lambda_s E_p/\rho_g D C_p E \qquad \eta_{ox} = by_{ox}$$

$$b = \rho^3 Z D/m_o^2 \qquad \eta_i = by_i$$

$$A = QR/nC_p E b \qquad \xi = \psi(m_o/\rho_g D)$$

$$\beta = Rh_v/C_p E \qquad \xi_s = \frac{x}{\Sigma^{1/2}}(m_o/\rho_g B)$$

$$\mu = \rho_g/\rho_s \qquad \tau = t(m_o^2/\rho_g^2 B)$$

and letting $H = \frac{\partial}{\partial \tau} + \omega\frac{\partial}{\partial \xi} - \frac{d^2}{d\xi^2}$ transforms equations 2.1 to 2.4

as

$$H(\eta_f) = H(\eta_{ox}) = -\frac{1}{A}H(\theta) = -\eta_f \eta_{ox} \exp(-1/\theta) \qquad 2.5$$

$$H(\eta_i) = 0 \qquad 2.6$$

and

$$\frac{d\theta_s}{d\tau} + \frac{\mu\omega}{\Sigma^{1/2}}\frac{d\theta_s}{d\xi_s} = \frac{d^2\theta_s}{d\xi_s^2} \qquad 2.7$$

subject to the following initial and boundary conditions:

$$\eta_f(\xi,0) = \eta_f(\infty,\tau) = 0 \qquad \eta_f(0,\tau) - \omega^{-1}\frac{d\eta_f(0,\tau)}{d\xi} = m_{bx}$$

$$\eta_{ox}(\xi,0) = \eta_{ox}(\infty,\tau) = \eta_{bx}^{\infty} \qquad \eta_{ox}(0,\tau) - \omega^{-1}\frac{d\eta_{ox}(0,\tau)}{d\xi} = b(1-\alpha)$$

$$\eta_i(\xi,0) = \eta_i(\infty,\tau) = \eta_i^{\infty} \qquad \eta_i(0,\tau) - \omega^{-1}\frac{d\eta_i(0,\tau)}{d\xi} = 0$$

$$\theta(\xi,0) = \theta(\infty,\tau) = \theta_0 \qquad \theta_s(0,\tau) = \theta(0,\tau)$$

$$\theta_s(-\xi_s,0) = \theta_s(-\infty,\tau) = \theta_{s0} \qquad \frac{\Lambda}{\Sigma^{1/2}}\frac{d\theta_s(0,\tau)}{d\xi_s} - \beta\omega = \frac{d\theta(0,\tau)}{d\xi}$$

2.8

Definition of ξ and ξ_s in the above fashion allows one to calculate the correct "double jump" temperature at the propellant surface when the equations are integrated numerically.

Of all the dimensionless groups listed above, the most important ones are 'b' which is the inverse of the first Damkohler number, A the dimensionless heat release parameter, and α the propellant composition parameter. The parameter (b) can also be written as $\frac{\rho^2 D}{m_s^2} / \frac{1}{rz}$ which is the ratio of characteristic diffusion times to characteristic chemical reactions time. Thus a large value of b indicates dominance of diffusional process compared to chemical processes in controlling ignition and vice-versa

For a given propellant, ignition in a shock tube operating under given conditions, the characteristic ignition delay τ^* is found to be a function of y_{ox}^{∞} alone. Thus,

$$\tau^* = f(y_{ox}^{\infty})$$

Experiments show a dependence of τ^* on y_{ox}^{∞} as $\tau^* \sim |y_{ox}^{\infty}|^{-\delta}$ where $1 \leq \delta \leq 3$; theory generally gives values of δ to be between 2/3 and 2 depending upon the choice of ignition criterion and the completeness of the theory.

2.3 Ignition Criteria

Discussion of several ignition criteria used in previous gas phase models are given in references 3 and 4. In all these cases, ignition was attributed to some state of gas phase distributions during the ignition period. In the past, three ignition criteria have been extensively employed for defining the ignition event. In his gas phase model McAlevy assumed that ignition occurred whenever heat generation at any point in the gas phase exceeds heat losses at that point. This is mathematically equivalent to stating that $\frac{\partial T}{\partial t} = 0$ at ignition. Hermance argued that this criterion is not appropriate since this criterion was satisfied much earlier in the ignition period, and need not necessarily lead to incipient ignition. In his calculations, Hermance employed another criterion which stated that ignition occurred when the maximum gas phase temperature at any station in the gas phase exceeds the initial gas phase temperature by a specified amount. Thus, at ignition, $T^* = \alpha T_o$ where $\alpha > 1$. For reporting the numerical results Hermance used a value of $\alpha = 1.5$. Statement of ignition in the above terms is equivalent to specifying a certain rate of temperature rise in the gas phase.

Another ignition criterion often employed is the integrated heat balance criterion. According to this criterion, ignition is defined as that instant at which the heat generation due to chemical reactions, integrated over the entire gas phase at a given time is equal to, and increasing more rapidly than, the heat conducted out of the boundary layer at the solid-gas interface. Mathematically expressed, ignition occurs when

$$Q(\text{generated}) + Q(\text{conducted}) \geq 0 \qquad t = t_{ign}$$

or

$$Q \int_0^{\infty} \rho^2 Z y_f y_{ox} \exp(-E/RT)\, dx + \lambda_g \left.\frac{dT}{dx}\right)_o \geq 0$$

Theoretical work[7] indicated that this criterion gives results close to McAlevy's criterion.

All the three criteria discussed above appear to be physically reasonable and constitute several approximate mathematical basis for defining ignition. However, it should be noted that these criteria have nothing in common with usual experimental ignition criteria, or so it appears. Unless a relationship can be established between a theoretical and an experimental ignition criterion, theoretical predictions are of limited significance.

2.4 Asymptotic Analysis at Short Times:

Since all the above mentioned ignition criteria correspond to ignition times very close to the beginning of the ignition period, certain approximations can be made:

1. Convective transport terms can be neglected compared to diffusive transport terms in equations 2.6 to 2.8.

2. Propellant surface temperature can be assumed constant with respect to time.

3. Reactant consumption up to ignition can be neglected.

Numerical computations by Hermance[3], have shown that neglecting convective terms does not introduce any significant error in the final results. Although it can be shown without much effort that assumption: (1) leads to a gross violation of the conservation law, convection is ignored in the approximate analysis. Assumption (2) is well justified for high initial pyrolysis rates, since feed back is not operative under these circumstances. Assumption (3) is also valid since for large initial oxidizer mole fractions and high pyrolysis rates, reactant consumption was indeed found negligible. With these it can be shown that [4,5] $\tau^* \sim (\omega A b^2 y_{ox}^{\infty})^{-2/3}$ for oxygen rich and $\tau^* \sim (nb^2 \omega A \alpha\overline{1-\alpha})^{-1/2}$ for neutral atmospheres respectively. These results are in good agreement with the behaviour of numerical solutions.

2.5 Asymptotic Analysis at Long Times:

At long times (order of few milliseconds), quasi-steady conditions prevail in the gas phase. There are two distinct reaction zones. First is a premixed, primary reaction zone of few microns thick adjacent to propellant surface. The conditions in the primary zone are unchanging and the zone remains fixed in space. There is a second, diffusion reaction zone, remote from the propellant surface which moves with a constant velocity relative to the propellant surface. The conditions in the secondary reaction zone are slowly varying functions of time. Since the behaviour of secondary reaction zone depends very strongly upon the external oxidizer, and we are only interested in the influence of external oxidizer upon ignition, we only need to consider the secondary reaction zone. This is facilitated by a change of co-ordinates and then examining the secondary reaction zone with respect to this new co-ordinate system in which the reaction zone remains stationary. Assuming that concentration profiles of oxidizer and fuel vapours can be approximated by power law expressions , the following relationship holds true in the secondary reaction zone:

$$\frac{\partial\theta}{\partial\tau} = \frac{\partial^2\theta}{\partial\xi^2} + A\eta_f\eta_{ox}\exp(-1/\theta)$$

$$\theta(0,\tau) = \theta_i,\ \theta(\xi,\tau) = \theta_\infty;\ \theta(\xi,0) = f(\xi/\xi) \qquad \text{2.9}$$

$$\eta_f = c_1 - m_1\xi^p$$

$$\eta_{ox} = c_2 + m_2\xi^q \qquad \text{2.10}$$

Here τ is measured from the instant at which a strong diffusion reaction zone is formed. The constants c_1, c_2, m_1 and m_2 can be determined by the requirements that at $\xi = 0$, $\eta_{ox} = 0$; $\zeta = \delta$, $\eta_{ox} = \eta^{\infty}_{ox}$, $\eta_f = 0$ and on the average stoichiometry is maintained in the secondary zone.

Thus,

$$\eta_f = \eta^{\infty}_{ox}\left[1 - (\xi/\delta)^b\right]$$

$$\eta_{ox} = \eta^{\infty}_{ox}\left[(\xi/\delta)^q\right] \qquad 2.11$$

Close to steady state, the total rate of heat generation from the secondary reaction zone is approximately equal to the rate of heat loss, which is approximately constant. Therefore:

$$Q_{gen} = A\eta^{\infty 2}_{ox}\int_0^{\delta}\left(\frac{\xi}{\delta}\right)^{q}\left[1-(\xi/\delta)^{b}\right]\exp(-1/\theta)\,d\xi \qquad 2.12$$

letting $\xi/\delta = \phi$ we get

$$Q_{gen} = A\eta^{\infty 2}_{ox}\delta\int_0^1 \phi^{q}(1-\phi^{b})\exp(-1/\theta)\,d\phi$$

$$= Q_{lost} \simeq \frac{\text{constant}}{\delta} = \frac{c}{\delta} \qquad 2.13$$

Since the integral in the above equation is approximately constant, we obtain $\delta \sim 1/A\eta^{\infty}_{ox}$. Consequently the energy equation takes the form

$$\frac{d\theta}{d\tau} = \frac{d^2\theta}{d\xi^2} + \frac{c}{\delta^2}\left(\frac{\xi}{\delta}\right)^{q}\left[1-(\xi/\delta)^{b}\right]\exp(-1/\theta) \qquad 2.14$$

subject to the conditions that $\theta(0,\tau) = \theta_1$, $\theta(\delta,\tau) = \theta_o$ and $\theta(\xi,0) = f(\xi/\delta)$. If we define τ and ξ as $\bar{\tau} = \tau\delta^2$ and $\bar{\xi} = \xi\delta$ to completely eliminate δ from the equation 2.14 and the corresponding boundary conditions, the solution then is of the form $\theta = \theta(\theta_1, \theta_o; \bar{\tau}, \bar{\xi})$ Thus for any suitable choice of ignition criteria, the ignition $\bar{\tau}^*$ is given by:

$$\tau^* \sim \left(A\eta^{\infty 2}_{ox}\right)^{-1}$$

Since $\eta^{\infty}_{ox} = b\, y^{\infty}_{ox}$ and $A \sim \frac{1}{b}$, it can be expected that at long times $t^* \sim (y^{\infty}_{ox})^{-2}$ and $t^* \not\sim (m_o)$.

The above analysis also applies to pure fuels igniting in oxygen rich atmospheres, since the effect of any ozidizer supplied by the solid is obliterated by the presence of primary reaction zone where the oxidizer from the solid is consumed, leaving pure fuel vapours to react with the external oxidizer. Furthermore, under conditions of small y^{∞}_{ox}, where the primary zone is dominant, the long time ignition delay is also independent of m_o.

For a propellant igniting in a neutral atmosphere, the power law expressions for η_f and η_{ox} become

$$\eta_f = nb\alpha\left[1-\left(\xi/\delta\right)^p\right] \qquad 2.15$$

$$\eta_{ox} = b(1-\alpha)\left[1-\left(\xi/\delta\right)^p\right] \qquad 2.16$$

Furthermore, close to steady conditions in the gas phase,

$$Q_{gen} = \beta\delta \int_0^1 (1-\phi^p)^2 \exp(-1/\theta)\, d\phi$$

$$= Q_{lost} = \frac{c}{\delta} \qquad 2.17$$

This gives the relationship $\delta \sim \beta^{1/2}$. Using this and substituting 2.15 and 2.16 into energy equation and redefining τ and ξ as $\tau = \bar{\tau}\,\delta^2$ and $\xi = \bar{\xi}\delta$, it can be verified that the energy equations becomes independent of all constants, from which the relationship $\tau^* \sim b^{-1}$ and $\tau^* \sim \alpha(1-\alpha)$. Since $b \sim (\frac{1}{m})^2$ and $\tau \sim m^2$, even for a propellant igniting in a neutral atmosphere, the ignition time is independent of volitility.

In the above analysis the assumption was that the reaction zone thickness depended upon heat losses. This is in contrast to that made in estimating the thickness of a steady state diffusion flame. In the former, one obtains $\delta \sim 1/\eta_{ox}^{\omega}$ whereas the latter gives $\delta \sim 1/\eta_{ox}^{\omega/2}$. The numerical computations indicate that $\delta \sim 1/\eta_{ox}^{\omega}$ is nearly true; in effect then, it can be concluded that finite reaction rate kinetics play an important role in the establishment of the steady state.

In the preceding derivation, no mention was made of any specific ignition criterion for the theoretical definition of ignition. The ignition criterion could be either $\theta^* = \alpha\theta_0$, where $\alpha > 1$ or $\partial\theta/\partial\tau \to 0$. For presenting numerical result a criterion of the type $\tau/\theta_m(\partial\theta_m/\partial\tau) \to 0$ was chosen. In reference (8) it is shown that this also is an appropriate criterion.

The key assumption in presenting the long-time analysis, was that the emission criterion employed in experimental detection of ignition must in some sense be related to the establishment of steady conditions. In other words, emission of light during propellant ignition is delayed until the establishment of steady burning conditions. Whether this is true is not known.

2.6 Emission Criterion

Theoretical studies are of limited significance unless they offer a means of comparison with experiments. Though all the gas phase theories discussed previously are quite elegant in their approach both physically and mathematically, their predictions cannot be compared directly with experiments since no relationship between experimental ignition criterion and mathematical criteria has been found. To make the present gas phase distribution is not known.

If at any instant, we consider an elementary volume 'dv' in the gas phase at a distance x from the propellant surface, the intensity of electro-

magnetic radiation emitted by the species emitting radiation at a frequency ν is given by[9]:

$$dI = N_m(h\nu)A_{mn}d\nu \qquad 2.18$$

where $N_m = N_{mo}(\frac{g_m}{Q})e^{-Eu/kT}$ is the number of molecules in the excited state and and

$$A_{mn} = \frac{64\pi^3 \omega^3_{mn}}{3h} |R_{mn}|^2$$

is the Einstein Coefficient of spontaneous emission. Absorption is neglected since it is generally compensated by the induced emission. The total number of molecules of species emitting radiation is related to the number of product molecular present as $N_{mo} = N_p f_r = N(1 - y_f - y_i - y_{ox})f_r$ where N is the total number of molecular present per unit volume of the gas at temperature T. Noting that $dv = a_c dx$ and defining L* as the characteristic slit width the expression for the intensity of light passing through the width becomes

$$I = K \int_0^{L^*} N(1 - y_f - y_{ox} - y_i) \exp(-h\nu/kT)\, dx \qquad 2.19$$

where $K = \frac{64}{3}\pi^4(\omega_{mn})^4 cf_r \frac{g_m}{Q} |R_{mn}|^2 a_c$, a_c being the cross sectional area of the shock tube.

This energy impinges on a photocell through an aperture with area 'a_r' at a distance 'r' from the centre of the shock tube through a suitable filter passing a very narrow region of the specturm. Assuming that the energy of all the excited states are sufficiently high, $Q = g_o + g_1 e^{-\varepsilon_1/kT} + g_2 e^{-\varepsilon_2/kT} + g_3 e^{-\varepsilon_3/kT} + \ldots = g_o$, the voltage output of the photocell is given by:

$$V_p \sim \bar{K} \int_0^{\psi^*} (1 - y_i - y_{ox} - y_f) \exp(-h\nu/kT)\, d\psi \qquad 2.20$$

where $\psi = \int_o^x \frac{\rho(x,t)}{\rho_g} dx$ and $\bar{K} = N_i K$. N_i is the number of gas molecules present in the initial gas phase per unit volume. The relative response of the photo-detector is

$$J(t) = \int_0^{\xi^*} (1 - y_i - y_{ox} - y_f) \exp(-m_t/\theta)\, d\xi \qquad 2.21$$

On the basis of light emission, the ignition delay is defined to be the time t*, required for J to reach some value J*. Thus the criterion is the achievement of $J = J^*$.

As a check on the applicability of this criterion in terms of capabilities of commonly used photo-detectors, the theoretical intensity of thermal light emission in the UV region was estimated. It was found to be of detectable magnitude. This was done for a 500μ thickness region of gas adjacent to the solid at 25 atms. and 3000°K, containing approximately 10^{20} product molecules. We assume that the radiation is due to characteristic strong CN emission bands in the UV region involving (Reference 10) transitions at 3883 Å and 3590 Å. The intensity of radiation falling on a detector given

by the right hand side of equation 2.19 assuming -- is on the order of 10^{-2} to 10^{-5} lumens. For an RCA type 935 photocell[11] preceded by a KODAK Wratten filter 18A[12] intensities on the order of 10^{-2} lumens are easily detectable. Therefore, it is concluded that thermally excited emission must comprise a part of the light detected in shock tube experiments.

It is possible that a part of the light detected by the photo-cell may be of chemiluminiscent nature. Since chemiluminiscence is attributed to radical-radical interactions, its dependence on gas phase properties is not known. One could argue that such interactions will not be frequent until relatively large concentrations exist, such as after the establishment of an intense, thick reaction zone involving external gas phase oxidizer. Such conditions would correspond to the 'long time" behaviour of the gas phase ignition process. Thus it can be argued that the thermally excited emission used in the present investigations is an adequate representation of reality.

The assumption was that CN emission is of thermal origin. There is some experimental evidence that this is so, as is discussed in reference 20. However, till conclusive experiments are performed, it is not possible to say with any certainty that CN emission is thermal or not. Till that time, it is assumed that the present analysis is valid. In case it becomes clear that CN emissions are not thermal, it is possible to consider the OH radical, which is known to undergo thermal excitations. The results obtained using this radical will not be very different from those of CN, since the characteristic parameters defining the emission have similar magnitudes.

The long time criterion discussed previously and the strong emission criterion[8] are somewhat related. Detailed analysis of this is given in reference. This gives some basis for the assertion previously made that detectable or strong emission occurs close to steady state.

CHAPTER III

NUMERICAL METHODS:

The set of differential equations 2.6 to 2.7 with their initial and boundary conditions are highly non-linear in nature and cannot be solved exactly. This leaves the only other alternative of solutions by difference approximations. There are several different schemes available and the most common ones are (1) explicit method (2) implicit method and (3) implicitly-explicit[13] method. There are other methods also in use, like predictor-corrector methods, Crank-Nicolson scheme, collocation method, etc. These methods have been found to be of not much value in the present case because of the large number of equations to be solved and their highly non-linear nature. The discussion of several numerical methods was done in reference (5) and only a discussion of implicitly-explicit method is presented here.

3.2 The Implicitly-Explicit Method:

In this method, one set of nodes is computed using a simple explicit scheme and alternate nodes are computed using an explicit scheme. For example, consider a differential equation of the type:

$$U_t = U_{xx} + a_0 U_x + f(x,t;U) \qquad 3.1$$

In this case, all the even nodes can be calculated using the explicit scheme. Thus

$$\frac{U_{2i}^{k+1} - U_{2i}^{k}}{\Delta t} = \frac{U_{2i+1}^{k} - 2U_{2i}^{k} + U_{2i-1}^{k}}{\Delta x^2} + a_0 \frac{U_{2i+1}^{k} - U_{2i-1}^{k}}{2\Delta x} + f_{2i}^{k} \qquad 3.2$$

where (i) refers to the space point and (k) to the time step. Δt and Δx are increments in time and space variables respectively. To compute intermediate odd nodes we use the implicit difference approximation

$$\frac{U_{2i-1}^{k+1} - U_{2i-1}^{k}}{\Delta t} = \frac{U_{2i}^{k+1} - 2U_{2i-1}^{k+1} + U_{2i-2}^{k+1}}{\Delta x^2} + a_0 \frac{U_{2i}^{k+1} - U_{2i-2}^{k+1}}{2\Delta x} + f_{2i-1}^{k+1} \qquad 3.3$$

The value of f_{2i-1}^{k+1} can be approximated by

$$f_{2i-1}^{k+1} = f_{2i-1}^{k+1}\left(x,t;\ U_{2i-2} + U_{2i}/2\right) \qquad 3.4$$

Since the equation 3.2 is explicit equation 3.4 is also explicit.

It can be seen from above that an implicitly-explicit method is basically an explicit method involving the same number of arithmetic operations as a simple explicit method. The advantage of an implicitly-explicit methos is obvious. Since an implicit method introduces positive error, i.e. consistent overestimation, and an explicit method constantly underestimates, the net error is greatly minimized. Hence, this method is more accurate for the same number of arithmetic operations involved. Alternatively, for the same accuracy as either implicit or explicit method alone, the number of operations are greatly reduced. Furthermore, the value of $\lambda = \frac{\Delta t}{(\Delta x)^2}$ which defines stability of the approximation is unity instead of $\frac{1}{2}$ as in the case of an explicit scheme. Since the stability criterion $\lambda = 1$ was deduced originally[13] for linear parabolic differential equations, for non-linear cases caution should be excercised to see that $\lambda < 1$. Convergence of the system has to be determined by trial and error procedure as are generally done for non-linear differential equations.

CHAPTER IV

DISCUSSION OF RESULTS:

Results on homogeneous propellant ignition are presented under three headings: (1) short time results, (2) long time results and (3) emission results. Short time results correspond to weak criterion on temperature, which is the establishment of a gas phase temperature 50% in excess of the initial gas phase temperature. Long time results are related to the attainment of quasi-steady gas phase conditions and emission results correspond to the achievement of a certain specified intensity of thermal radiation emitted by igniting gases gases.

4.1 Short Time Results:

At short times, the ignition behaviour can be deduced analytically by some simplifying assumptions. The validity of some of these assumptions can be justified from excellent agreement in behaviour between the numerical solutions and asymptotic solutions.

Figure (3) shows a logarithmic plot of dimensionless ignition delay versus the Damkohler number b, for both feed back and non- feed back cases. For large initial pyrolysis rates, i.e. low b values, both feed back and non-feed back models give almost identical results indicating that feed back is not important under these conditions. At low pyrolysis rates, however, feed-back becomes very important. Without feed-back, the gas phase will be starved of fuel supply and ignition delay tends to become extremely large as indicated by sharp upturns of dashed curves of Figure 3. In the feedback model, the surface temperature keeps on rising till the fuel pyrolysis rate is sufficient to cause rapid ignition. At high initial pyrolysis rates both feedback and non feed back models give -2/3 slope in(Figure 3)which is in agreement with asymptotic prediction. At large y^{∞}_{ox} values, the stoichiometric ratio (n) has virtually no effect on the ignition behaviour. Only at low y^{∞}_{ox} when the evolved oxidizer plays an important role in causing ignition does the stoichiometric ratio (n) become effective. This can be seen by comparing Figures 3 and 4.

It is also evident from Figures (4) and (5) that pure fuels ignite faster than propellants which is in variance with experimental results. Also in contradiction with experiments is the theoretically predicted weak dependence of ignition delay upon y^{∞}_{ox}. Employing short time criteria, both numerical and asymptotic results show that $t^* \sim (y^{\infty}_{ox})^{-2/3}$ as shown in Figure 10, curves 3 and 4. Experiments on the other hand indicate that $t^* \sim (y^{\infty}_{ox})^{\delta}$ where δ ranges from -1 to -3. The findings of the present investigations employing short time criterion show the same basic trends as in reference (4) and (5).

4.2 Long Time Results:

Continued numerical integrations -- beyond the achievement of weak ignition criterion -- of system of partial differential equations presented in Chapter II reveals very interesting fact that quasi-steady burning

conditions prevail soon after the weak temperature criterion is satisfied. In the period between the attainment of quasi-steady conditions and the achievement of weak temperature criterion, the conditions in the gas phase change continuously and rapidly. Figure (6) shows gas phase distributions at the time when weak temperature criterion was satisfied. Oxidizer mole fractions are nearly constant everywhere and equals to the free stream oxidizer mole fractions. This strengthens the original hypothesis that at short times reactant consumption can be neglected. Also can be seen from the Figure 6 is a thin intense reaction zone adjacent to solid surface. This later on shall be termed, for convenience, as primary reaction zone. Primary zone is a pre-mixed reaction zone. Figures (7) and (8) are schematic representations of gas phase distributions soon after and a long time after the short time temperature criterion is satisfied. Between t = 0.5 milliseconds and t = 2.0 milliseconds, conditions in the gas phase are changing slowly. Conditions in the primary zone are nearly steady. The secondary zone, so-called because of its structure is a diffusion reaction zone similar to the diffusion reaction zone in the flames studied by Burke-Schumann. The secondary reaction zone is thick compared to the primary zone. The fuel which is not consumed in the primary zone is used up in the secondary zone. Another noticeable feature of the secondary zone is that it is steadily moving away from the propellant surface. It has been found from numerical computations that this type of behaviour is established for a wide range of initial pyrolysis rates of the solid composition of the initial gas phase and a range of stoichiometric ($2 \leq n \leq 6$) of the gas phase chemical reactions.

Situations similar to that revealed in Figures (7) and (8) are more appropriately described by the term 'quasi-steady'. The quasi-steady state requiring an order of magnitude greater in time than the weak ignition criterion that $\theta^* = 1.5\theta_o$, is still achieved rapidly with ignition times on the order of the few milliseconds, even in a neutral gas phase. The behaviour of the model in this time domain is termed as 'Long time' behaviour. An interesting result occurring in the long time domain is the formation of twin flame zone structure in the gas phase whenever conditions permit. The secondary zone, as explained earlier, is formed between the hot fuel and the external oxidizer, the strength of which depends upon: (1) the mole fraction of the oxidizer present in the initial gas phase, (2) the stoichiometric ratio (3) propellant composition. A strong diffusion reaction zone exists for sufficiently large values of α and n. The strength of the reaction zone is measured by the amount of heat released in the reaction zone. At $\alpha = 1$, i.e. for pure fuel, only secondary zone exists and for $y_{ox}^{\infty} = 0$ only primary zone exists.

As in all previous models, the apparent ignition characteristics exhibited by the present model in the long time domain depend upon the choice of ignition criteria. In this domain several ignition criteria exist, for example; (1) time to achieve maximum absolute reaction rate (2) time required for a zero oxidizer mole fraction to occur at any location (3) a specified low rate of change of heat released in the secondary zone, etc. The results of these choices are indicated in Figure (9). In determining the closeness of the system to steady state, the important quantity is $(\frac{1}{q}\frac{\delta q}{\delta t})$-- i.e., the percentage change in heat release rate in the secondary zone. This quantity may be

represented by

$$\frac{1}{T_{max}}\left(\frac{\delta T_{max}}{\delta t}\right) \quad \text{or} \quad \frac{1}{\theta}\left(\frac{\delta \theta_{max}}{\delta \tau}\right)$$

Curves 5 and 6 of Figure (9) illustrate the ignition behaviours when a specified value of

$$\frac{1}{\theta_m}\left(\frac{\delta \theta_m}{\delta t}\right)$$

was chosen. The most satisfactory criterion was $\frac{\Delta\theta_m/\theta_m}{\Delta\tau/\tau} = \varepsilon$, where ε can have any specified value. This criterion tends to compensate for small values of

$$\frac{1}{\theta_m}\left(\frac{\delta \theta_m}{\delta \tau}\right)$$

when y^{∞}_{ox} is on the order of 0.1. As discussed elsewhere, this criterion is also appropriate.

Figure (10) shows a plot of t* versus y^{∞}_{ox} for several initial pyrolysis rates and propellant composition. As can be seen from the graph, it is interesting to note that there is a strong dependence of t* upon y^{∞}_{ox} as was observed during shock experiments. The results are also in agreement with the asymptotic analysis. at long times. It is also demonstrated from numerical results that the ignition delay is independent of initial pyrolysis rates, in agreement with experimental results[7]. Another interesting observation that can be made from Figure (10) is that a pure fuel ignites slower than a propellant under similar conditions, as has been found experimentally.

4.3 Emission Results

The results of present investigation emphasize, still further, the conclusions of the previous investigations on the characteristics of gas phase ignition process of solid materials - that choice of ignition criterion is decisive in determining the apparent ignition behaviour. The results also demonstrate the importance of choice of ignition criteria in the interpretation and reporting of experimental data.

Figures 12(a) and 12(b) are plots of calculated relative response of a hypothetical photo-detector, J, versus time for two values of activation energies assuming equal reaction rates for both energy values at a temperature of 1800°K. Values of J of 0.1 indicate an absolute intensity on the order of 10^{-2} lumens as detected by the photo-cell. These results can either be used to produce theoretical oscilloscope traces, or achievment of a particular value of J = J* to obtain t* versus y^{∞}_{ox} plots for a particular J* value.

Figure 13(a) is a linear plot of relative detector response versus time for y^{∞}_{ox} = 1.0, and 0.5 and illustrates the theoretical prediction of the way similar experimental curves should look for a solid undergoing gas phase ignition process. Figure 13(b) is a replot of experimental photo-cell response versus time during the ignition of a composite solid propellant for y^{∞}_{ox} = 1, and 0.5 exposed to a reflected. shock wave. As was done in experiments, if we choose the first discernable upward deflection or 'breakup' for determining the ignition event, it is obvious that sensitivity of the detecting equipment is important in determining the instant of ignition. For example, a decrease in sensitivity by a factor of 3 in Figure 13(a)

(i.e. a replot with a vertical scale contracted by a factor of three) would produce curves that look very much like those in Figure 13(b) indicating that the ignition behaviour predicted by theory and observed from experiments may change considerably depending upon the sensitivity of the detecting device.

Figure 14(a) and 14(b) are plots of t* versus y_{ox}^{∞} with ignition criteria of J* = 0.01, 0.05 and 0.1. The figures also include the so-called break-up criterion which is the ignition delay obtained from theoretical oscilloscope traces. As can be seen, the dependence of t* upon y_{ox}^{∞} becomes stronger and stronger as the value of J* is increased from 0.01 to 0.1. Beyond 0.1, any further increase in J* does not change the dependence of t_{ign} upon y_{ox}^{∞} very much, though the magnitude of ignition delay changes. Values of $J^* \geq 0.1$ correspond to long time criterion and J = 0.01 correspond to weak temperature criterion. It can also be seen from Figures 14 (a) and 14 (b) that ignition data for an E/R of 6000°K do not differ much from those for an E/R of 12000°K. This is expected since the chemical time for both activation energies was taken to be the same at 1800°K.

Figure 15(a) and 15(b) allow comparison of the present theoretical results using several ignition criteria and experimental results. For description of curves in Figures 15(a) and 15(b) reference should be made to Tables 2(a) and 2(b) respectively. The long time ignition Curve 5 and the emission criterion Curve 4 exhibit the same slope for high initial oxidizer mole fractions. Curve (1) is the data obtained at ONERA and Curves 2 and 3 were taken from reference (7). The slopes of Curves 1 and 3 are in good agreement with those of 4 and 5. Magnitudes of ignition delays are of the same order of magnitude for both theoretical and experimental curves, except for Curve (5) which is an order of magnitude higher and probably would correspond to ONERA data, Curve 1.

Figure 15(b) illustrates a further comparison of the present theoretical results with those of experiments. Curves 1 and 3 are experimental, and curves 2 and 4 are theoretical. Comparison of Figures 15(a) and (b) illustrates, to some extent, the diversity of the experimental data existing for composite propellant ignition under shock tube conditions. They also indicate with reference to Table II, the effect of different experimental and theoretical ignition criteria on the apparent ignition behaviour.

Figure (16) illustrates the difference between the behaviour of ignition of pure fuels and a homogeneous propellant when an emission criterion is employed. It can be seen that the ignition of a pure fuel is far more sensitive to the initial oxidizer mole fraction in the gas phase than is the propellant. At large y_{ox}^{∞} values a pure fuel ignites faster than a propellant for equal J* values and the situation reverses as y_{ox}^{∞} is decreased. The long time ignition data shows that a pure fuel ignites slower than a propellant at larger values of y_{ox}^{∞}. This perhaps is due to the fact that quasi-steady conditions are attained in the gas phase sooner for a propellant than for a pure fuel. However, it is not clear why an emission criterion shows a different behaviour than the long time behaviour.

4.4 Pressure Dependence of Ignition:

Under shock tube conditions, an increase in the initial gas pressure has a profound effect on the jump temperature at the propellant surface. Since the propellant pyrolysis rate is an exponential function of surface temperature it can be expected that gas phase total pressure has considerable effect on

ignition times. In Chapter II, asymptotic analysis at short times revealed that $\tau^* \sim (A\omega b^2 y_{ox}^{\infty})^{-2/3}$, where $\omega = \frac{m}{m_o}$. In this case m is the pyrolysis rate at the jump temperature and m_o is the pyrolysis rate at 400°K. Since $\rho^2 D \sim p$, $\tau \sim t(m_o^2/\rho^2 D)$, $b \sim (\rho^3 Z D / m_o^2)$ and $A = QR/nC_p E b$

we have

$$(m_o^2/\rho^2 D)t \sim \left[(m/m_o)\frac{\rho^3 Z D}{m_o^2}\right]^{-2/3}$$

or

$$t^*/p \sim \left[m/m_o\, p^2\right]^{-2/3}$$

To find the dependence of (m) upon the initial pressure we assume a power law relationship of the form:

$$\frac{m}{m_o} = \left(\frac{T - T_{s,o}}{400 - T_{s,o}}\right)^n$$

and equating that at any jump temperature other than 400°K, this ratio should be the same as

$$\exp(-E_p/RT_s) \,/\, \exp(-E_p/400R)$$

from which it was found that n = 2 for an E_p/R of 6000°K. Thus we obtain the pressure dependence of ignition delay as $t_{ign}^p \sim p^{-5/3}$. At long times, however, since $t^* \sim (An_{ox}^{\infty 2})^{-1}$ it can be expected that $t^* \sim p^{-1}$.

Figure 17(a) and (b) are theoretical oscilloscope traces for mass fluxes of 0.05 and 0.005 g/cm^{2}sec., respectively at $y_{ox}^{\infty} = 1$. The ignition delays obtained from these graphs with J* = 0.1, J* = 0.05 and the break-up criterion are plotted on lnt* versus lnp to give ignition delay as a function of pressure, in Figures 18(a) and (b). It is obvious from these figures that t*-p relationship strongly depends upon the choice of ignition criteria.

With break-up criterion (weak emission) or short time temperature criterion, numerical solutions give results in very good agreement with short time asymptotic relationship deduced above. Thus, from the graphs it is found that $t^* \sim p^{-1.77}$ where as asymptotic relationship gives $t^* \sim p^{-1.67}$. This is also in agreement with experimental observations.

As the value of J* increases to 0.05 or 0.1, the dependence of t* upon p, predicted by the theory, decreases approaching a limiting value of $t^* \sim p^{-1}$ for large J* values. Here again large emission results are in agreement with long time asymptotic analysis. Thus it can be said that more sensitive device may indicate a strong pressure dependence whereas an insensitive device may do otherwise.

The response of the predicted ignition delay of feed back model to changes in concentration of the oxidizer in the gas phase is shown in figure 18(c). It is important to note that under physical situation assumed in the present analysis, and in end wall shock tube experiments, the real ignition delay is not purely a function of oxidizer concentration alone. Different ignition delay oxidizer concentration relationships are predicted for the cases of (1) variable mole fraction at constant pressure and (2) variable total pressure with constant oxidizer mole fraction, as shown in Figure 18(c).

CHAPTER V

CONCLUSIONS

The present theory succeeded in explaining several experimental observations made on both double base and composite propellants. The present model is an improvement over the previous ones in that it can adequately represent a propellant igniting both in oxygen rich and neutral environments and the theoretical predictions can be directly compared with experiments. This was not possible in previous models. In addition, it has been possible to evaluate the validity of some simplifying assumptions that have been made in previous studies of this type.

One of the most important results of the present investigations is that completely transient conditions, including feedback, do indeed allow the solid itself to achieve quasi-steady burning conditions. It is found that feedback is operative over a wide range of decomposition rates of the solid. Nevertheless, feedback can be neglected for sufficiently high decomposition rates of the solid without significantly affecting the final results.

For solids producing fuel and oxidizing decomposition products in non-stoichiometric amounts, it has been found that a twin reaction zone structure exists in the gas phase soon after the short time criterion of the form $\theta^* = 1.5\theta_g$ is satisfied. The size and strength of the secondary zone strongly depends upon the amount of oxidizer initially present in the gas phase. It has been found from numerical solutions that for a given propellant, the size and strength of the primary reaction zone is independent of the initial oxidizer mole fraction. This supports the hypothesis that, any criterion corresponding to the development of the primary reaction zone, like short time or weak emission criterion indeed should exhibit a weak dependence upon the external oxidizer. Since experiments indicate a stronger dependence of t^* on y^{∞}_{ox} it is to be concluded that experimental detection does not correspond to the development of the primary zone.

The reason for the existence of secondary zone is discussed in the previous chapter. It is only to be mentioned here that since most propellants are fuel rich and shock tube experiments are conducted at sufficiently high oxidizer mole fractions one can always expect a twin flame structure in the gas phase. The implications of this statement is obvious. It points out that any criterion related to the development of a strong secondary zone should reveal properties entirely different from those revealed by weak criterion. Since the strength of the secondary zone greatly depends upon the initial oxidizer mole fraction it is clear that ignitionbbehaviour should do likewise.

The above fact is demonstrated very well from the fact that both long time criterion and large emission criterion indicate the same result that $t^* \sim (y^{\infty}_{ox})^{-2}$ and $t^* \neq f(m_o)$. Experiments show similar behaviour.

The development of emission criterion helps to compare theoretical results with those of experiments under the criterion of detectable amount of light emission for the hot gases as detected by a photo-cell. The light emission criterion was derived by determining the time required for a quantity J, proportional to the output of a hypothetical photo-cell detector to reach some selected value J*. This detector sensed the calculated intensity of thermally stimulated light incident on it.

The new criterion can be considered as a reasonable theoretical equivalent of the experimental criterion employed during shock tube experiments and helps to clarify the diversity present in the experimental data and type of ignition data needed to ascertain the ignition mechanism. The theory based on emission criterion predicts that a highly sensitive device should indicate a weak ignition dependence on external oxidizer mole fraction and a less sensitive device should do so otherwise. Hence the theory calls for experiments using at least two greatly different sensitivities of the photo detector to determine the mechanism of ignition.

It has also been found that the secondary zone is responsible for the majority of the light detected. The weak emission criterion gives essentially the same results as with short time temperature criterion and the strong emission criterion corresponds to long time criterion. This is quite well substantiated in Chapter II.

It was shown that purely thermal excitation of certain radical was of sufficient magnitude to produce light intensities detectable by an ordinary photo-cell similar to RCA 935. It is possible that some of the light detected experimentally may be due to chemi-luminiscence. Present analysis ignores this. Thermally excited light emission used in the present investigation can be considered as an adequate respresentation of reality. Thus it can be concluded that ignition of fuels and homogeneous propellants under shock pulse cause explained by pure gas phase mechanisms.

In the above discussion it was assumed that ignition was triggered by pure gas phase mechanisms. However, in reference (6) it is shown that both simple heterogeneous, and simple gas phase theories predict nearly the same ignition behaviour. From this point of view, the theoretical analysis carried out so far is not really conclusive as to the exact mechanism of ignition during shock tube tests, since equivalent work has not been carried out for heterogeneous model. In reality, it may be possible that both mechanisms play their part in the ignition process. The purpose of the present investigations is therefore not to invalidate the surface reaction theory but to show the characteristic behaviour of purely gas phase ignition process, and such a mechanism can, in fact, explain all the experimentally observed ignition behaviour -- something which has not been demonstrated previously.

CHAPTFR VI

6.1 Introduction:

In all the previous theories on gas phase ignition under shock tube conditions it was assumed that either the solid was a pure fuel or contained an oxidizer which had the same physico-chemical properties as the external oxygen. Thus it was found that the dependence of ignition times y_{ox}^{∞} became weaker as the amount of oxidizer present in the propellant was increased. If the evolved oxidizer is less active than the ambient oxidizer, it is obvious that the ambient oxidizer is the controlling factor in deciding the ignition characteristics. Therefore, previous analysis applicable to pure fuels, discussed in Chapter II, can be employed in estimating the ignition behaviour of the propellants. On the other hand it would be interesting to evaluate the situation in which the evolved oxidizer is far more active than the ambient oxidizer. In such a case one would anticipate that ignition behaviour should less strongly depend upon the external oxidizer. An example of a propellant which produces an oxidizer more reactive than the ambient oxidizer is an ammonium perchlorate based propellant. This type of propellant, on decomposition produces an oxidant, perchloric acid, which is very active. Hence it is of interest to find out what happens in such a case. This is discussed in the following sections.

6.2 Description of the Model:

The assumptions made here are the same in Chapter II except that the two oxidizer diffusion processes are treated separately and the evolved oxidizer is assumed to have different kinetic properties than the ambient oxidizer. With these in mind, the equations for conservation of reactants and energy can be written as below:

Defining the operator $H \equiv \frac{\partial}{\partial \tau} + \omega \frac{\partial}{\partial \xi} - \frac{\partial^2}{\partial \xi^2}$

the equations after proper non-dimensionalization may be written as

$$H(\eta_f) = -\eta_f \left[\eta_{ox}'' + \pi \eta_{ox}' \exp \frac{1}{\theta}\left(1 - \frac{1}{\varepsilon}\right) \right] \exp(-1/\theta) \qquad 6.1$$

$$H(\eta_{ox}') = -n \eta_f \pi \eta_{ox}' \exp \frac{1}{\theta}\left(1 - \frac{1}{\varepsilon}\right) \cdot \exp(-1/\theta) \qquad 6.2$$

$$H(\eta_{ox}'') = -\eta_f \eta_{ox}'' \exp(-1/\theta) \qquad 6.3$$

$$H(\eta_i) = 0 \qquad 6.4$$

$$H(\theta) = A\eta_f\left[\eta_{ox}'' + \pi Q \eta_{ox}' \exp\frac{1}{\theta}\left(1 - \frac{1}{E}\right)\right]\exp\left(-\frac{1}{\theta}\right) \qquad 6.5$$

and

$$\frac{\partial \theta_s}{\partial \tau} + \frac{M\omega}{\Sigma^{1/2}} \frac{\partial \theta_s}{\partial \xi_s} = \frac{\partial^2 \theta_s}{\partial \xi_s^2} \qquad 6.6$$

Subject to the initial and boundary conditions

$$\eta_f(\xi,0) = \eta_f(\infty,\tau) = 0 \qquad \eta_f(0,\tau) - \omega^{-1}\frac{\partial \eta_f(0,\tau)}{\partial \xi} = n_2 b\alpha$$

$$\eta_{ox}''(\xi,0) = \eta_{ox}''(\infty,\tau) = \eta_{ox}^{\infty} \qquad \eta_{ox}''(0,\tau) - \omega^{-1}\frac{\partial \eta_{ox}''(0,\tau)}{\partial \xi} = 0$$

$$\eta_{ox}'(\xi,0) = \eta_{ox}'(\infty,\tau) = 0 \qquad \eta_{ox}'(0,\tau) - \omega^{-1}\frac{\partial \eta_{ox}'(0,\tau)}{\partial \xi} = (1-\alpha)b$$

$$\eta_i(\xi,0) = \eta_i(\infty,\tau) = \eta_i^{\infty} \qquad \eta_i(0,\tau) - \omega^{-1}\frac{\partial \eta_i(0,\tau)}{\partial \xi} = 0$$

$$\theta(\xi,0) = \theta(\infty,\tau) = \theta_0 \qquad \theta_s(0,\tau) = \theta(0,\tau)$$

$$\theta_s(\xi_s,0) = \theta_s(-\infty,\tau) = \theta_{s,0} \qquad \frac{\Lambda}{\Sigma^{1/2}}\frac{\partial \theta_s(0,\tau)}{\partial \xi_s} - \beta\omega = \frac{\partial \theta(0,\tau)}{\partial \xi}$$

. . . 6.7

For simplicity it was assumed that $\Lambda = 1$, $E = Q = n = 1$, but $Z_1 \neq Z_2$. All the dimensionless groups are defined as in Chapter II, except for the additional ones which are defined as $E = E_1/E_2$, $\pi = Z_1/Z_2$, $Q = Q_1/Q_2$ and

$$n = \frac{n_1}{n_2}$$

6.3 Approximate Solutions:

Limiting solutions can be obtained either for large or small values of π.

Case I, Small π:

Equations 6.1 to 6.6 simplify to

$$H(\eta_f) = -\eta_f \eta''_{ox} \exp(-1/\theta)$$

$$H(\eta'_{ox}) = H(\eta_i) = 0$$

$$H(\eta''_{ox}) = -\eta_f \eta''_{ox} \exp(-1/\theta) \qquad 6.8$$

$$H(\theta) = A\eta_f \eta''_{ox} \exp(-1/\theta)$$

$$\xi \qquad \frac{d\theta_s}{d\tau} + \left[\frac{\mu\omega}{\Sigma^{1/2}}\right]\frac{d\theta_s}{d\xi_s} = \frac{d^2\theta_s}{d\xi_s^2}$$

The boundary conditions remain unaltered. A procedure similar to pure fuel case lead to the relationship that $\tau^* \sim (Ab^2\, \omega n_2 y^{\infty}_{ox})^{-2/3}$ for short times and $\tau^* \sim (A\eta^{\infty}_{ox}{}^2)^{-1}$ for long times.

Case 2, Large Π

For large Π, equations 6.1 to 6.6 reduce to:

$$H(\eta_f) = -\eta_f \eta'_{ox} \pi \exp\tfrac{1}{\theta}\left(1 - \tfrac{1}{E}\right) \cdot \exp(-1/\theta)$$

$$H(\eta'_{ox}) = n H(\eta_f)$$

$$H(\eta''_{ox}) = -\eta_f \eta''_{ox} \exp(-1/\theta)$$

$$H(\theta) = A\eta_f \eta'_{ox} \pi Q \exp\tfrac{1}{\theta}\left(1 - \tfrac{1}{E}\right) \cdot \exp(-1/\theta)$$

6.9

and $$\frac{\partial \theta_s}{\partial \tau} + \frac{\mu \omega}{\Sigma^{1/2}} \frac{\partial \theta_s}{\partial \xi_s} = \frac{\partial^2 \theta_s}{\partial \xi_s^2}$$

With the initial and boundary conditions same as before, the solution in this case is similar to the case of a propellant igniting in neutral atmosphere; thus the ignition delay should be almost independent of external oxidizer mole fraction.

6.4 Results and Conclusions:

In this section, only the emission criterion is employed. Further, for the reasons mentioned above, only the case of evolved oxidizer more reactive than the gas phase oxidizer is considered. Figure (18) is a plot of t* versus y_{ox}^{∞} for $Z_1 = 5Z_2$ or an evolved oxidizer five times as reactive as the ambient oxidizer, at the same initial gas phase temperature. It was found that for a selected ignition criterion of the type J=J*, dependence of t* upon y_{ox}^{∞} decreases as the reactivity of the evolved oxidizer increases. To illustrate this effect, Figure (18) contains two curves for $\alpha = 0.5$ and $E1/R = 6000^{\circ}K$ for the cases of $Z_1 = Z_2$ and $Z_1 = 5Z_2$. It is evident that for J* = 0.1, the slope of the curve for $Z_1 = 5Z_2$ is lower than that for $Z_1 = Z_2$. However, steeper slopes can be expected at large J* values since the fuel that is not used up in the primary zone forms a strong secondary zone with the external oxidizer.

The snake like character of the lowest curve in Figure (19) resulted from making a theoretical oscilloscope trace similar to Figure 13(a) and applying a break-up criterion for the case of $Z_1 = 5\ Z_2$. This probably is due to the difficulty of ascertaining the exact break-up point from the theoretical oscilloscope traces. It is interesting that it bears a marked resemblence to composite propellant ignition data recently presented by Summerfield et al[13]. Such ignition characteristics may be interpreted as indicating a gas phase ignition process in which the evolved oxidizer is considerably more reactive than the oxidizer initially present in the gas phase.

Since shock tube experiments in composite propellants indicate a large effect of y_{ox}^{∞} on t*, the gas phase theory currently formulated leads to the conclusion that either little or no oxidizer was decomposed during the primary ignition process or the evolved oxidizing species have kinetic properties similar to oxygen during shock tube experiments.

CHAPTER VII

GAS PHASE IGNITION OF HETEROGENEOUS SOLID PROPELLANTS UNDER SHOCK TUBE CONDITIONS

7.1 Introduction:

The present day propellants are heterogeneous in nature. They consist of oxidizer crystals, like ammonium or potassium perchlorate, finely ground and dispersed in a fuel matrix. Upon decomposition of such a propellant, the fuel oxidizer vapours may diffuse both axially and radially, probably affecting the ignition behaviour considerably. Since the size of the oxidizer particle is of the same order of magnitude as the reaction zone thickness ($\simeq$ 20 to 200 μ) it can be expected that radial diffusion may play a significant role in determining the overall ignition characteristics. To extend the analysis of gas phase ignition characteristics, making the model more realistic and applicable to heterogeneous propellants, a two dimensional model is considered, and a detailed description of the model is presented in the following sections.

7.2 Physical Model:

A schematic representation of the physical model and the propellant geometry are shown in Figures (20) and (21). The assumptions made during the equations are the same as in Chapter II, except for a few additional ones. They are:

1. The diffusion in both axial and radial
2. The decomposition rates of fuel and oxidizer are assumed to proceed according to an Arrhenius law.
3. Negligible amount of propellant is decomposed during ignition and the propellant surface remains planar during rapid ignition process (although there may exist a radial surface temperature, and hence mass flux, distribution).
4. Density is constant in the gas phase.
5. Oxidizer and fuel have identical thermal properties.

It should be noted that although the assumption (3) is not necessary, assuming a planar interface simplifies the problem considerably. In principle, it is possible to set up boundary conditions which take into consideration the variation of mass flux with radius and the surface geometry acquired by the propellant surface because of this. But the computational labour and time involved did not permit the consideration of a more exact model. Nevertheless it was felt that the effect on the ignition behaviour of the boundary movement would be insignificant.

7.3 Mathematical Formulation:

With the definition of an operator H as

$$H \equiv \frac{\partial}{\partial \tau} + \bar{u}\frac{\partial}{\partial \xi} + v_\rho \frac{\partial}{\partial \rho} - \left[\frac{\partial^2}{\partial \xi^2} + \frac{1}{\rho}\frac{\partial}{\partial \rho}\left(\rho \frac{\partial}{\partial \rho}\right)\right]$$

the equations for the conservation of the species and energy can be written as follows:

CONTINUITY

$$\frac{\partial}{\partial \xi}(\rho \bar{u}) + \frac{\partial}{\partial \rho}(\rho v_\rho) = 0 \qquad 7.1$$

MOMENTUM

$$H(\bar{u}) = 0 \qquad 7.2$$

SPECIES AND ENERGY

$$H(\eta_f) = H(\eta_{ox}) = -\frac{1}{A} H(\theta) = -\eta_f \eta_{ox} \exp(-1/\theta) \qquad 7.3$$

$$\frac{\partial \theta_f}{\partial \tau} + \frac{\mu\omega}{\Sigma^{1/2}}\frac{\partial \theta_f}{\partial \xi_s} = \frac{\partial^2 \theta_f}{\partial \xi_s^2} + \frac{\Sigma}{\rho}\frac{\partial}{\partial \rho}\left(\rho \frac{\partial \theta_f}{\partial \rho}\right) \qquad 7.4$$

$$\frac{\partial \theta_{ox}}{\partial \tau} + \frac{\mu\omega}{\Sigma^{1/2}}\frac{\partial \theta_{ox}}{\partial \xi_s} = \frac{\partial^2 \theta_{ox}}{\partial \xi_s^2} + \frac{\Sigma}{\rho}\frac{\partial}{\partial \rho}\left(\rho \frac{\partial \theta_{ox}}{\partial \rho}\right) \qquad 7.5$$

subject to the following initial and boundary conditions:

$\tau \le 0,\ \xi > 0,\ \xi_s < 0;\ \tau > 0,\ \xi = \infty,\ \xi_s = -\infty$

$\eta_f = 0,\ \eta_{ox} = \eta_{ox}^{\infty},\ \eta_i = \eta_i^{\infty}$

$\theta = \theta_\infty,\ \theta_f = \theta_{ox} = \theta_{-\infty}$

$\bar{u} = v_\rho = 0$

$\tau > 0,\ \xi = \xi_s = 0$

$$\eta_f - \bar{u}^{-1}\frac{d\eta_f}{d\xi} = nb,\ \rho_1 \le \rho \le \rho_2$$
$$= 0,\ 0 \le \rho < \rho_1$$

$$\eta_{ox} - \bar{u}^{-1}\frac{d\eta_{ox}}{d\xi} = b,\ 0 \le \rho < \rho_1$$
$$= 0,\ \rho_1 \le \rho \le \rho_2$$

$$\eta_i - \bar{u}^{-1}\frac{d\eta_i}{d\xi} = 0,\ 0 \le \rho \le \rho_2$$

$$\theta_s = \theta,\ \frac{d\theta_s}{d\xi_s} = \frac{d\theta}{d\xi} \pm \beta$$

$\xi > 0,\ \tau > 0,\ \xi_s < 0$

$$\rho = 0:\quad \frac{d\eta_f}{d\rho} = \frac{d\eta_{ox}}{d\rho} = \frac{d\eta_i}{d\rho} = \frac{d\theta_{ox}}{d\rho} = \frac{d\theta_f}{d\rho} = \frac{d\bar{u}}{d\rho} = \frac{d\theta_f}{d\rho} = 0 = \frac{d\theta}{d\rho}$$

$$\rho = \rho_1:\quad \frac{d\theta_f}{d\rho} = \frac{d\theta_{ox}}{d\rho} = 0$$

$$\rho = \rho_2:\quad \frac{d\eta_f}{d\rho} = \frac{d\eta_{ox}}{d\rho} = \frac{d\eta_i}{d\rho} = \frac{d\theta_{ox}}{d\rho} = \frac{d\theta_f}{d\rho} = \frac{d\theta}{d\rho} = \frac{d\bar{u}}{d\rho} = v_\rho = 0$$

In the above analysis it was assumed that the evolved oxidizer had the same physical and kinetic properties as the free stream oxidizer. The dimensionless quantities appearing in the above equations are defined as follows:

$$\xi = x\left(m_o/\rho_g D\right),\quad \bar{u} = \frac{u}{u_o},\quad u_o = \frac{m_o}{\rho_g}$$

$$\tau = t\left(m_o^2/\rho_g^2 D\right),\quad v_\rho = \frac{v_r}{u_o},\quad \eta_f = nby_f$$

$$\xi_s = \xi/\Sigma^{\frac{1}{2}},\quad \omega = \bar{u}$$

$$\rho = r\left(m_o/\rho_g D\right),\quad \eta_{ox} = by_{ox},\quad \eta_i = by_i$$

$$\theta = RT/E,\quad \theta_{ox} = RT_{ox}/E_{ox},\quad \theta_f = RT_f/E_f$$

For a significant part of the work it was assumed that the decomposition rates of both oxidizer and fuel were the same at equal surface temperatures. The above equations were numerically solved on an IBM 360/75 digital computer. The results of numerical computations are presented in Section 7.6.

7.4 Asymptotic Solutions:

Solutions applicable under special conditions can be obtained by neglecting reactant consumption up to ignition. If we further assume that each fuel strand is surrounded by huge oxidizer strand inverse geometry of the previous section), the equations discussed above can be reduced to

$$\frac{\partial \eta_f}{\partial \tau} = \frac{\partial^2 \eta_f}{\partial \xi^2} + \frac{1}{\rho}\frac{\partial}{\partial \rho}\left(\rho \frac{\partial \eta_f}{\partial \rho}\right) \qquad 7.7$$

$$\frac{\partial \theta}{\partial \tau} = \frac{\partial^2 \theta}{\partial \xi^2} + \frac{1}{\rho}\frac{\partial}{\partial \rho}\left(\rho \frac{\partial \theta}{\partial \rho}\right) + A\eta_f \eta_{ox} \exp(-1/\theta) \qquad 7.8$$

with $\eta_{ox} = \eta_{ox}^{\infty}$ for a large y_{ox}^{∞} values. Wall temperature was assumed constant and convection neglected. Negligible amount of oxidizer decomposes during ignition.

Equations 7.7 and 7.8 are subjected to initial and boundary conditions:

$$\frac{\partial \eta_f}{\partial \xi} = -nb, \quad 0 \le \rho \le \rho_2 \; ; \quad \frac{\partial \eta_f}{\partial \xi} = 0, \quad \rho > \rho_2 .$$

$$\left.\frac{\partial \eta_f}{\partial \rho}\right)_{\rho=0} = \left.\frac{\partial \eta_f}{\partial \rho}\right)_{\rho=\rho_2} = 0; \quad \xi \to \infty, \; \eta_f \to 0 .$$

Also at $t = 0$, $\eta_f = 0$ for all ξ and ρ.

Successive application of Hankel and Laplace transform gives the solution for η_f as

$$\eta_f = \frac{nb\rho_2}{2}\int_0^{\infty} J_1(p\rho_2) J_0(p\rho)\left[e^{-\xi p}\operatorname{erfc}\left(\frac{\xi}{2\tau^{1/2}} - p\tau^{1/2}\right) - e^{\xi p}\operatorname{erfc}\left(\frac{\xi}{2\tau^{1/2}} + p\tau^{1/2}\right)\right]\frac{dp}{p}$$

If we define ξ, ρ, τ and ϕ as

$$\bar{\xi} = (A\eta_{ox}^{\infty} n b \rho_2/2)^{\frac{1}{2}} \xi$$
$$\bar{\rho} = (A\eta_{ox}^{\infty} n b \rho_2/2)^{1/2} \rho \qquad 7.10$$
$$\bar{\tau} = (A\eta_{ox}^{\infty} n b \rho_2/2) t$$
$$\phi = \beta \tau^{1/2}$$

then, substitution of 7.9 in 7.8 gives

$$\frac{d\theta}{d\bar{\tau}} = \frac{d^2\theta}{d\bar{\xi}^2} + \frac{1}{\bar{\rho}} \frac{d}{d\bar{\rho}}\left(\bar{\rho} \frac{d\theta}{d\bar{\rho}}\right) + \eta_{ox}^{\infty} e^{-\frac{1}{\theta}} \int_0^{\infty} J_1\left(\frac{\phi \bar{\rho}_2}{\bar{\tau}^{1/2}}\right) J_0\left(\frac{\phi \bar{\rho}}{\bar{\tau}^{1/2}}\right) \psi \frac{d\phi}{\phi} \qquad 7.11$$

where $\psi = e^{-\phi\bar{\xi}} \operatorname{erfc}\left(\frac{\bar{\xi}}{2\bar{\tau}^{1/2}} - \phi\right) - e^{\phi\bar{\xi}} \operatorname{erfc}\left(\frac{\bar{\xi}}{2\bar{\tau}^{1/2}} + \phi\right)$ $\frac{1}{\xi}$ $\bar{\rho}_2 = (A\eta_{ox}^{\infty} n b/2)^{\frac{1}{2}} \rho_2^{3/2}$

Solution of 7.11 is of the form $\theta = \theta(\bar{\tau}, \bar{\xi}, \bar{\rho}, \bar{\rho}_2 \sqrt{\bar{\tau}})$ and thus for an ignition criterion of the type $1/\theta = \theta^*$ occurring at $\bar{\tau} = \tau^*$ we get $\tau^* \sim 1/(A \eta_{ox}^{\infty} n b \rho_2)$ or $t^* \sim (y_{ox}^{\infty})^{-1}$. This is an interesting result, indicating the ignition delay depends inversely on the oxidizer mole fraction, which is in good agreement with some experiments. The present result that $t^* \sim (y_{ox}^{\infty})^{-1}$ is an interesting contrast to the previous result for homogeneous propellants of $t^* \sim (y_{ox}^{\infty})^{-2/3}$ and is a direct result of the 2-dimensional nature of the problem.

The above result is equally valid for a fuel igniting in a shock tube, rich in oxygen, if the shock tube diameter is much larger than the propellant strand, as is the case in the experiments reported.

7.5 Numerical Methods:

Both explicit and implicit schemes discussed in Chapter III can be employed in the present situation also. However, it is obvious that either of the method will take extremely long computational times. For example, for the same number of axial nodes and the same number of time steps, a 2-D problem will take roughly M times the computational time needed by a 1-D problem, where M is the number of nodes in the radial direction. The so-called alternating implicit-explicit method would seem to be promising, and a rough estimation indicates that this method is several times as fast as either the implicit or explicit method. However, it is quite cumbersome and hence only the explicit method is considered here.

Consider a differential equation of the type

$$u_t = u_{xx} + u_{rr} + \frac{u_r}{r} + f(x,r,t;u) \qquad 7.12$$

At all grid points except at r = 0, and r = R the equations can be approximated by the forward difference approximation:

$$\frac{u_{ij}^{k+1} - u_{ij}^{k}}{\ell} = \frac{u_{i+1\,j}^{k} - 2u_{ij}^{k} + u_{i-1\,j}^{k}}{h_1^2} + \frac{u_{ij+1}^{k} - 2u_{ij}^{k} + u_{ij-1}^{k}}{h_2^2} + \frac{u_{ij+1}^{k} - u_{ij-1}^{k}}{2h_2 j} + f(ih_1, jh_2, \ell k; u) \qquad 7.13$$

where $x = i\,h_1$, $r = jh_2$ and $t = \ell k$.

The above scheme offers no computational problem except at r = 0. At r = 0, a singularity exists in the term $\frac{1}{r}\frac{\partial u}{\partial r}$. Since it was assumed that at r = 0, $\frac{\partial u}{\partial r} = 0$ because of symmetry. the term $\frac{1}{r}\frac{\partial u}{\partial r}$ is of the form 0/0 at r = 0 which is indeterminate. If however, u'(r) is expanded in McLaurin series and the limiting process is carried out by application of L'Hopital's rule, one obtains

$$\lim_{r \to 0} \left[\frac{1}{r}\left(\frac{du}{dr}\right) \right] = u''(0) \qquad 7.14$$

Hence along the line r = 0, the equation to be solved is:

$$\frac{du}{dt} = \frac{d^2u}{dx^2} + 2\frac{d^2u}{dr^2} + f(x,0,t;u) \qquad 7.15$$

At the outer boundary r = R and $\frac{\partial u}{\partial r} = 0$ and therefore equation becomes

$$\frac{du}{dt} = \frac{d^2u}{dx^2} + \frac{d^2u}{dr^2} + f(x,r,t;u) \qquad 7.16$$

With these precautions in mind, equation 7.12 can be solved in a straight forward manner.

Stability and Convergence:

Though rigorous proofs of stability and convergence are not possible for the above equations, many times stability of the approximation is assumed. For a two-dimensional linear problem it can be shown that all explicit schemes are stable as long as $\lambda \leq \ell/h_1^2 + \ell/h_2^2$

If we choose that $h_1 = h_2 = h$, then the restriction on the grid size for stability becomes $\lambda = \ell/h^2 \leq 1/4$, a more stringent restriction than that for a one dimensional case.

As far as convergence is concerned, it can only be tested by a trial and error procedure. If the grid size is reduced to half of its original size and the solutions thus obtained do not differ very much from each other then the difference approximation can be considered convergent. Computer trials indicated this to be true in the present instance.

7.6 Ignition Criteria:

Similar to homogeneous propellant ignition data, data for heterogeneous propellants are presented using short time and emission criteria. The form of expression for the intensity of emitted radiation in terms of output of photocell is modified to

$$V_p \sim \frac{2K}{\rho_2^2} \int_0^{\xi''} \int_0^{\rho_2} (1 - y_f - y_{ox} - y_i) \exp\left(-\frac{M_t}{\theta}\right) \rho \, d\rho \, d\xi \qquad 7.17$$

where ρ_2 is the outer diameter of one composite microstrand. For presenting the theoretical ignition data, the quantity calculated during numerical computation was

$$J' = \sum_{i=j=0}^{N} \sum^{M} j f(x)_j \exp\left(-\frac{t_c}{\theta_{ij}}\right) \qquad 7.18$$

which is related to the homogeneous propellant ignition criterion J as

$$J = \frac{2J'}{M^2}$$

where M is the number of nodes in the radial direction, assuming that the grid size in the axial direction is the same for both homogeneous and heterogeneous propellants.

CHAPTER VIII

8.1 Discussion of Results:

Ignition behaviour of a heterogeneous propellant differs from that of a homogeneous propellant in many ways. Firstly, as can be expected, there is diffusion in both axial and radial directions and thus the degree of chemical reaction varies from point to point. Hence it is not possible to talk of one or two discrete reaction zones as was possible in the case of a homogeneous propellant. Secondly, since the surface temperature of the propellant varies radially, the mass flux at the propellant surface is not uniform resulting in widely differing rates of cross diffusion of fuel and oxidizer vapour as a function of time.

Figure (22) is a plot of reactant mole fraction versus dimensionless distance, ξ, at a time $\tau = 0.153$ which is only a short time after the achievement of a gas phase temperature equal to $1.5\theta_o$. As can be seen from the figure, close to the outer radius of the propellant strand, the propellant behaves like a pure fuel since there is more fuel at the outer radius than at the inner radius. Towards the centre of the propellant strand the concentration profile of the reactant changes. It appears that for small values of r/r_o, where r_o is the outer radius of the propellant strand (i.e. close to the centre of the propellant strand), there is a fuel hill established in between the evolved and the external oxidizer. The fuel vapours flow down the hill on either side to form a double reaction zone which reduces to a single reaction zone as r/r_o is increased. It is obvious from the figure that the concept of a single reaction zone is not applicable to heterogeneous propellant ignition. Hence the long time ignition criterion employed in the case of homogeneous propellants becomes meaningless.

Figure (23) throws more light on the structure of the gas phase during the ignition of a heterogeneous propellant. The fuel concentration is maximum at the outer radius and the oxidizer mole fraction is maximum at the centre all the time. Further, the fuel mole fraction falls off very sharply with distance. The distributions at $\tau = 0.753$ do not differ very much from those at $\tau = 0.153$ except that as the radius increases, the oxidizer mole fraction first decreases and then increases.

Figure (24) is a plot of relative emission intensities versus time for y_{ox}^{∞} of 1, 0.5 and 0.1, for a particle size of 70 microns. In Figure 25, Curve (1) is obtained from short time data and exhibits a slope of approximately -0.8 on the log-log plot and is in good agreement with the approximate solution discussed in t the previous chapter. However, it should be remembered that the approximate solutions are valid only for large oxidizer particles, i.e. for small values of R_2-R_1/R_2. Curve (2) is obtained from emission characteristics and as can be seen from the figure, is in good agreement with the experimental curve (3) for large y_{ox}^{∞} values. Curve (3) is extracted from reference (7). The slope of curve (4) is not very much different from that of curve (2). Only the magnitude of the ignition delay is higher.

Figure (26) is again a linear plot of J versus t, for a particle size of 200 microns. It can be seen from the figure that even at the 'break-up' point, ignition delays are very sensitive to the initial oxidizer mole fraction. However, if we take a certain specified deflection on the oscilloscope to define the instant of ignition, as can be seen from Figure 27, for a J* value of 0.05, then the dependence of ignition, delay upon the initial oxidizer mole fraction becomes weaker. A J* value of 10^{-4} on Figure (27) corresponds to the weak temperature criterion and exhibits a slope of almost -1 on the log-log plot. This justifies the validity of approximations made in obtaining the asymptotic solutions. It is obvious that consideration of inverse geometry, i.e. fuel surrounded by oxidizer crystals, should essentially give the same results as the normal geometry, i.e. oxidizer particles surrounded by the fuel matrix. Figure (27) again demonstrates that a highly sensitive equipment detects the ignition behaviour to be weaker than a low sensitivity device.

Comparison between Figures (25) and (27) shows that the particle size has a strong effect upon the ignition delay. For example, curve (2) of Figure (25), which is obtained by applying the break-up criterion has a slope of -1.2 and the curve (2) of Figure (27) obtained by applying the same criterion indicates a slope of -2.0. It can be expected from these that as the particle size increases, the apparent ignition behaviour exhibits a stronger dependence upon the external oxidizer. As the particle size is reduced, the propellant becomes less and less heterogeneous in nature and the ignition behaviour should essentially be the same as predicted for homogenous propellants.

From numerical computations it has been found that the emission from a heterogeneous propellant is lower than the emission from a homogeneous propellant. This is to be expected since, in the case of a homogeneous propellant, the temperature inside the secondary reaction zone is high and uniform across the section whereas in the case of a heterogeneous propellant, the temperature is high at fuel-rich areas and low at fuel-poor areas.

Continued numerical integration of the differential equations describing the ignition of a heterogeneous propellant indicated that quasi-steady burning conditions are attained even for heterogeneous propellants. It has been found from computations that emission intensities become constant with time when quasi-steady gas phase conditions are attained. Hence steady burning conditions can be said to be attained when the emission intensities become constant with respect to time.

Pressure Dependence of Ignition Delay:

As discussed in Chapter IV, Section 4, a change in the total pressure results in a corresponding change in the initial jump temperature at the propellant surface and hence a pressure dependence similar to that of homogeneous propellants can be expected. The asymptotic solution of Section 7.4 indicates that ignition delay should at least be inversely proportional to pressure at high mass fluxes and large y_{ox}^{∞} values. Figure 28(a) and 28(b) are theoretical 'oscilloscope' traces for mass fluxes of 0.05 and 0.005 g/cm^{2}sec at $y_{ox}^{\infty} = 1$ and are used to obtain ℓnt^* versus log p curves for several ignition criteria.

Figure (29) is a plot of lot t* versus log p for a mass flux of 0.05 g/cm^2-sec at $y_{ox}^{\infty} = 1.0$. As can be seen from the figure, at break-up, the dependence of ignition times upon the gas phase total pressure can be read as

$t^* \sim p^{-1.5}$. The dependence does not seem to change very much if higher values of J^* are chosen. Only the magnitude of the ignition delay changes.

At low mass fluxes the pressure dependence of ignition delay becomes much stronger. Figure (30) is again a plot of log t* versus log p for a mass flux of 0.005 $g/cm^2 sec$ & $y_{ox}^{\infty} = 1.0$. As can be seen from the graph, the pressure dependence at break-up is much stronger than at high emission intensities. The dependence can be read as $t^* \sim p^{-2.5}$ at break-up and $t^* \sim p^{-2.0}$ if an ignition criterion of $J^* = 0.1$ is chosen. These are in excellent agreement with the experimental results[1]. Since, after the short time criterion is satisfied, the mass flux from the propellant surface becomes sufficiently high -- irrespective of the initial mass fluxes due to high surface temperatures attained in the feed back model -- the initial mass flux should not have much effect on the pressure dependence if a strong emission criterion ($J^* \geq 0.1$) is employed.

8.2 Conclusions

The present theoretical investigations on the ignition of heterogeneous propellants have revealed some interesting aspects. Firstly, with the present model, it is possible to explain the experimentally observed ignition behaviour of composite propellants. Even with a weak temperature criterion one theoretically obtains slope of -1 on a log-log plot of t* versus y_{ox}^{∞}, which is in good agreement with some experiments[7]. With more stringent ignition criteria $t^* \sim (y_{ox}^{\infty})^{-2}$ or stronger is found theoretically as well as in experiments[1]. The theory indicates that a sensitive equipment, detecting ignition, should indicate a behaviour similar to short time criteria. Theoretical plots similar to experimental oscilloscope traces reveal that a criterion similar to experimental criteria of ignition can explain the strong sensitivity of ignition behaviour upon the initial oxidizer mole fraction and the diversity of experimental results. A weaker dependence of ignition upon the external oxidizer should be observed for propellants with finely ground oxidizer particles. This is because the heterogeneity of the propellant decreases as the particle size is decreased, and faster mixing is achieved in the radial direction.

In the limiting case where the particle size is extremely small the system should behave like a homogeneous system. (This can also be explained by the fact that the diffusion mixing time in the radial direction is proportional to the square of the particle size and consequently a reduction in the particle size by 50% reduces the diffusional mixing time by a factor of 3 thus making the system more homogeneous). The present model also exhibits a strong dependence of ignition times upon external total pressure which is in good agreement with the experimental results under shock tube conditions. On the basis of the present investigations, it can therefore be concluded that ignition of composite and homogeneous propellants under shock tube conditions can be explained by pure gas phase mechanisms, employing light emission criteria.

8.3 Comparison Between Homogeneous and Heterogeneous Propellant Ignition:

It has been found from the present investigations that under similar conditions both homogeneous and heterogeneous propellants behave similarly. In the case of a homogeneous propellant one can speak of two distinct reaction zones, primary and secondary reaction zones, whereas in the case of the heterogeneous propellants, theoretically speaking, the concept of distinct reaction zones is not valid. For similar kinetic and physical properties, emission from a homogeneous propellant is more intense than from a heterogeneous pro-

pellant. This is because the temperature at any section of the gas phase is uniform for a homogeneous propellant and the temperature varies radially for a heterogeneous propellant with low temperatures near the oxidizer rich regions. For some sensitive photo detector read-outs, heterogeneous propellants exhibit stronger sensitivity for external oxidizer than do homogeneous propellants, providing the oxidizer particle size is large. This situation disappears as the particle size decreases.

Ignition Behaviour of a Low Oxidant Propellant:

It is obvious from what has been said so far that a propellant containing more than 50% oxidizer by weight attains steady burning conditions after the ignition transients are over. A propellant with less than 20% oxidizer behaves like a pure fuel. Therefore it can be expected that a propellant containing oxidizer between 20 and 50%, should behave like a pure fuel at low initial oxidizer mole fractions and like a propellant at high initial oxidizer mole fractions. This effect is observable if the decomposition rates of oxidizer and fuel are assumed to be different.

Figure (31) shows a lot t* plotted against log y^{∞}_{ox} for a propellant containing 50% oxidizer and 35% oxidizer respectively. The particle size (i.e. diameter of oxidizer cyrstals) is 50 to 60% microns. A two dimensional model was used to compute the ignition data. It was assumed in the numerical computations that the activation energy of pyrolysis of the oxidizer particles is twice that of fuel and both fuel and oxidizer have equal decomposition a rates at $400^{o}K$. As can be seen from the figure; increasing the content of oxidizer in the propellant only slightly increases the ignition delay at high initial oxidizer mole fractions. For an α of 0.5 as y^{∞}_{ox} is decreased, the $t^* - y^{\infty}_{ox}$ curves bends over and at very low y^{∞}_{ox} values, ignition delay is initially independent of y^{∞}_{ox}. For $\alpha < 0.3$ it has been found that ignition delay steadily increases as y^{∞}_{ox} is decreased. At $\alpha < 0.35$, there is a bend over or independency of t* on y^{∞}_{ox} over a short range of y^{∞}_{ox} values and for sufficiently low values of y^{∞}_{ox}. The bend over is expected to occur at higher values of y^{∞}_{ox} for a stronger emission criterion, $J^* > 0.005$. However, computational times are already very large and to attain J* values of 0.05 or 0.1 may take computational times on the order of an hour or so.

A behaviour similar to the above has been found during shock tube ignition of composite propellant[16]. Thus it can be said that a two-dimensional gas phase model described in the present situation can explain a variety of shock tube ignition data presented by McAlevy & Summerfield[1], and Kashiwagi[16].

CHAPTER IX

RADIANT IGNITION OF HOMOGENEOUS SOLID PROPELLANTS

9.1 Introduction:

Arc image or radiant ignition of solid propellants has become a wide spread practice for screening propellants according to their ignitability. However, the validity of application of such data to the ignition of propellants in practical rockets is questionable. In fact, there is as much justification for the application of shock tube experimental data to the operational motor systems as there is for the application of arc image experimental data. Even though direct application of arc image or shock tube ignition data for propellants igniting in practical rocket motors is not possible, still, some understanding of the ignition behaviour of propellants is achieved by these experiments.

The importance or significance of experimental data often times cannot be appreciated or properly utilized without an adequate theoretical model. Based on certain experimental observations, generally, a simple theoretical model is proposed and the predictions of the theoretical model are compared with experimental observations. Any discrepancy is then corrected by refining the original model or by proposing a new model. This has been the situation in the theoretical studies on ignition of solid propellants.

As already mentioned in Chapter I, theoretical studies on the ignition of solid propellants subjected to radiant heating were initiated by Hicks. His original theoretical model remained untouched for quite some time, till the development of composite propellants. Somehow, the predictions of Hicks model did not agree with the ignition behaviour of composite propellants. Many experiments on composite propellants indicated that the original hypothesis of Hicks -- that ignition was caused by solid phase reactions -- was not correct. This led to the emergence of gas phase and heterogeneous ignition models. Definitive arguments and proof, for or against either of the new theories, is beyond the scope of present work. It is assumed here that ignition in arc image experiment is due to gas phase processes; the purpose is to provide information on just what kind of ignition behaviour might be expected if, indeed, the ignition process in a real propellant were entirely due to gas phase reactions.

The gas phase ignition model developed by McAlevy and Summerfield to describe the ignition behaviour under shock tube conditions was applied successfully by Shannon and Deverall[17] to study the ignition behaviour of solids igniting in an arc image furnace. A similar model, with some refinement, was later on developed by Ohlemiller and Summerfield[18]. Both these models showed considerable qualitative agreement with experimental observations. Discussion of Ohlemiller's model is only qualitative and exact solutions, either analytical or numerical, have not been presented as yet. The object of the present investigation is to refine the model of Ohlemiller to take into consideration the effect of absorption of radiant energy by gas phase reactants and products and make the model describe the ignition of propellants, in general, rather than pure fuels only.

No orginality is involved in the derivation of the equations and therefore only their final form is presented here. Employing the assumptions listed in Chapter II, the equations of conservation of species are written

as follows:

SOLID

$$\frac{\partial \theta_s}{\partial \tau} + \frac{\mu\omega}{\Sigma^{1/2}} \frac{\partial \theta_s}{\partial \xi_s} = \frac{\partial^2 \theta_s}{\partial \xi_s^2} - \Gamma_1 \exp\left(-\frac{1}{\theta_s}\right) + \Gamma_2 \exp(-\Delta \cdot \xi_s) \quad 9.1$$

GAS

$$H(\eta_f) = \frac{1}{n} H(\eta_{ox}) = -\frac{1}{A} H(\theta) = -\eta_f \eta_{ox} \exp\left(-\frac{1}{\theta}\right) \quad 9.2$$

$$H(\eta_i) = 0 \quad 9.3$$

Subject to the boundary conditions

$$\theta(\xi,0) = \theta(\infty,\tau) = \theta_0 \qquad \eta_f(0,\tau) - \omega^{-1} \frac{\partial \eta_f(0,\tau)}{\partial \xi} = -nb\alpha$$

$$\eta_f(\xi,0) = \eta_f(\infty,\tau) = 0 \qquad \eta_{ox}(0,\tau) - \omega^{-1} \frac{\partial \eta_{ox}(0,\tau)}{\partial \xi} = (1-\alpha)b$$

$$\eta_{ox}(\xi,0) = \eta_{ox}(\infty,\tau) = \eta_{ox}^{\infty} \qquad \eta_i(0,\tau) - \omega^{-1} \frac{\partial \eta_i(0,\tau)}{\partial \xi} = 0$$

$$\eta_i(\xi,0) = \eta_i(\infty,\tau) = \eta_i^{\infty} \qquad \theta_s(0,\tau) = \theta(0,\tau) \quad 9.4$$

$$\theta_s(\xi_s,0) = \theta_s(-\infty,\tau) = \theta_{s,0} \qquad \frac{\partial \theta_s}{\partial \xi_s} = \frac{\Lambda}{\Sigma^{1/2}} \frac{\partial \theta}{\partial \xi}$$

where: $$H \equiv \frac{\partial}{\partial \tau} + \omega \frac{\partial}{\partial \xi} - \frac{\partial^2}{\partial \xi^2}$$

The in-depth pyrolysis is given by:

$$m_f = \int_{-\infty}^{0} \Sigma^{\frac{1}{2}} \rho_g^2 D \left(\frac{Z_s}{m_0}\right) \frac{1}{\mu} \exp\left(-\frac{1}{\theta_s}\right) d\xi_s$$

In the above treatment, photomeric dissociation of the propellant is not considered. All the dimensionless groups are defined as in Chapter II. Γ_1 and Γ_2 and Δ are constants with

$$\Gamma_1 = \frac{R}{E}\left(\frac{\rho_g^2 D}{m_0^2}\right)\left(\frac{Q_h Z_s}{c\rho_s}\right), \quad \Gamma_2 = \frac{R}{E}\left(\frac{\rho_g^2 D}{m_0^2}\right)\left(\frac{\beta \bar{Q}}{\rho_s c}\right)$$

and

$$\Delta = \beta \rho_g D / m_0$$

respectively. $\bar{Q}$ is the flux incident on the propellant surface and is related to the source flux as

$$\bar{Q} = Q_0 \exp\left(-\rho_g k_v x_m\right)$$

where x_m is the mean distance in the gas phase containing fuel species through

which the radiation passes before impinging on the propellant surface. It is approximated as

$$x_m = \int_0^\infty y_f \, dx \,/\, y_{fw}$$

where y_{fw} is the wall fuel mole fraction. Radiation passes entirely through oxygen and nitrogen. At later stages, when significant amount of products are formed, the absorption by products should also be considered. However, during radiant ignition negligible amount of products are formed till the fuel is ignited. Also, it is generally assumed that $\rho_g K_\nu$ remains constant with respect to pressure. At constant pressure this is the grey body assumption.

Since, during arc image experiments, the only source of heat supply to the gas phase is the propellant surface upon which the radiant energy is incident, the assumption that exothermic chemical reactions are nearly absent till ignition occurs appears to be quite valid. However, at extremely high rates of energy supply to the grey propellant surface, the surface temperature attains a sufficiently high value very rapidly; hence the chemical-diffusion time, t_{cd}, comprises the major portion of the delay period. One can rest assured that such a situation will not exist until the flux level reaches several hundred calories/cm^2-sec., when the propellant is not truly opaque and energy is absorbed in depth. In reference (18) it is shown that:

$$t_{ign} \simeq t_{cd} \quad \text{for large } Q_o$$

$$t_{ign} \simeq \frac{1}{\beta}\left[\frac{\rho_s c \Delta T^*}{Q_o(1-r)}\right] \quad \text{for moderately high } Q_o$$

and

$$t_{ign} \simeq \frac{\pi}{4}\lambda_s \left[\frac{\rho_s c \Delta T^*}{Q_o(1-r)}\right]^2 \quad \text{for low } Q_o$$

where $Q_o(1-r)$ is that portion of the incident flux which is absorbed by the propellant and ΔT^* is the characteristic temperature rise at the propellant surface at the instant of ignition. In the general case, the ignition time is a combination of these and hence

$$t_{ign} \simeq t_{cd} + \frac{1}{\beta}\left[\frac{\rho_s c \Delta T^*}{Q_o(1-r)}\right] + \frac{\pi}{4}\lambda_s \left[\frac{\rho_s c \Delta T^*}{Q_o(1-r)}\right]^2 \qquad \cdots 9.7$$

which has shown by Ohlemiller to be in agreement with experimental results. Present numerical calculations show that even for Q_o of 100 cal/cm^2-sec., $t_{cd} \ll t_{ign}$ based on $\theta^* = 1.5\theta_o$ or emission or $\Delta\theta^* =$ constant, criterion, unless a very low value of $\Delta\theta^*$ is assumed. A detailed discussion of the numerical results is presented in the following section.

9.2 Discussion of Results:

In the solution of differential equations 9.1 to 9.5 it was assumed that the incident flux is monochromatic in nature. This considerably simplifies the problem of selective absorption of radiation by the propellant. Such a situation practically exists in ignition experiments using laser beams. Since the gas phase reactions are almost negligible up to ignition, there is a tremendous build up of reactant concentration and once the exothermic reactions are triggered, an enormous amount of energy is released in the gas phase almost instantaneously. Chemical-diffusional times are extremely short compared to

the overall ignition time. For example, in a typical case, the chemical delay time is on the order of a millisecond whereas the total delay period is on the order of 200 milliseconds. Hence the ignition criterion based on a certain surface temperature rise seems to be quite realistic. Only at extremely high rates of heating, does the system of gas phase equations really need to be considered. At high heating rates, the ignition behaviour under arc image furnace conditions should be very much similar to shock tube ignition data.

At very low heating rates ($Q_o \approx 5$ to 10 cal/cm^{2}sec), conduction in the solid becomes an important factor and again conventional methods can be employed to predict the ignition behaviour. All in all, it appears that although gas phase reactions play an important role in establishing a gas phase flame, as far as the ignition behaviour is concerned, gas phase processes can be considered secondary. Pressure seems to have little effect on ignition behaviour except at sub-atompsheric or atmospheric pressures. For example, reference to Figures (32), (33) and (34) reveal that above 25 atmospheres, the effect of any further increase in the gas pressure has virtually no effect on ignition delay.

It is interesting to note that the exact numerical calculations of the present investigations are in excellent agreement with the calculations performed in reference (18) using approximate methods. It was also found that at low or moderately high heating rates and/or at low pressures, the effect of initial gas phase oxidizer mole fraction had no effect on the ignition behaviours. However, this may not be the case at extremely high heating rates.

The effect of absorption of radiation of the gas phase media upon the ignition behaviour is very little. This is understandable because radiation passess through the gaseous medium virtually unabsorbed, except at very short wave lengths. Even a grey gas absorbs very little radiation in the visable and infrared regions unless it passes through an extremely dense medium or the radiation has to be passed through an extremely thick region.

In the present calculations, reflection of the radiation from the propellant surface is not considered. Since the reflection of radiation from the propellant surface depends entirely upon the surface roughness, opacity etc., the effect of considering the reflectivity (r) is equivalent to considering an incident effective flux equal to $Q_o(1-r)$.

9.3 Conclusions:

The present investigations has revealed that in sofar as slow ignition is considered, like ignition in arc image furnaces, the simple theory based on conduction and absorption of energy in solid phase, neglecting the gas phase, can be used to predict the ignition behaviour of solid propellants at high and moderate pressures. Only at very low pressures -- in fact, sub-atmospheric pressures -- when chemical-diffusion reaction times become very large, does the overall ignition time depend strongly upon phase chemical kinetics.

9.4 Suggestions for Future Work:

The gas phase theory of ignition treated so far can successfully explain several aspects of propellant ignition found during experiments. It is necessary for successful application of the present theory that more precise experiments be performed. Without sensitive experiments, it is less meaningful to develop a mole precise theoretical model. As said in previous chapters, strong emission

may be occurring close to the establishment of steady state. To detect light emission in early stages, it is advisible to employ a photo-multiplyer which is extremely sensitive.

Further improvement in the theory can be brought about by considering small spherical oxidizer crystals embeded in fuel matrix and writing the appropriate differential equations and boundary conditions. This represents a mole realistic composite propellant model.

It is also of interest to consider theoretically the ignition of a heterogeneous propellant model by radiant energy. These combined with sensitive experimental should hopefully lead to a better understanding of the ignition behaviour of solid propellants.

REFERENCES:

1. McAlevy, R.F., III, Cowan, P.L. and Summerfield, M., "The Mechanism of Ignition of Composite Solid Propellants", Solid Propellant Rocket Research, Vol. 1 of ARS series on Progress in Astronautics and Rocketry, Academic Press, 1960, pp. 623, also McAlevy, R.F., Department of Aeronautical Engineering Laboratory Report No. 557, Princeton University, June 1961.

2. Anderson, R., Brown, R.S., Thompson, G.T. and Ebelling, R.H., Theory of Hypergolic Ignition of Solid Propellants", AIAA. Preprint 63-514 (Dec. '63).

3. Hermance, C.E., Shinner, R. and Summerfield, M., "Ignition of an Evaporating Fuel in a Hot Oxidizing Gas, including the Effect of Heat Feed Back", ASTRO ACTA 12, 2, 95-112 (1966), see also Hermance, C.E., Aerospace and Mechanical Sciences, Report No. 752, Princeton University, February 1966.

4. Hermance, C.E. and R.K. Kumar, "Gas Phase Ignition of a Solid Fuel Containing an Oxidizer", AIAA Paper 68-496, presented at ICRPG/AIAA 3rd Solid Propulsion Conference, Atlantic City, N.J., June 4-6, 1968.

5. Kumar, R.K., "Ignition of a Solid Propellant in a Hot Oxidizing Atmosphere", M.A.Sc. Thesis, Department of Mechanical Engineering, University of Waterloo, May 1968.

6. Waldman, C.H., Cheng, S.I., Sirignano, W.A. and Summerfield, M., "Theoretical Studies of Diffusion Flame Structures", AMS Report No. 860, Department of Aerospace and Mechanical Sciences, Princeton University, Princeton, N.J.

7. Kurylko, L. "Progress Report of Research on Solid Propellant Ignition", AMS Report No. 770, Princeton University, N.J. 1966.

8. Kumar, R.K. "Ignition of Homogeneous and Heterogeneous Solid Propellants Under Shock Tube Conditions", Ph.D Thesis, Department of Mechanical Engineering, University of Waterloo, 1971.

9. Herzberg, G., Spectra of Diatomic Molecules, Second Edition, Van Nostrand Co. Inc., Princeton, N.J.

10. Pearse and Gaydon, The Identification of Molecular Spectra, Chapman and Hall Co., London, England.

11. RCA Technical Manual PT-60, Phototubes and Photo-cell, RCA Victor Co. Ltd., Electron Tube Division, Montreal, P.Q. (1963)

12. Filters for Scientific and Technical Use, Eastman Kodak Co., 22nd Edition.

13. Saul'yev, V.K., "Integration of Equations of Parabolic Type by the Method of Nets", International series of monographs of pure and applied mathematics, Vol. 41, Pergamon Press.

14. Summerfield, M. and Kashiwagi, T., supplied "Experimental Oscilloscope Traces", Department of Aerospace and Mechanical Sciences, Princeton University, Princeton, N.J.

15. Summerfield, M. and Krier, P., Research presentation given at Air Force Office of Scientific Research, Combustion Dynamics Contractors' Meeting, Denver, Colorado, July 1969.

16. Kashiwagi, T., McDonald, B.W., Isota, H., Summerfield, M. "Ignition of Polymeric Fuels by Hot Oxidizing Gases", AFOSR Scientific Report AFOSR-70-2935, Department of Aerospace and Mechanical Sciences, Princeton University, Princeton, N.J.

17. Shannon, L.J. and Deverall, L.I., "A Model of Solid Propellant Ignition in a Neutral Environment", pp. 497, AIAA Journal, March 1969.

18. Summerfield, M. and Ohlemiller, T.J., "A Critical Analysis of Arc Image Ignition of Solid Propellants", Air Force Scientific Report No. 67-1534, Department of Aerospace and Mechanical Sciences, Princeton University, Princeton, N.J.

19. Hermance, C.E., "Variable Density and the Theory of Gas Phase Ignition of Solids". To be published in Astronautica Acta.

20. Kumar, R.K. and Hermance, C.E., "Ignition of Homogeneous Solid Propellants Under Shock Tube Conditions : Further theoretical developments". AIAA 8th Aerospace Sciences Meeting, New York, Jan. 19-21, 1970; AIAA preprint No. 70-120; to be published in AIAA Journal.

TABLE 1

Curve No.	Description
1	Long time data, m_o = 0.05, 0.005 E/R = 12000, ε = 0.01
2	Long time data, m_o = 0.05, 0.005 E/R = 6000, ε = 0.01
3	Short time data, m_o = 0.005, E/R = 6000 [$L^*(\theta) = 1.5\theta_o$]
4	Short time data, m_o = 0.05, E/R = 6000 ($L^*(\theta) = 1.5\theta_o$)

TABLE 2(a)

CURVE DESCRIPTION FOR FIGURE

No.	Curve	Reference
1	ONERA 20% PBAA + 80% NH_4ClO_4	6
2	McAlevy (Double base)	14
3	McAlvey (22.5% Polyester + 77.5% NH_4ClO_4)	6
4	Emission Criterion, $J^* = 0.1$	
5	'Long Time Criterion' (ε=0.01, note the values on the curve are to be multiplied by 10)	
6	Emission Criterion $J^* = 0.01$	

TABLE 2(b)

CURVE DESCRIPTION FOR FIGURE

No.	Curve	Reference
1	McAlevy (20% Epoxy -- 80% NH_4Clo_4)	6
2	'Light Emission Criterion' $J^* = 0.1$, $E/R = 12000^oK$	
3	Kurylko, L. (20% PBAA + 80% NH_4ClO_4	6
4	Cmission Criterion $J^* = 0.01$, $E/R = 6000^oK$	

TABLE 3

ASSUMED VALUES OF PHYSICAL PARAMETERS USED IN THEORETICAL CALCULATIONS

Quantity	Value
m_o, g/cm^2-sec at 400^oK	0.05 and 0.005
c_p, cal/g-^oK	0.3
λ_s, λ_g, cal/cm-sec-^oK	0.005
h_v, cal/gm	120
D, cm^2/sec	0.1
$T_{s,o}$, ^oK	300
T_o, ^oK	1800
$Q_1 = Q_2$, cal/mole	12000
D_p/R, ^oK	6000

Unless specified the gas density ρ_g is taken as 0.005 gm/cm^3.

TABLE 4

VALUES OF THE PHYSICAL PARAMETERS USED
IN RADIANT IGNITION CALCULATIONS

Quantity	Value
Q/Cp	$40{,}000^{\circ}K$
Zo	10^8 $cm^3/gm/sec.$
E_p, E_r	12000 cal/gm
α	0.5
Y_{ox}^{∞}	1.0
η	4.0
T_{∞}, $T_{-\infty}$	$300^{\circ}K$
M_o at $400^{\circ}K$	0.001 gm/cm^2-sec.
β	100/cm
K_{ν}	100

SCHEMATIC OF PHYSICAL MODEL

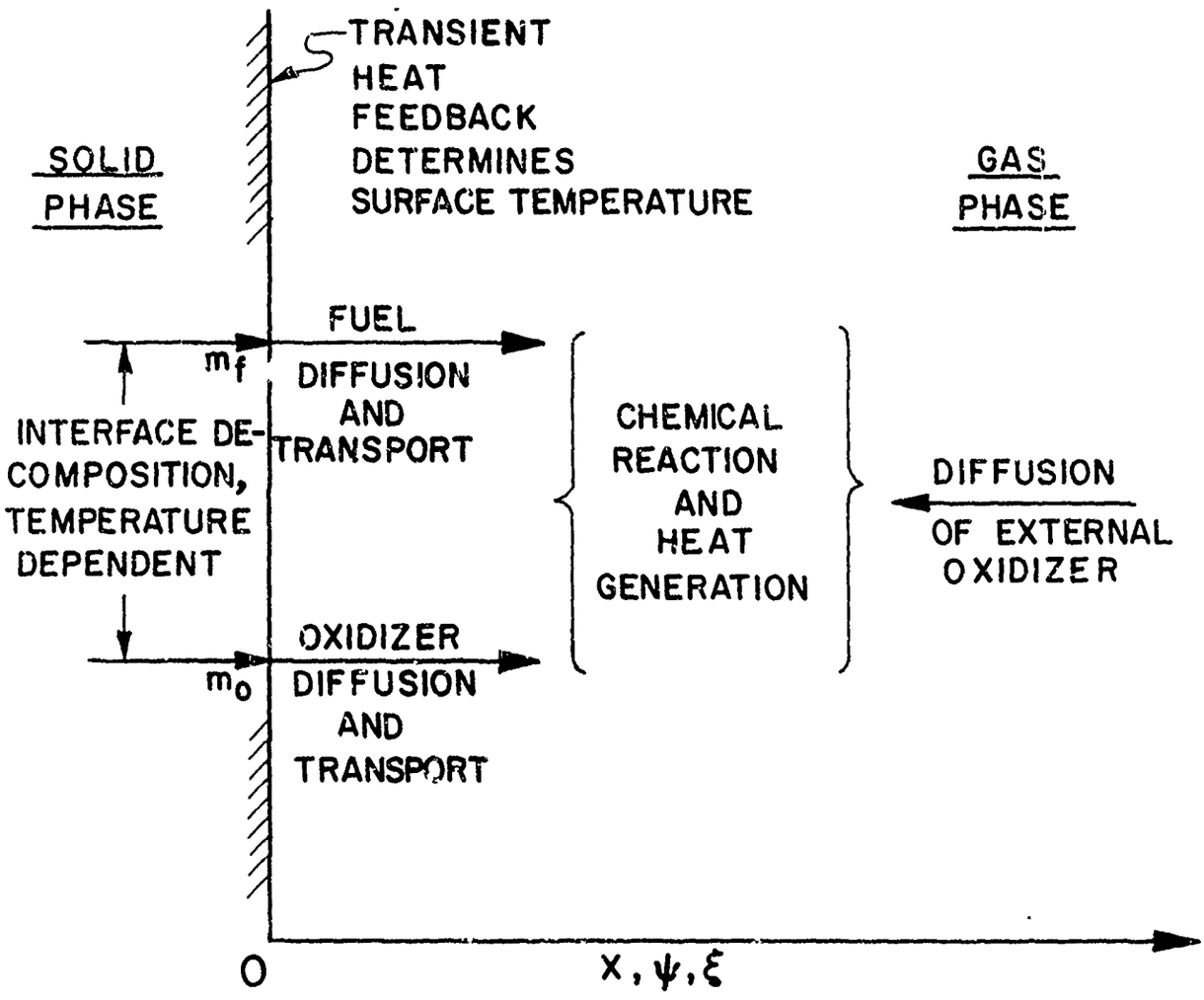

FIGURE 1

SKETCH OF NEAR STEADY STATE SPATIAL DISTRIBUTION OF FUEL, η_f , OXIDIZER, η_f, AND TEMPERATURE, θ, IN SECONDARY REACTION ZONE

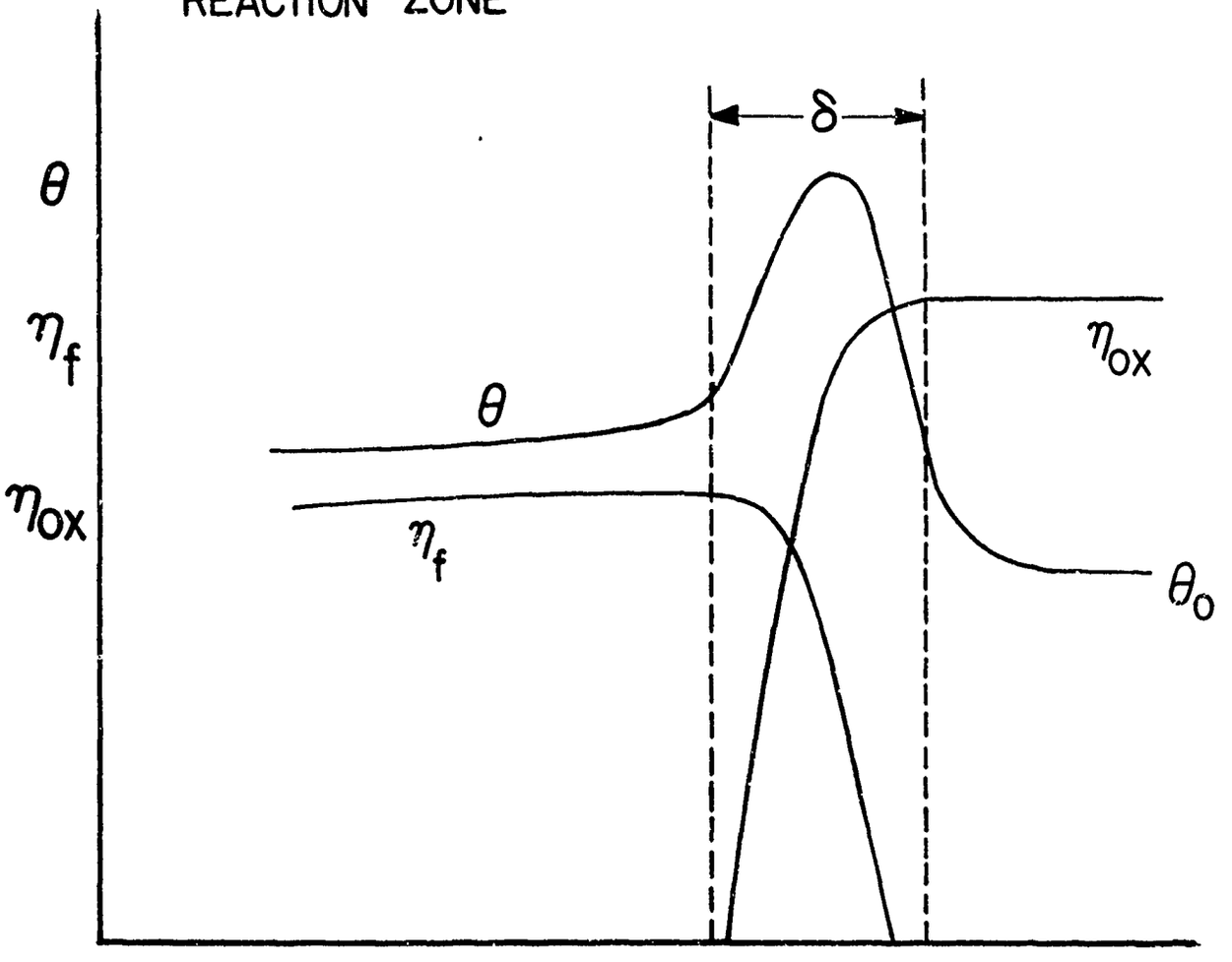

FIGURE 2

THE EFFECT OF FEEDBACK ON IGNITION AS THE MASS FLUX PARAMETER IS VARIED

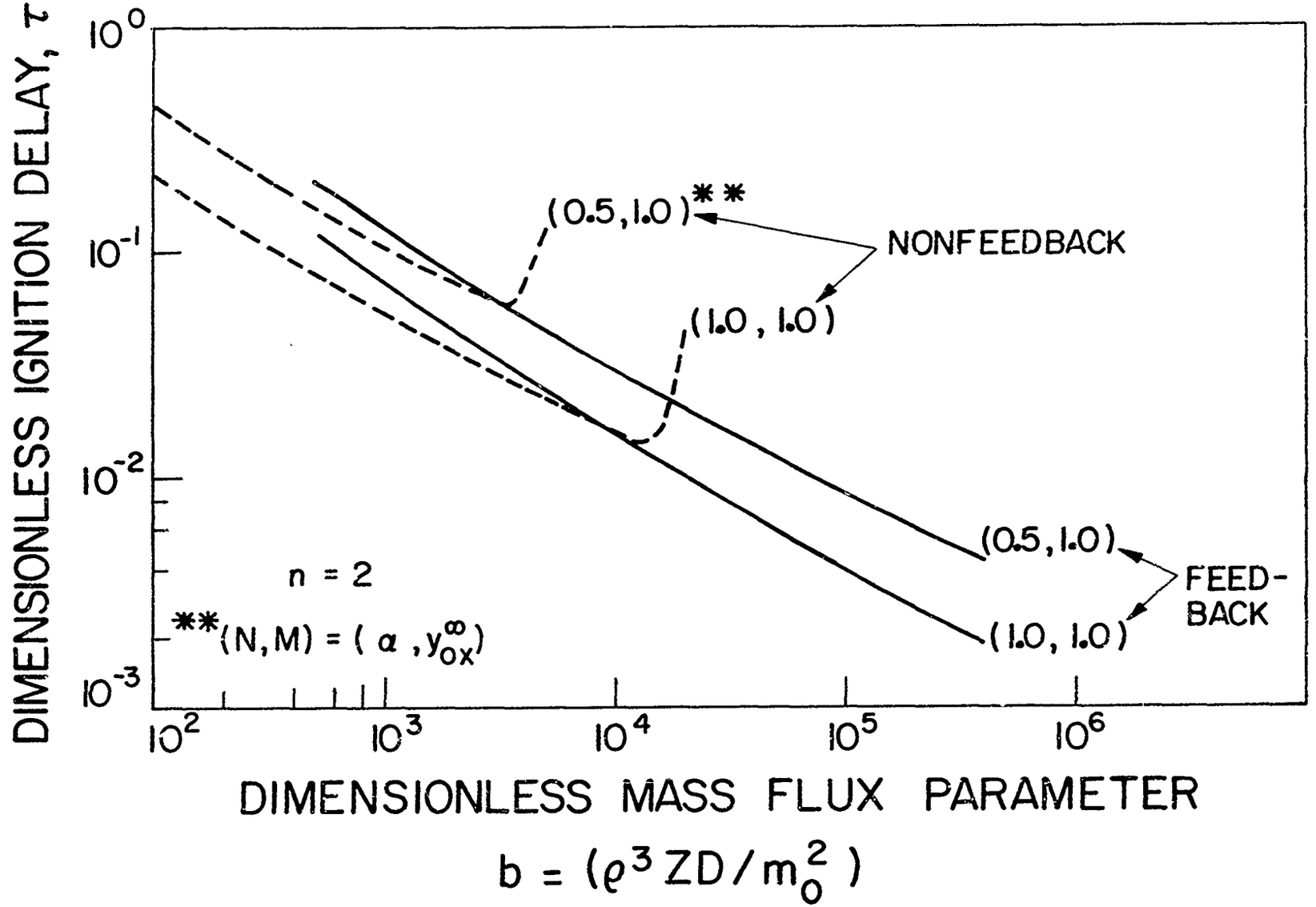

FIGURE 3

VARIATION OF DIMENSIONLESS IGNITION DELAY WITH DIMENSIONLESS MASS FLUX FOR VARIOUS PROPELLANT AND AMBIENT GAS PHASE COMPOSITIONS

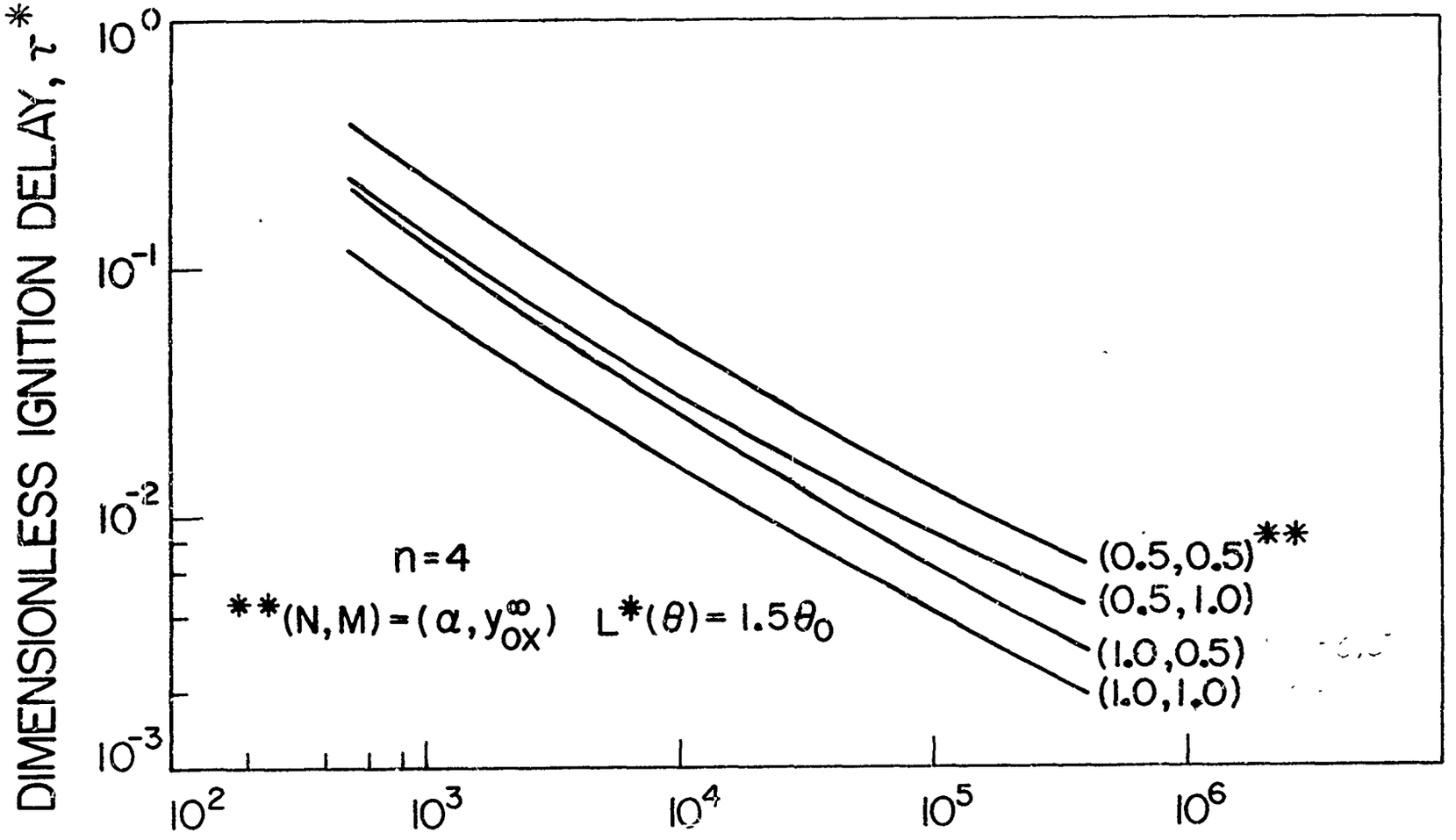

FIGURE 4

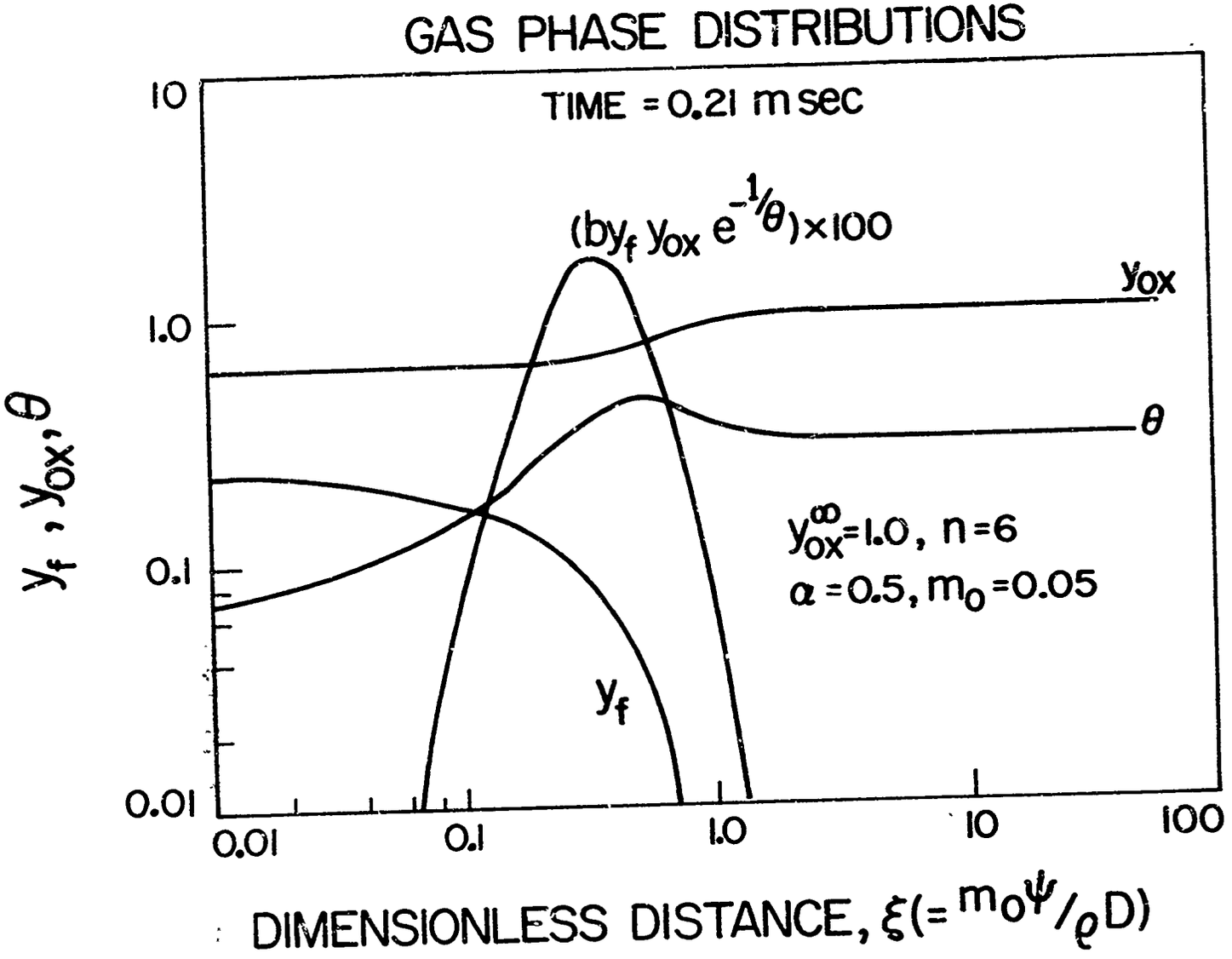
GAS PHASE DISTRIBUTIONS
TIME = 0.21 m sec
$(by_f\, y_{ox}\, e^{-1/\theta}) \times 100$
y_{ox}
θ
y_{ox}^{∞}=1.0, n=6
α =0.5, m_0 =0.05
y_f
y_f , y_{ox}, θ
10
1.0
0.1
0.01
0.01
0.1
1.0
10
100
DIMENSIONLESS DISTANCE, $\xi (= m_0 \psi / \rho D)$

FIGURE 6

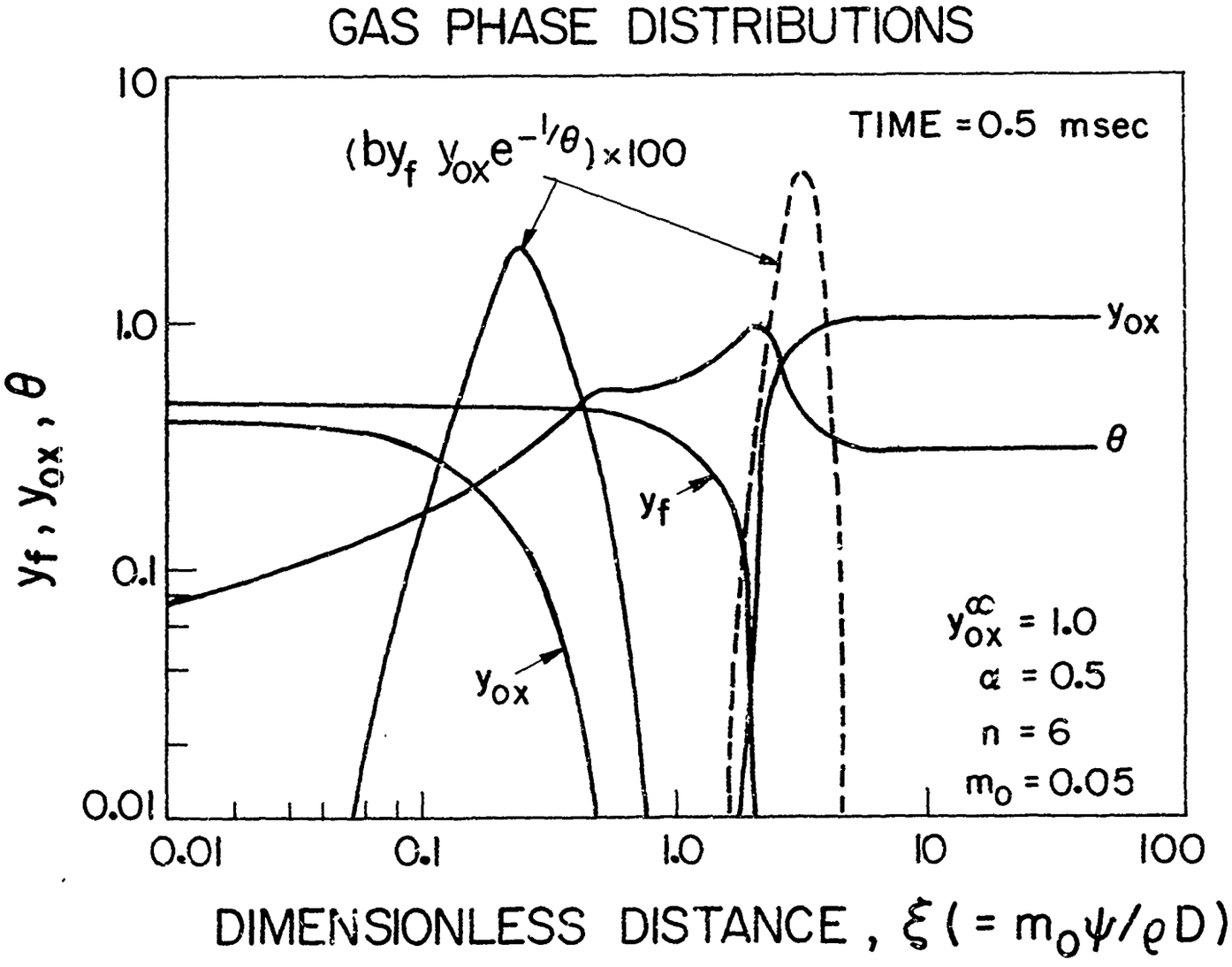
GAS PHASE DISTRIBUTIONS
TIME = 0.5 msec
$(by_f\ y_{ox}e^{-1/\theta})\times 100$
y_{ox}
θ
y_f
y_{ox}
$y_{ox}^{\infty} = 1.0$
$\alpha = 0.5$
$n = 6$
$m_0 = 0.05$
10
1.0
0.1
0.01
0.01
0.1
1.0
10
100
y_f, y_{ox}, θ
DIMENSIONLESS DISTANCE, $\xi\ (= m_0\psi/\rho D)$

FIGURE 7

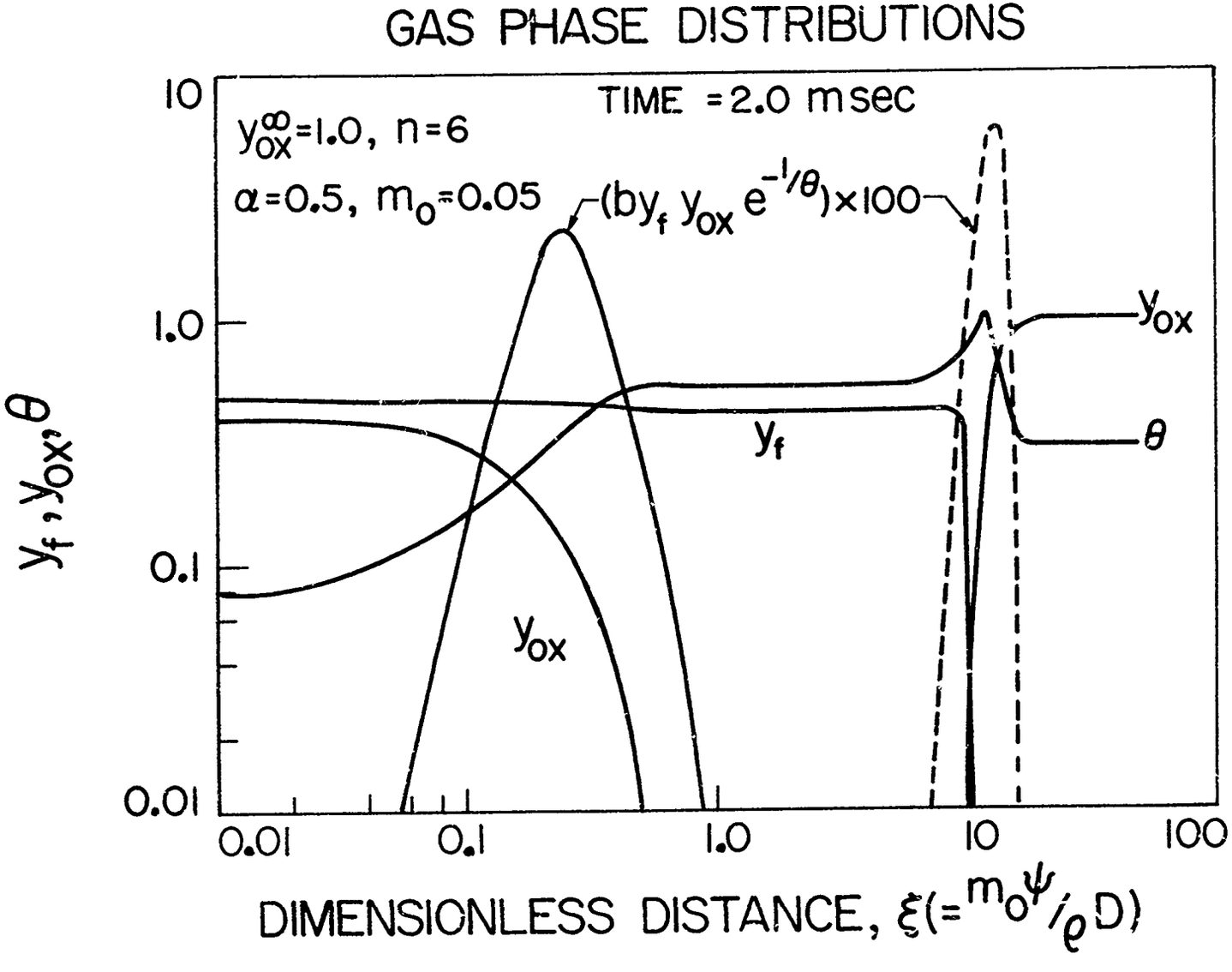
GAS PHASE DISTRIBUTIONS
TIME = 2.0 msec
y_{ox}^{∞}=1.0, n=6
α=0.5, m_0=0.05
$(by_f\, y_{ox}\, e^{-1/\theta})\times 100$
y_{ox}
y_f
θ
y_f, y_{ox}, θ
10
1.0
0.1
0.01
0.01
0.1
1.0
10
100
DIMENSIONLESS DISTANCE, $\xi(=m_0\psi/\rho D)$

FIGURE 8

EFFECT OF CHOICE OF IGNITION CRITERION UPON IGNITION DELAY

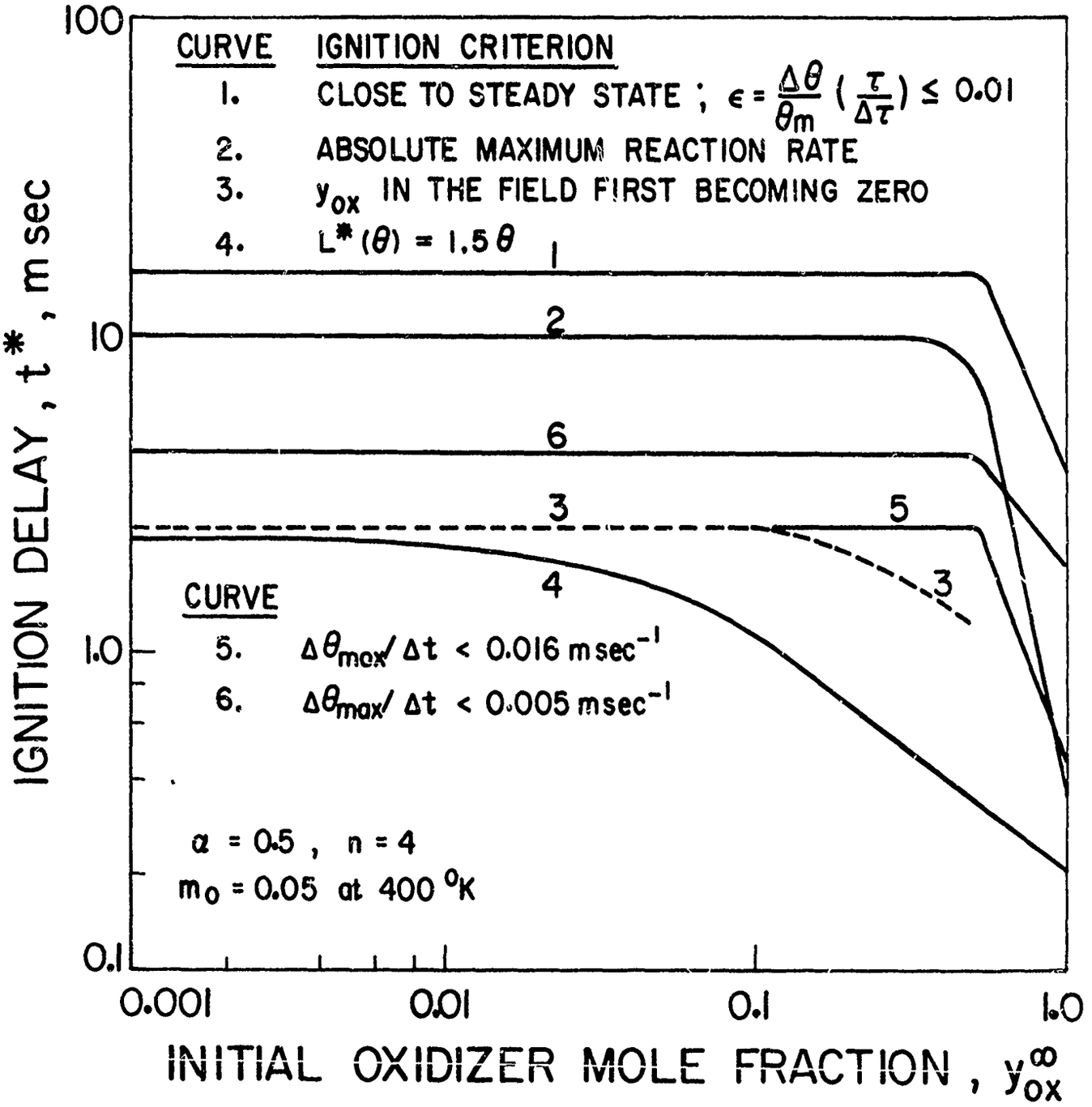

FIGURE 9

EFFECT OF INITIAL OXIDIZER MOLE FRACTION ON THE IGNITION DELAY PREDICTED BY THE FEEDBACK MODEL USING DIFFERENT IGNITION CRITERIA

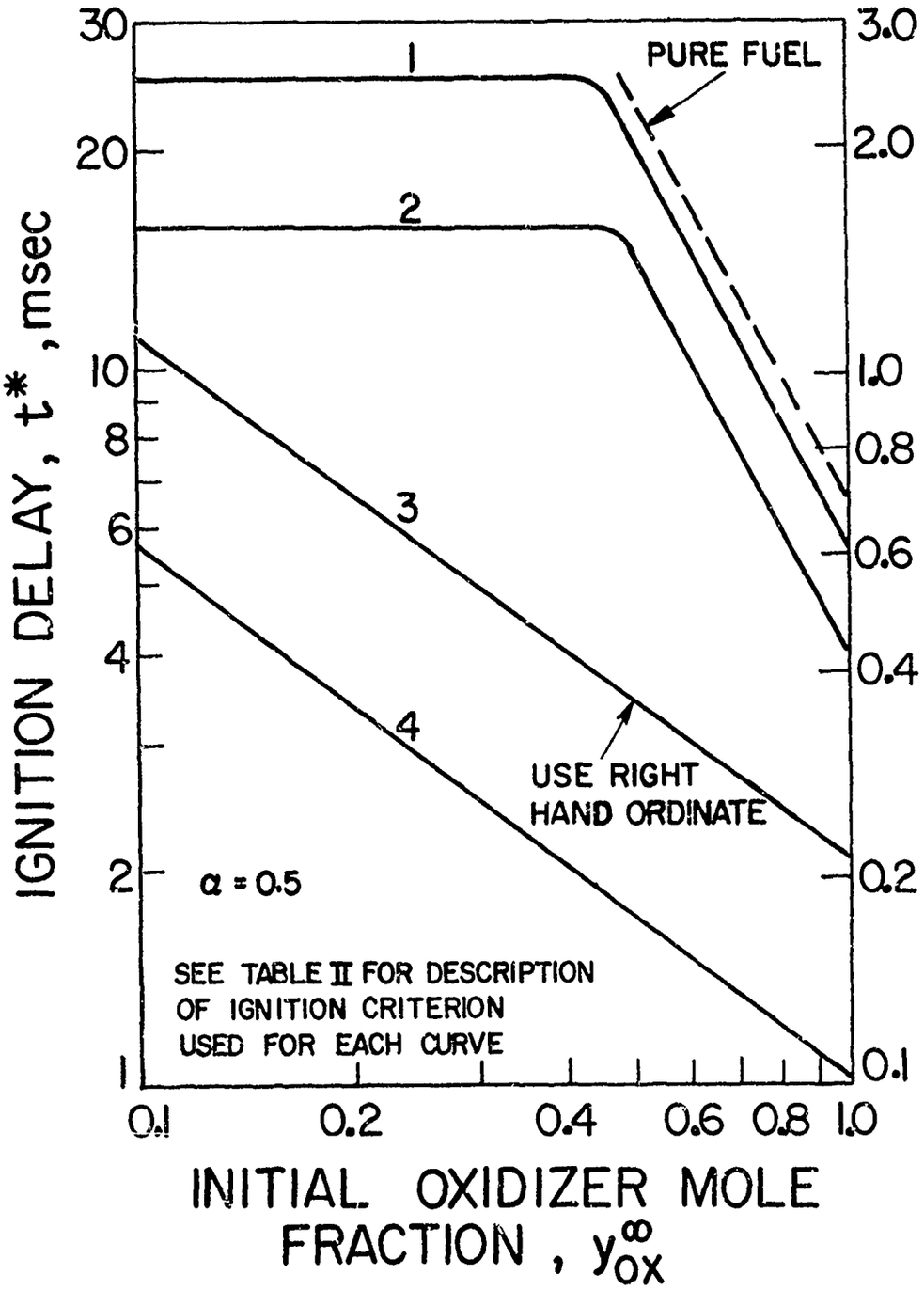

FIGURE 10

OPTICAL DETECTION SYSTEM

(From reference 1)

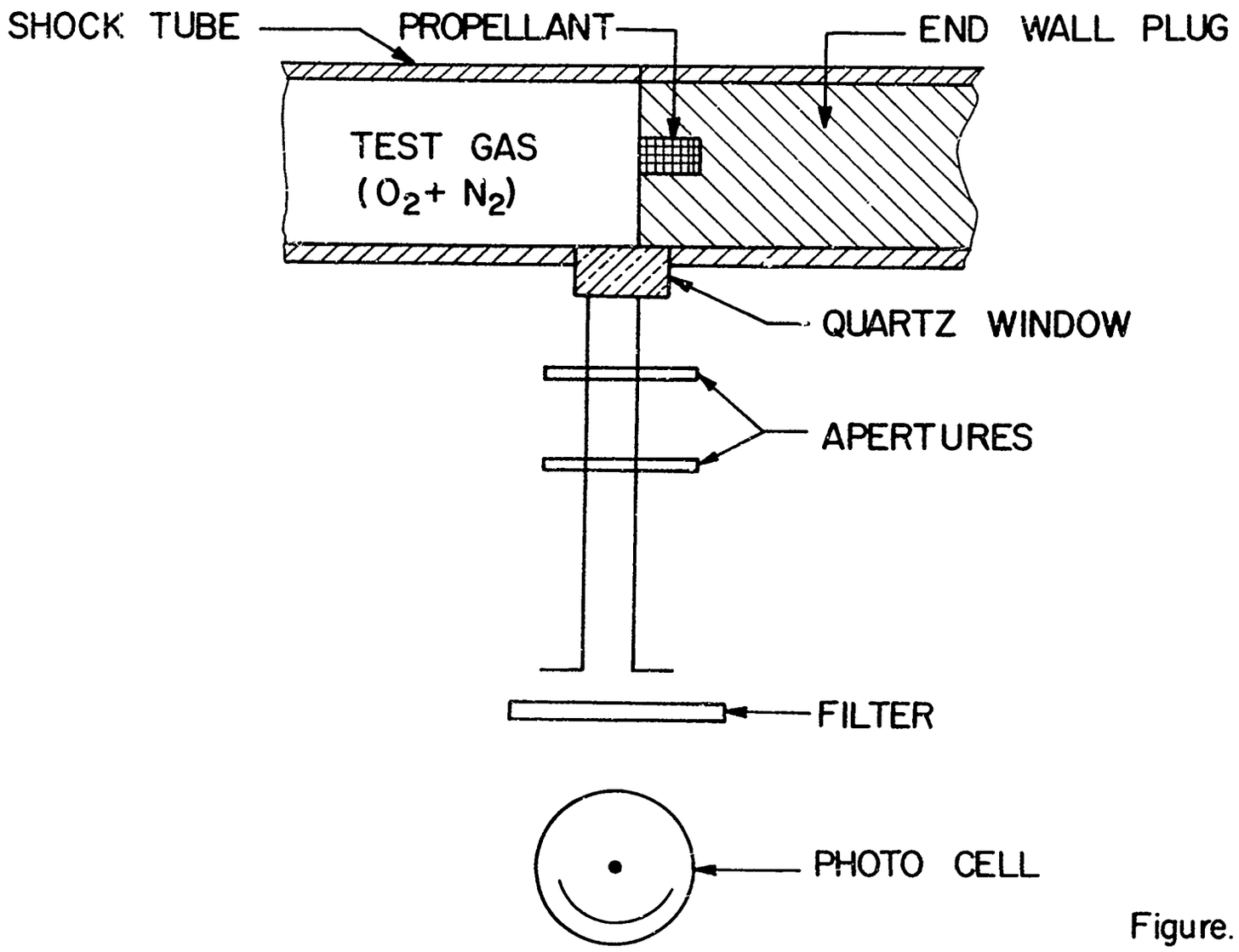

Figure. II

RELATIVE THEORETICAL RESPONSE, J, OF A LIGHT EMISSION DETECTOR VERSUS TIME.

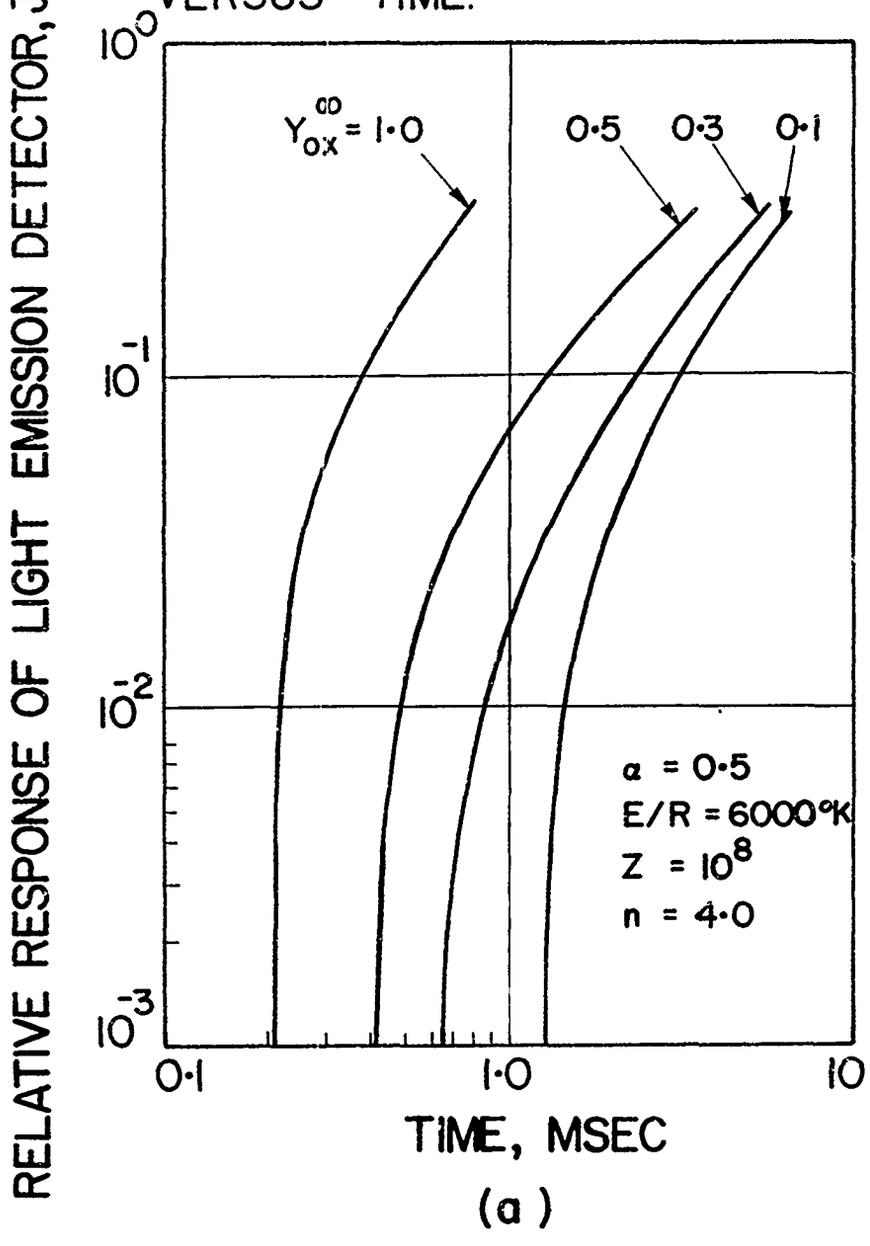

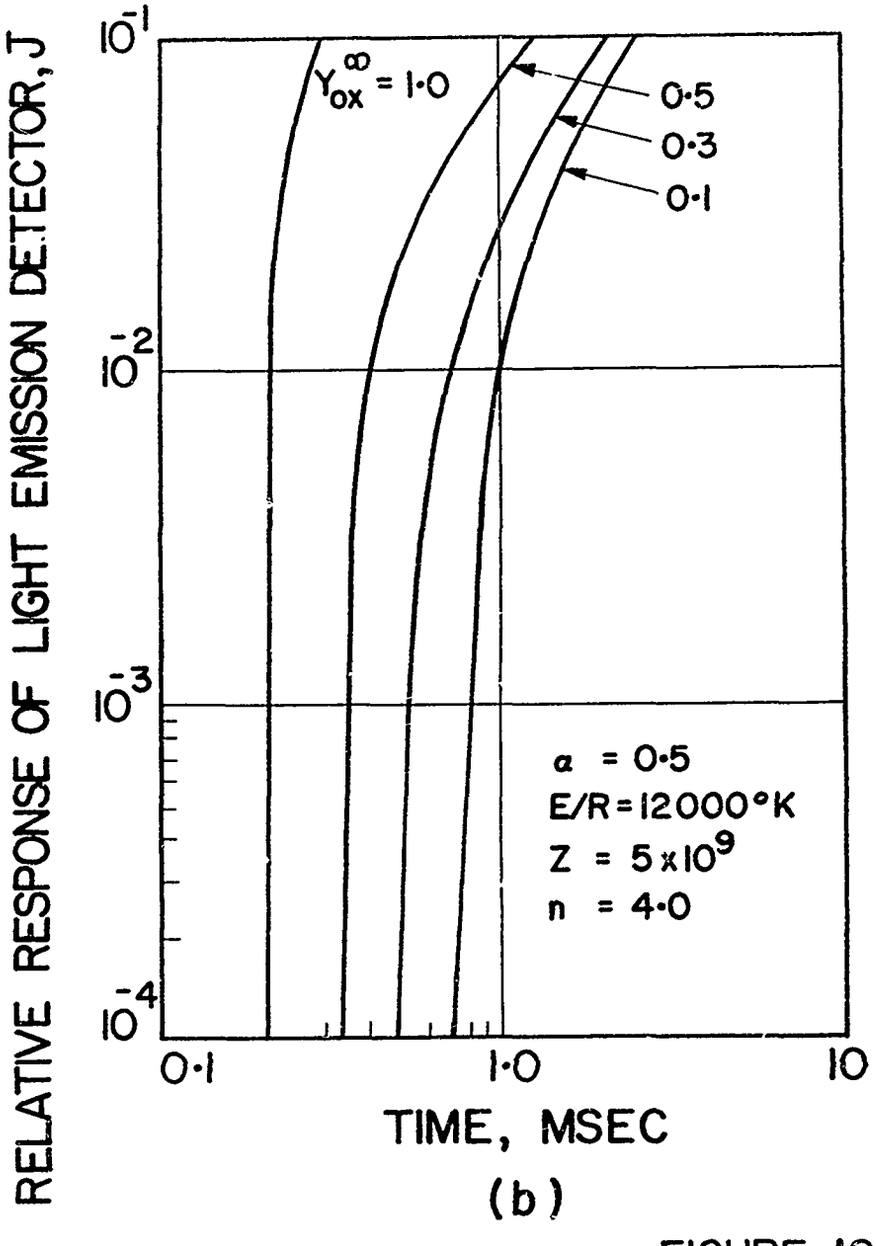

FIGURE 12

THEORETICAL AND EXPERIMENTAL CURVES OF THE RESPONSE OF A LIGHT EMISSION DETECTOR VERSUS TIME IN THE FORMAT OF EXPERIMENTAL DATA.

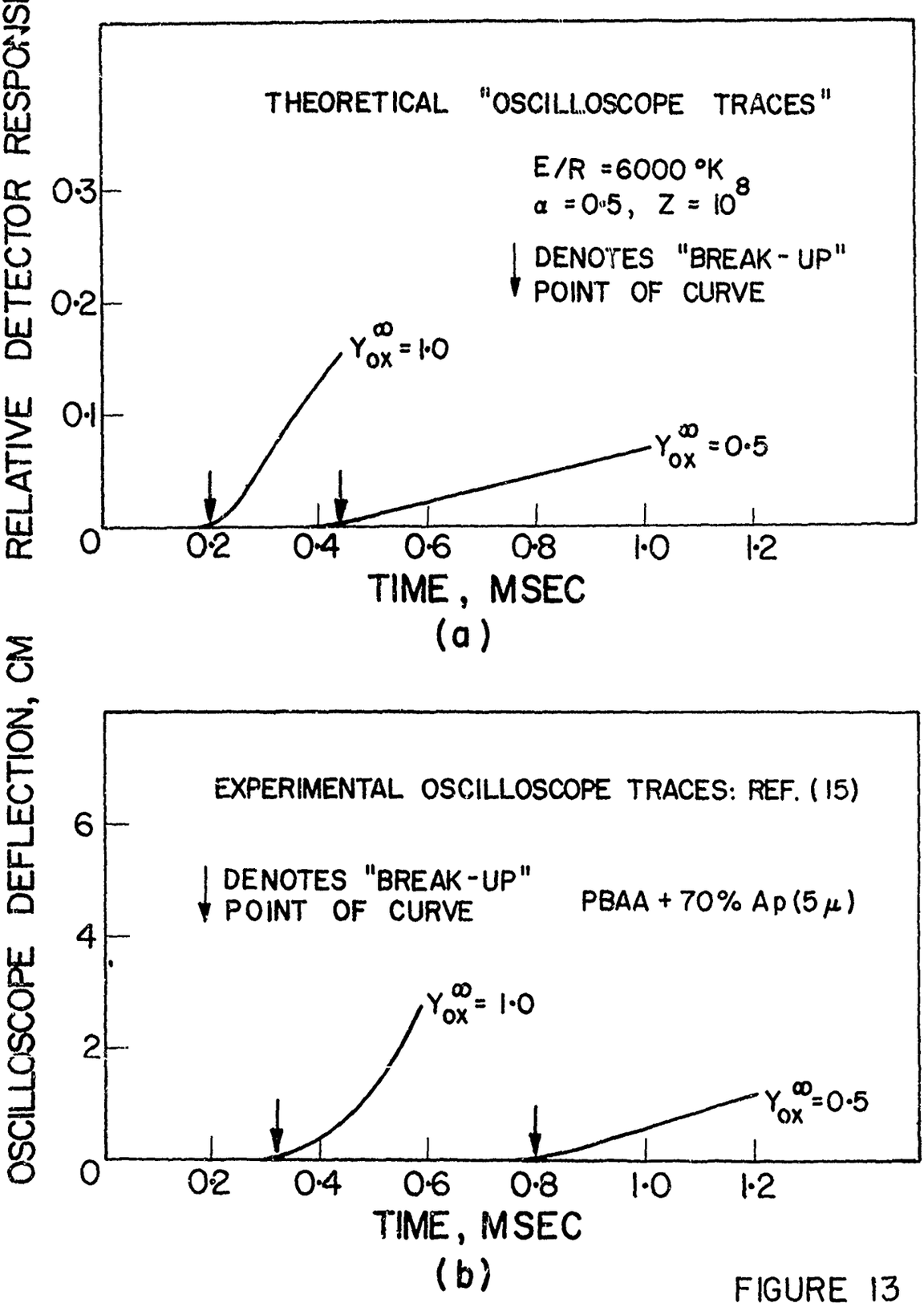

FIGURE 13

EFFECT OF INITIAL OXIDIZER MOLE FRACTION UPON IGNITION BEHAVIOUR WITH DIFFERENT LIGHT EMISSION IGNITION CRITERIA.

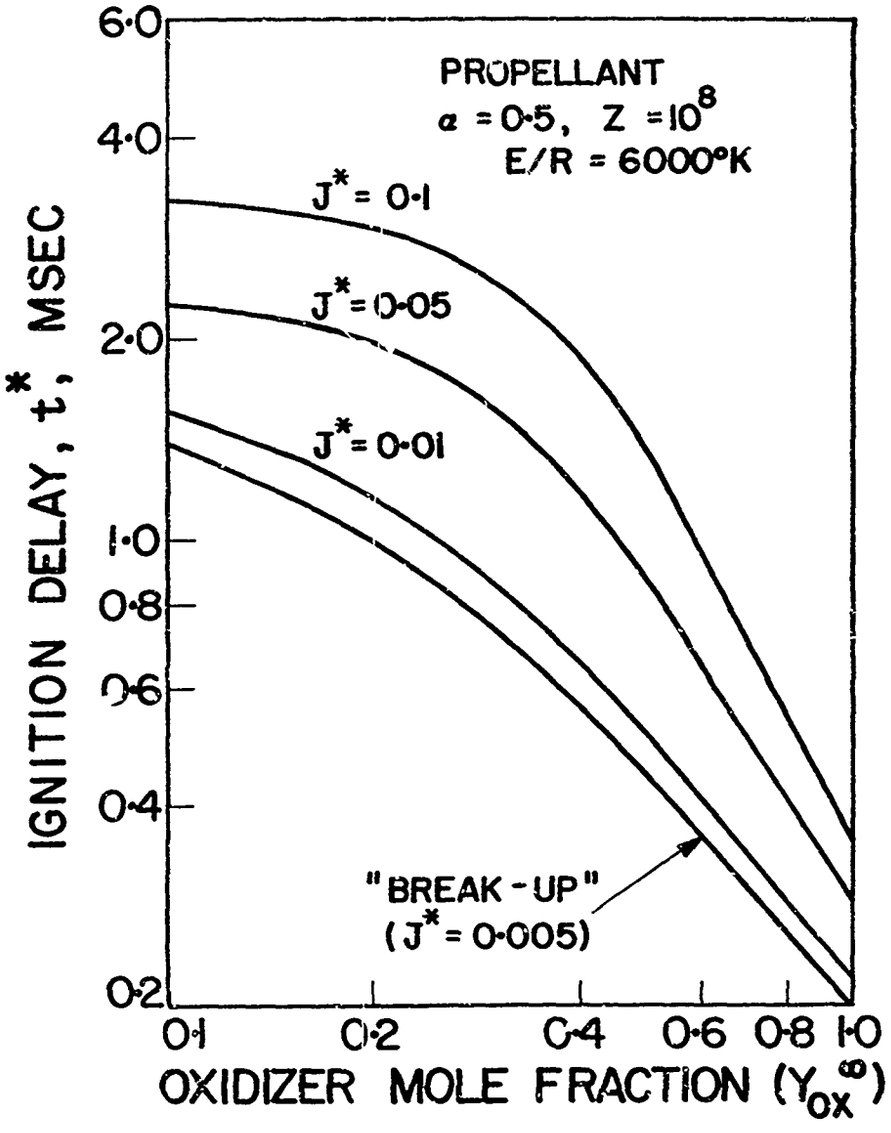

(a)

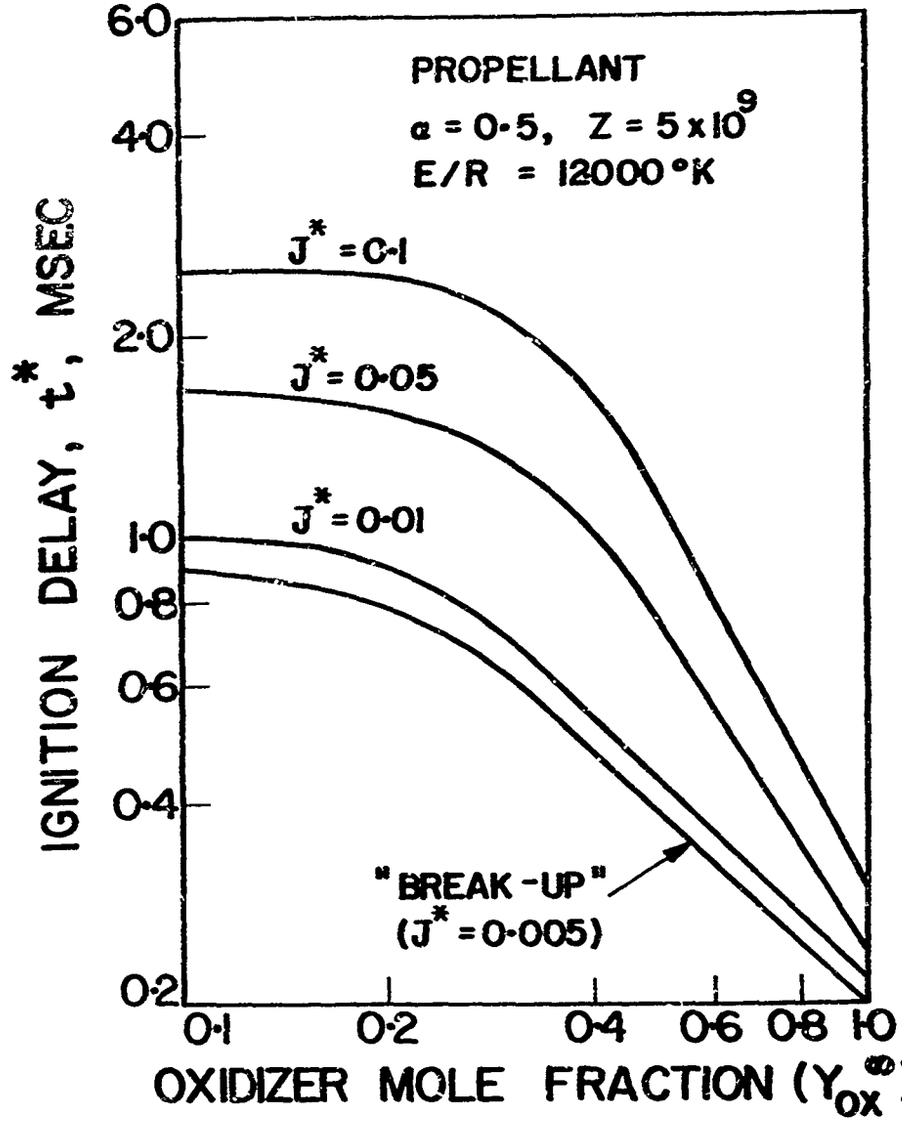

(b)

FIGURE 14

COMPARISON OF THEORETICAL IGNITION BEHAVIOR, USING VARIOUS IGNITION CRITERIA, WITH EXPERIMENTAL RESULTS.

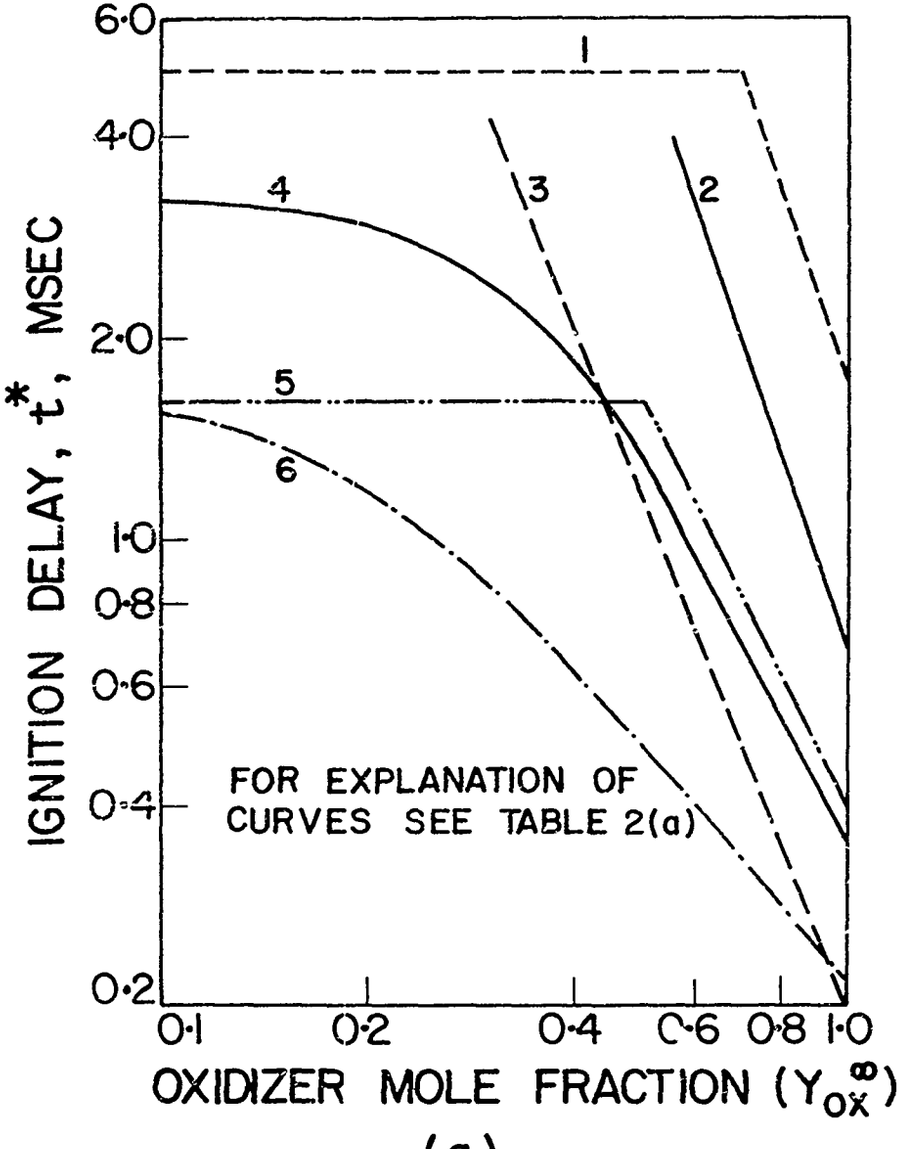

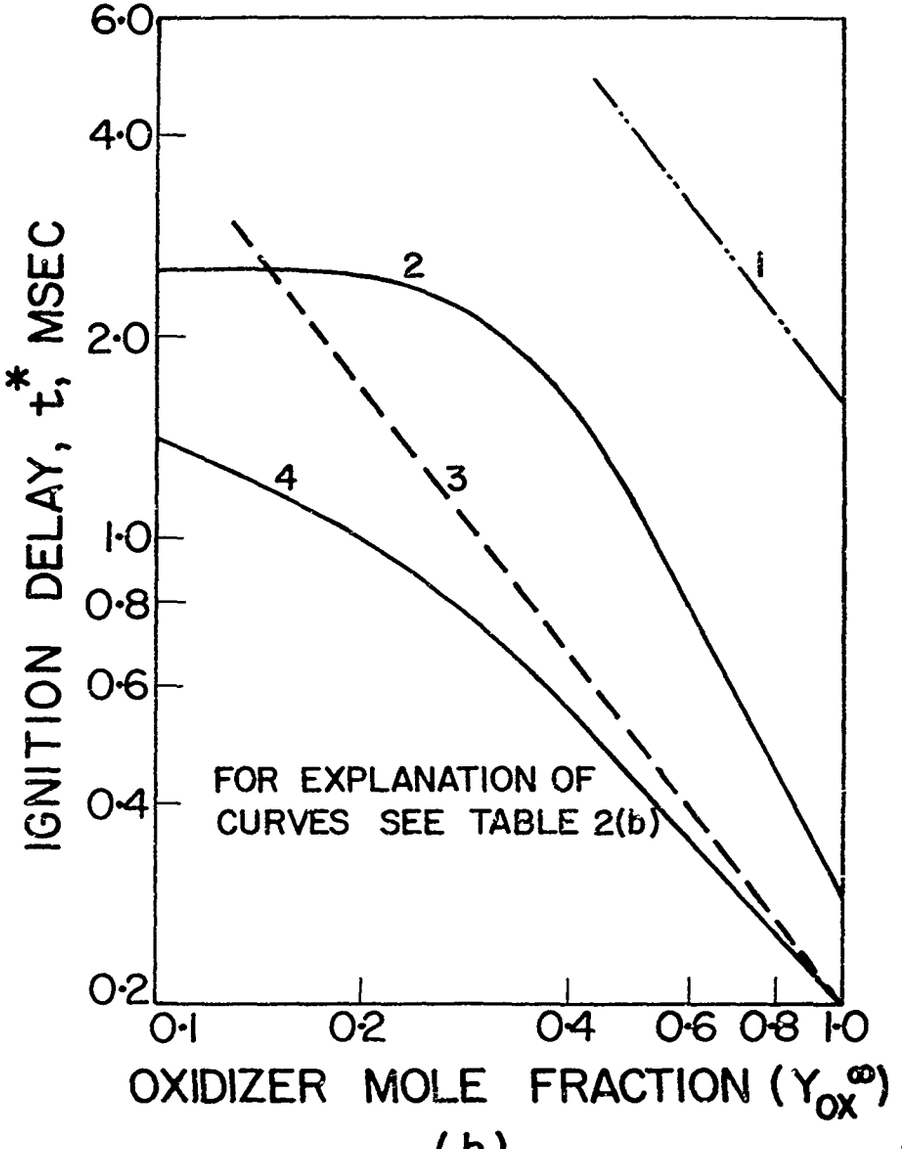

FIGURE 15

EFFECT OF INITIAL OXIDIZER MOLE FRACTION ON THE THEORETICAL IGNITION DELAY, FOR PROPELLANTS AND PURE FUELS, USING VARIOUS LIGHT EMISSION CRITERIA

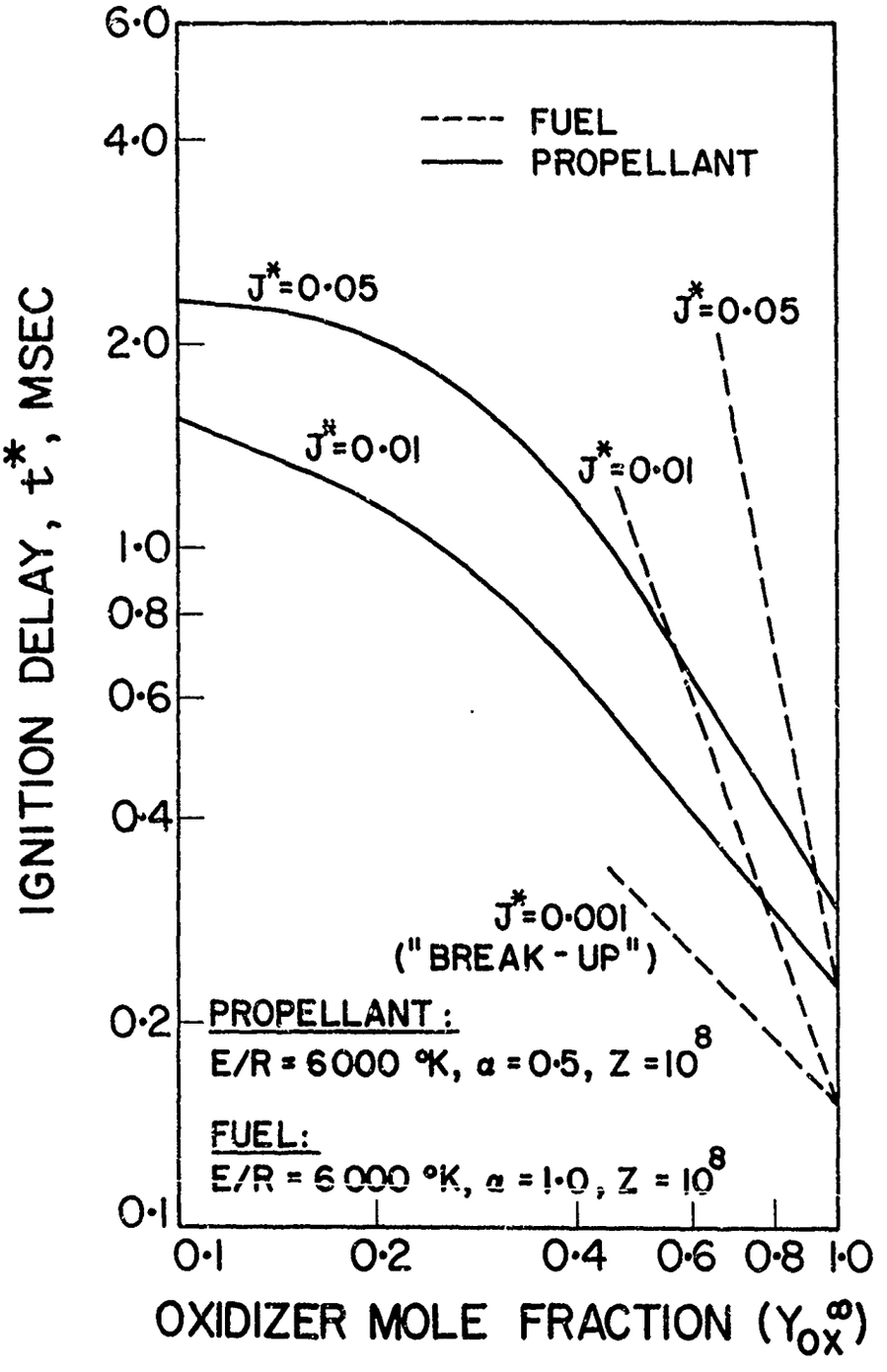

FIGURE 16

THEORETICAL OSCILLOSCOPE TRACES FOR A HOMOGENEOUS SOLID PROPELLANT

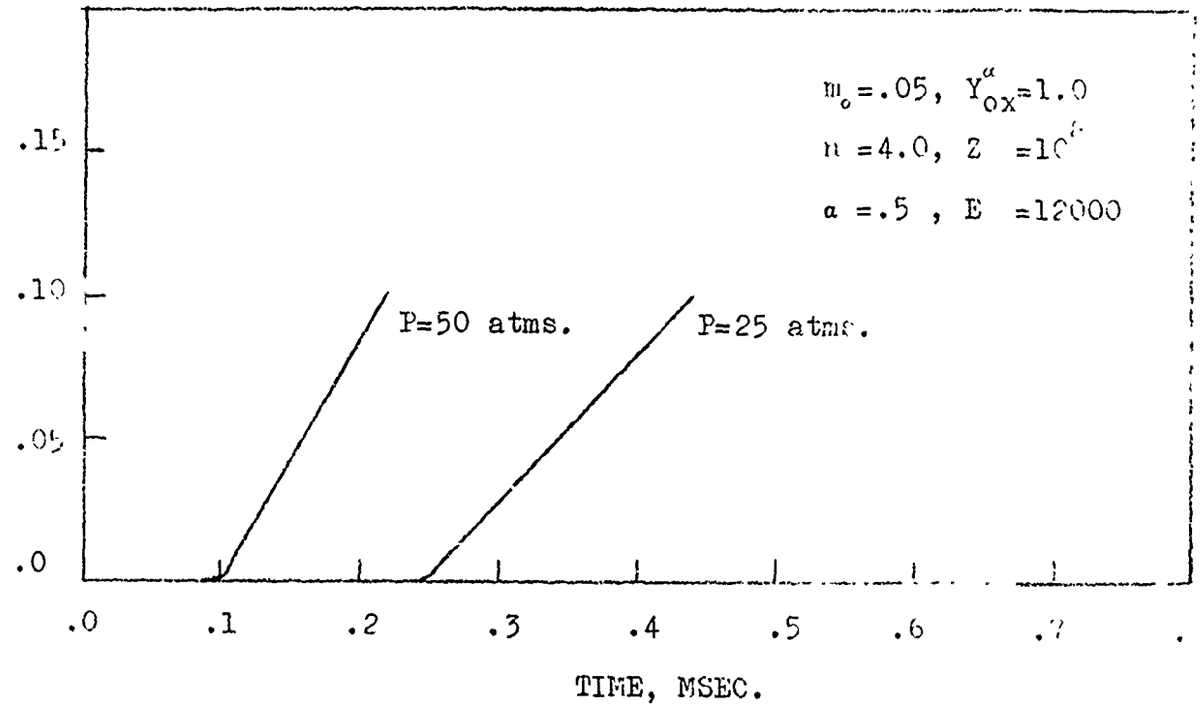

(a)

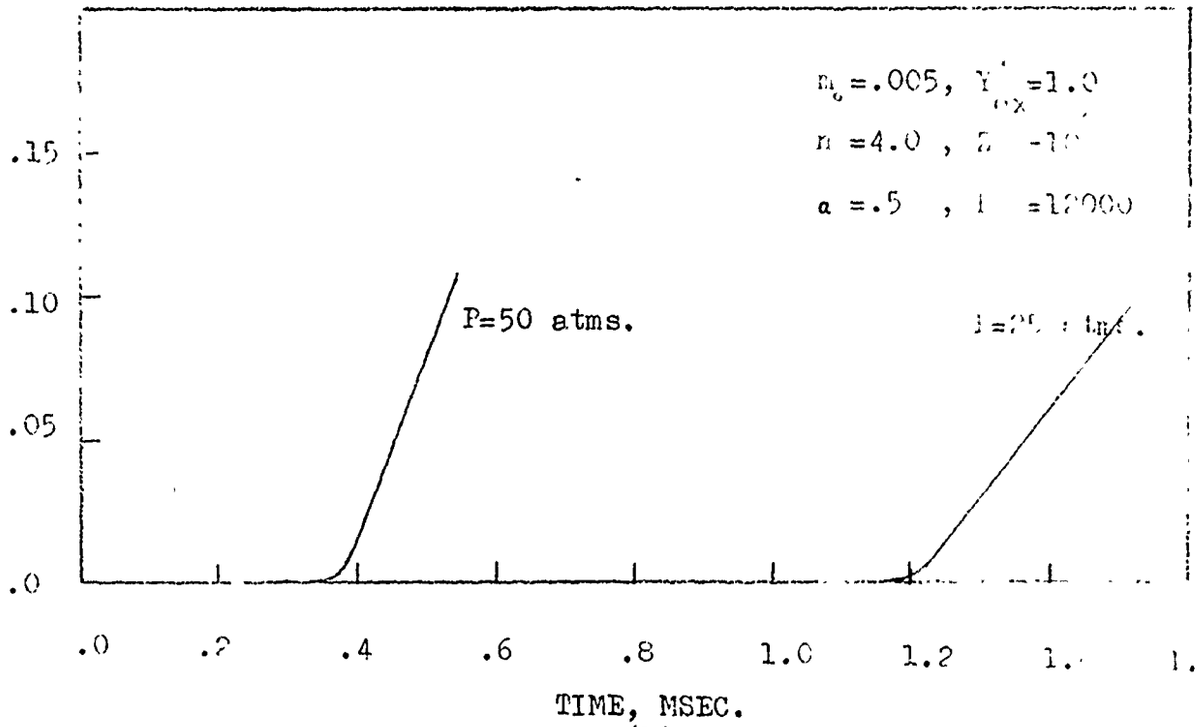

(b)

FIGURE 17

EFFECT OF GAS PHASE TOTAL PRESSURE ON IGNITION DELAY FOR A HOMOGENEOUS SOLID PROPELLANT

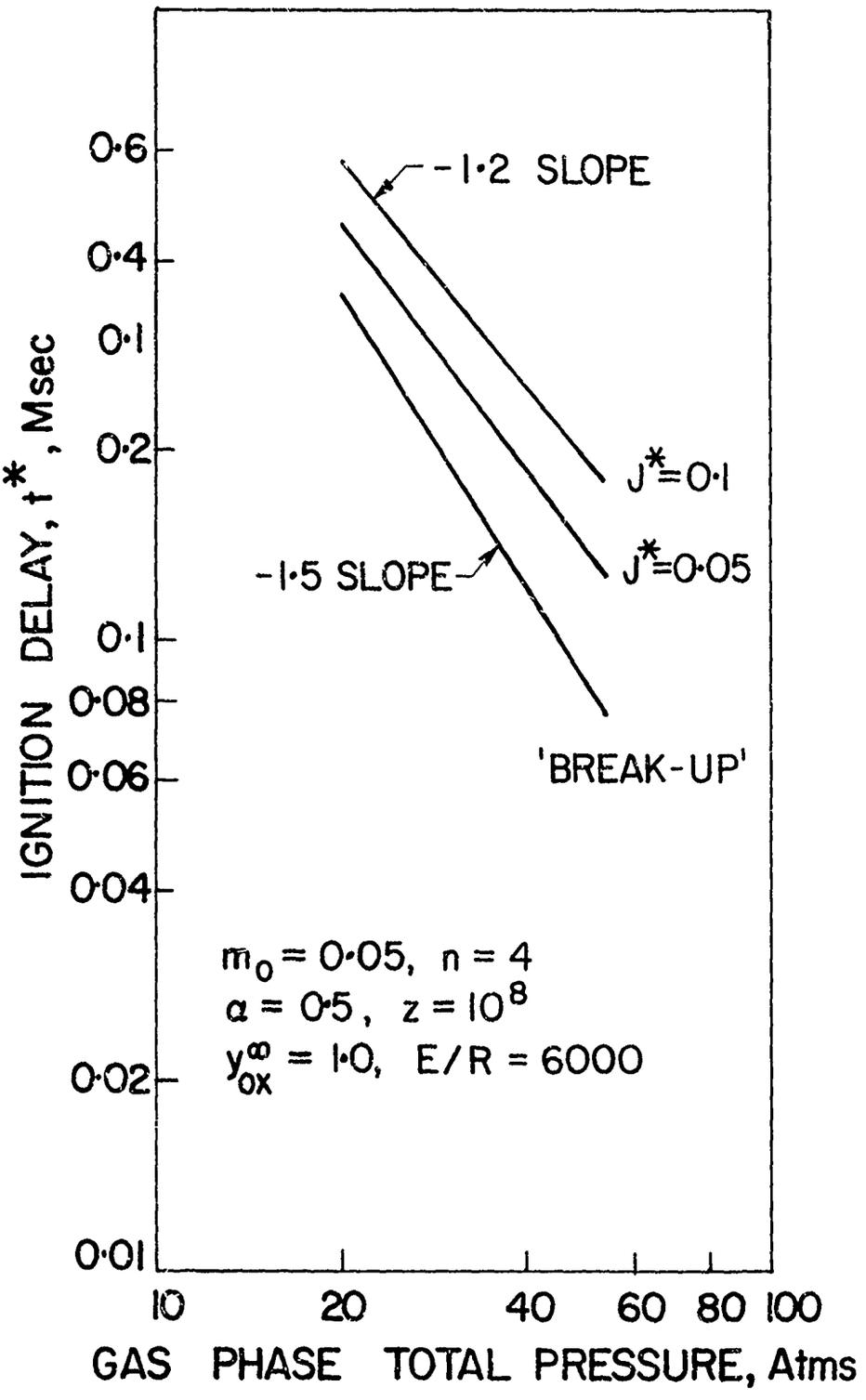

FIGURE 18a

EFFECT OF GAS PHASE TOTAL PRESSURE ON IGNITION DELAY FOR A HOMOGENEOUS SOLID PROPELLANT

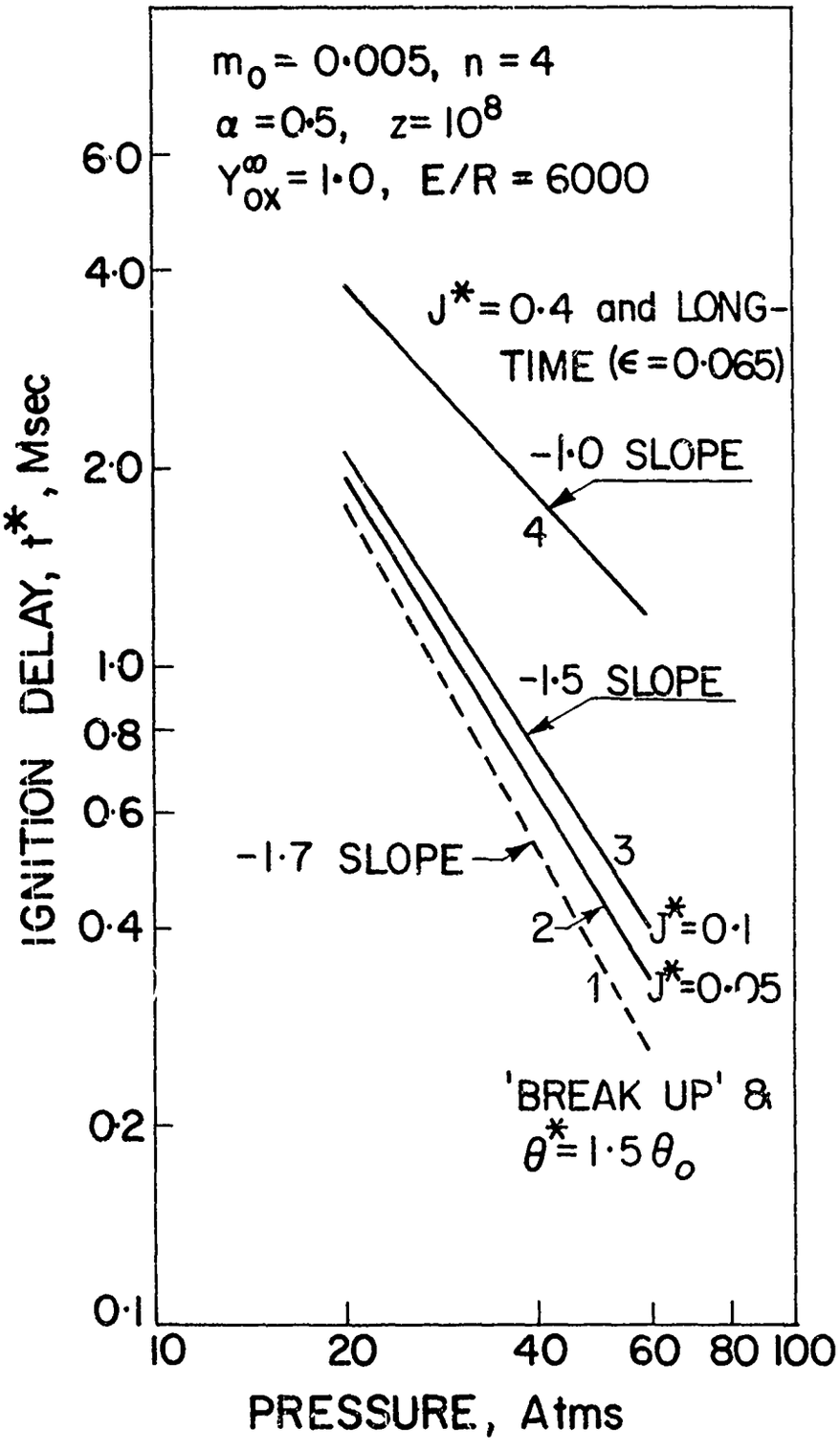

FIGURE 18 b

EFFECT OF OXYGEN PARTIAL PRESSURE ON IGNITION DELAY FOR A HOMOGENEOUS SOLID PROPELLANT

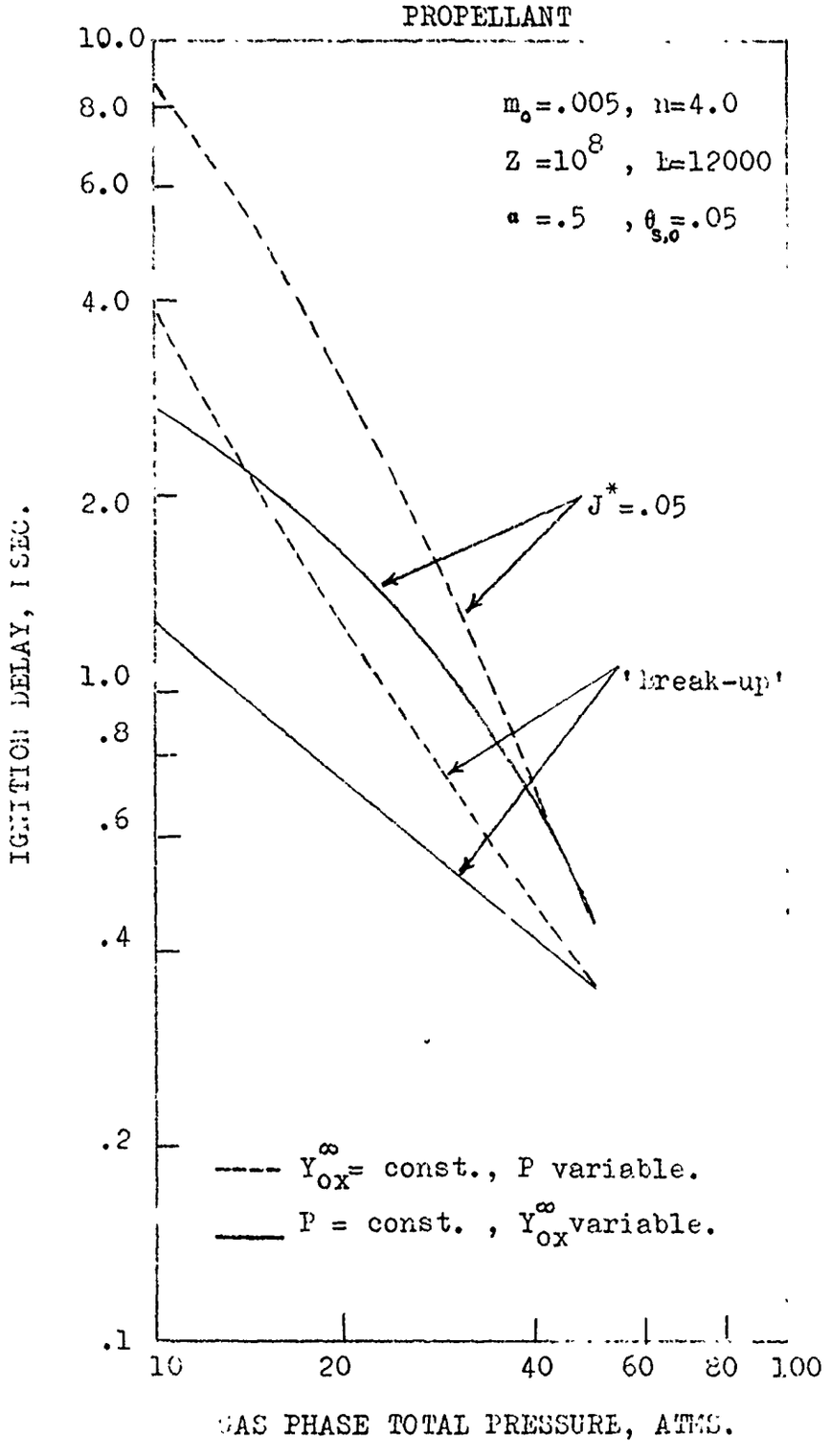

FIGURE 18(a)

BEHAVIOR OF THE IGNITION DELAY WHEN THE OXIDIZER SUPPLIED BY THE SOLID IS MUCH MORE REACTIVE THAN THAT INITIALLY IN THE GAS PHASE ($\alpha = 0.5$, $E/R = 6000°K$ FOR ALL CURVES)

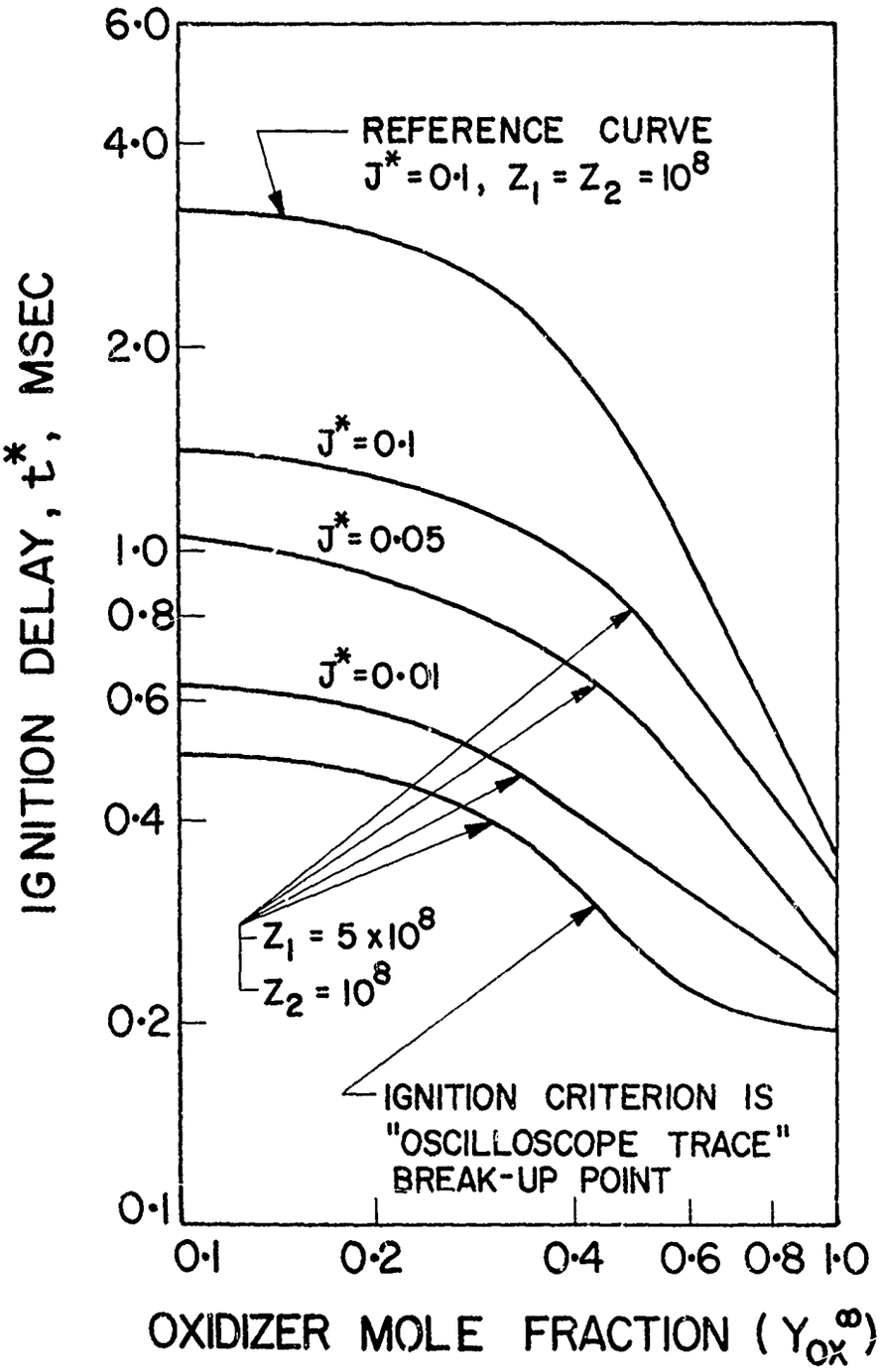

FIGURE 19

SCHEMATIC OF PHYSICAL MODEL FOR
HETEROGENEOUS SOLID PROPELLANT

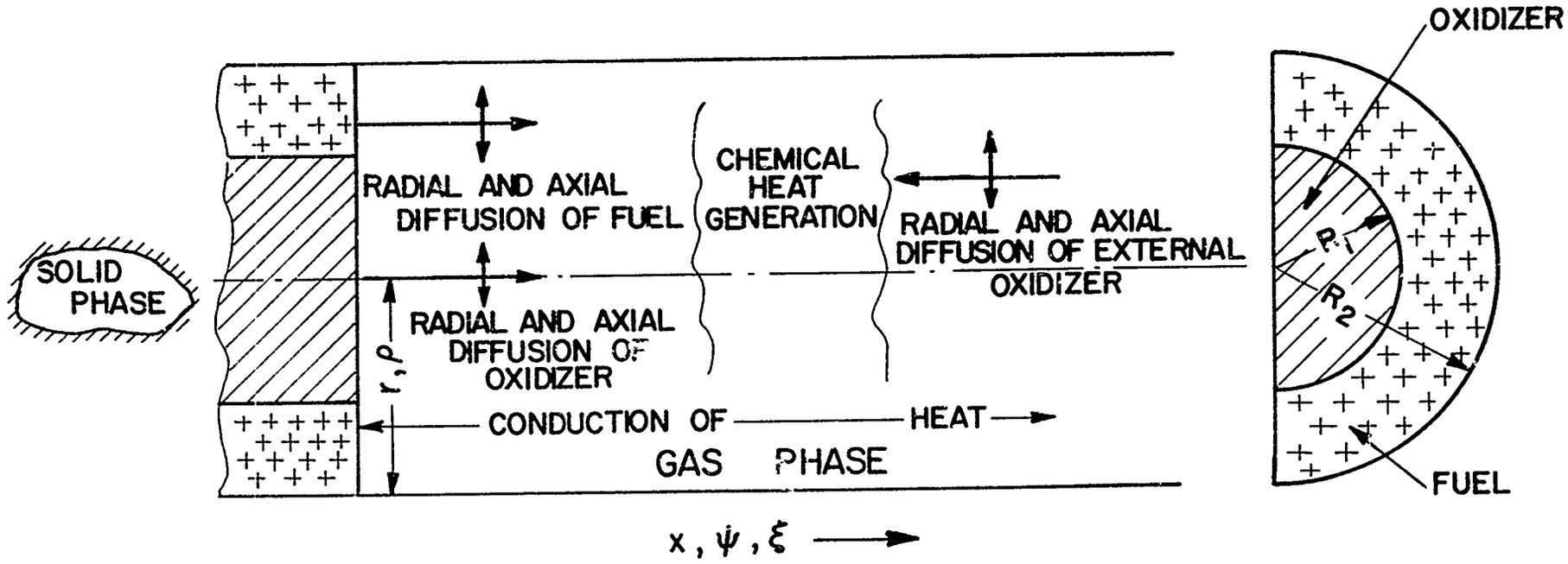

Figure 20

GEOMETRY OF A HETEROGENEOUS PROPELLANT

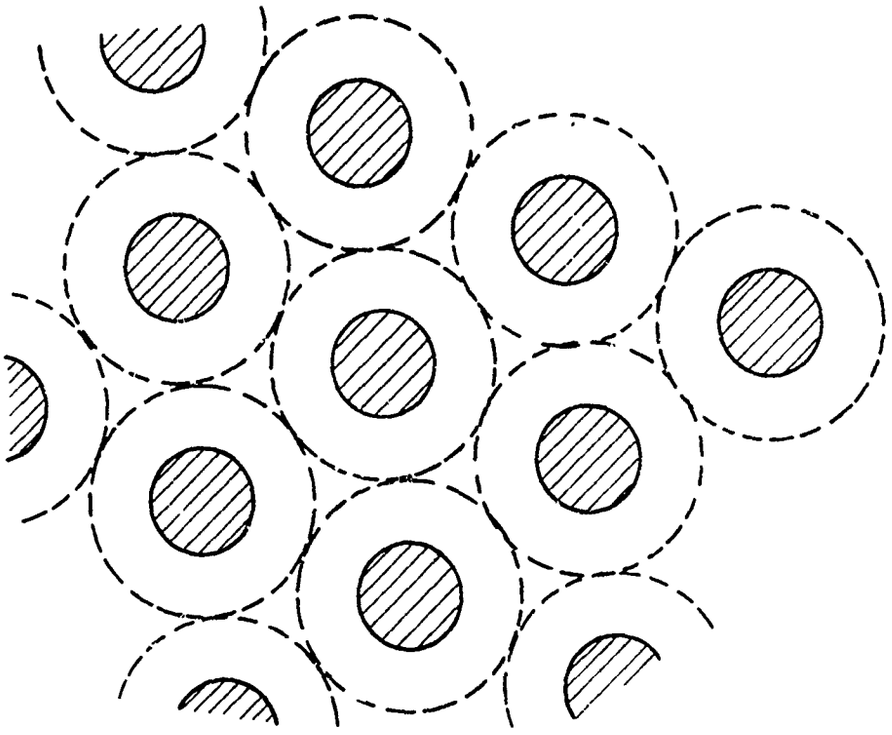

HATCHED POSTIONS REPRESENT OXIDIZER PARTICLES AND THE DOTTED LINES, THE BOUNDARY OF FUEL SURROUNDING IT.

Figure 21

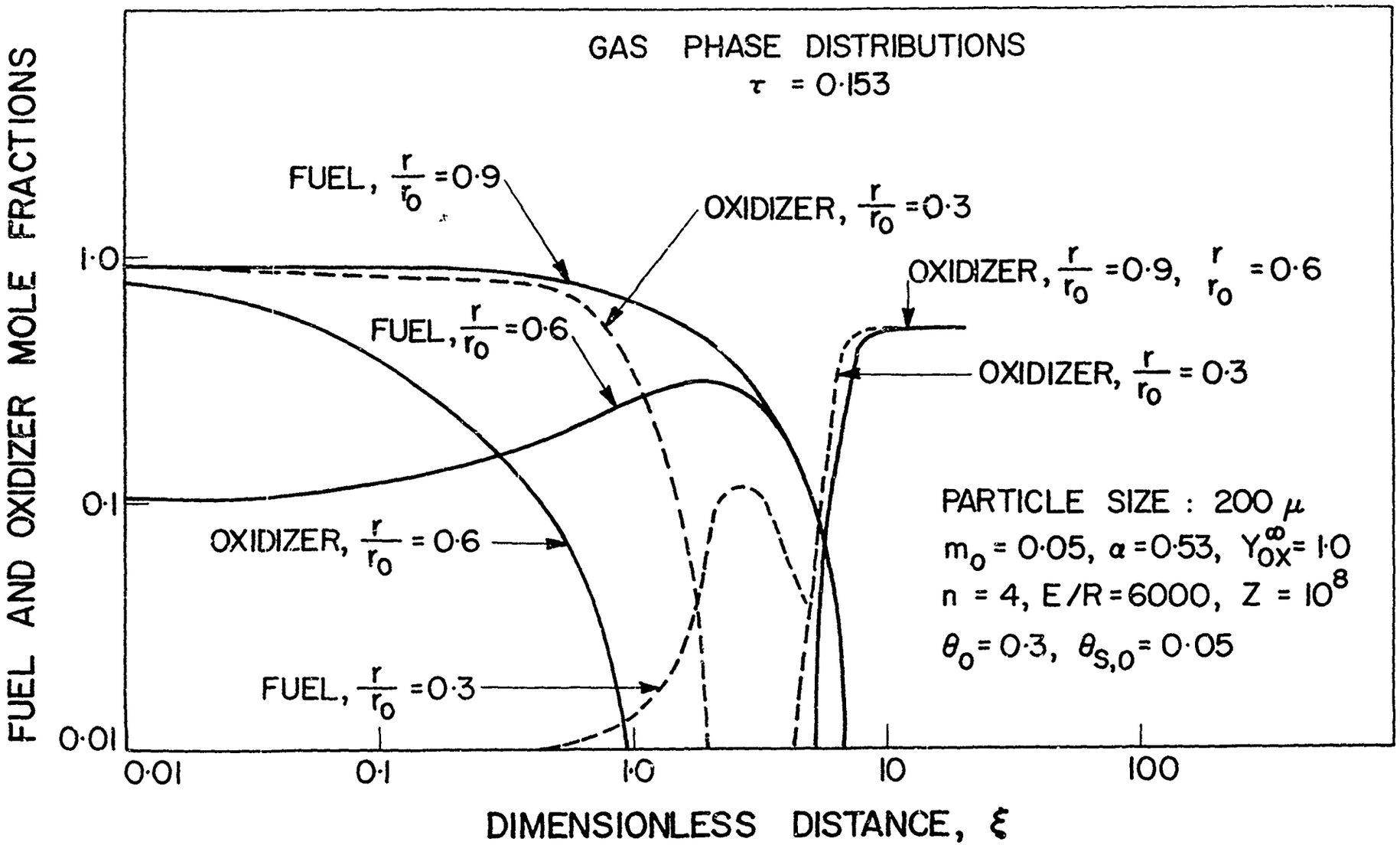
GAS PHASE DISTRIBUTIONS
τ = 0·153
FUEL, r/r0 = 0·9
OXIDIZER, r/r0 = 0·3
OXIDIZER, r/r0 = 0·9, r/r0 = 0·6
FUEL, r/r0 = 0·6
OXIDIZER, r/r0 = 0·3
OXIDIZER, r/r0 = 0·6
FUEL, r/r0 = 0·3
PARTICLE SIZE : 200 μ
m0 = 0·05, α = 0·53, Y_OX^∞ = 1·0
n = 4, E/R = 6000, Z = 10^8
θ0 = 0·3, θS,0 = 0·05
FUEL AND OXIDIZER MOLE FRACTIONS
1·0
0·1
0·01
0·01
0·1
1·0
10
100
DIMENSIONLESS DISTANCE, ξ

Figure 22

RADIAL DISTRIBUTION OF FUEL AND OXIDIZER
IN THE GAS PHASE

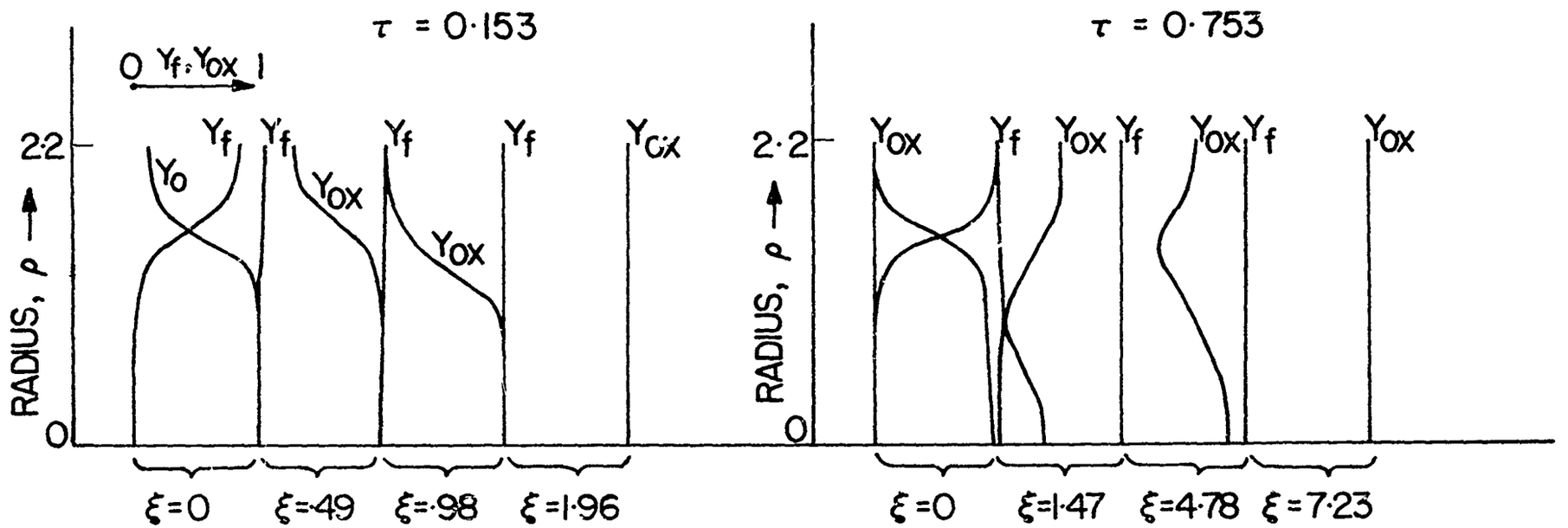

$m_0 = 0{\cdot}05$, $\alpha = 0{\cdot}53$, $Y_{OX}^{\infty} = 1{\cdot}0$
PARTICLE SIZE : $200\,\mu$
$n = 4$, $E/R = 6000$, $Z = 10^8$

Figure 23

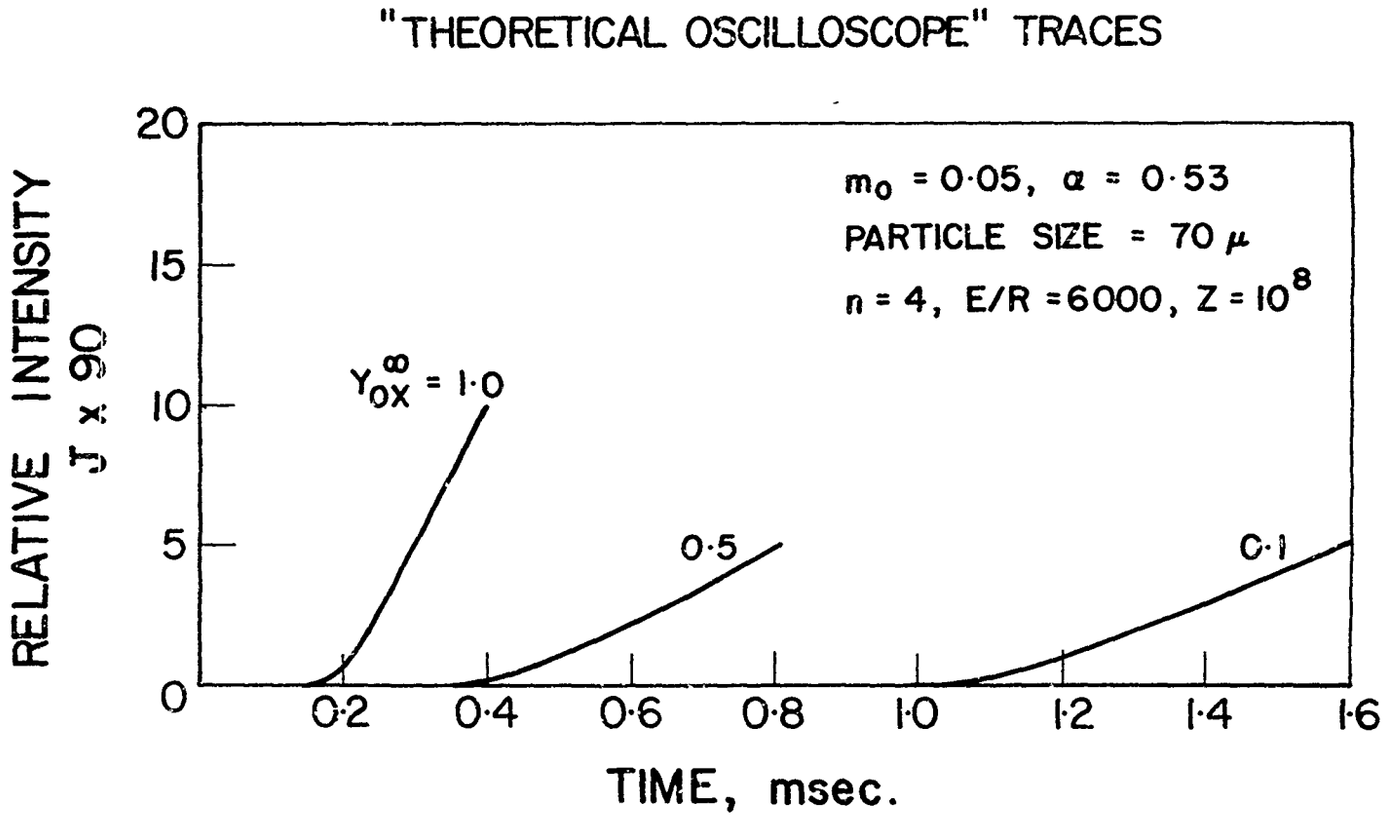
"THEORETICAL OSCILLOSCOPE" TRACES
RELATIVE INTENSITY
J x 90
20
15
10
5
0
m_0 = 0·05, α = 0·53
PARTICLE SIZE = 70 μ
n = 4, E/R = 6000, Z = 10^8
Y_{ox}^{∞} = 1·0
0·5
0·1
0·2
0·4
0·6
0·8
1·0
1·2
1·4
1·6
TIME, msec.

Figure 24

EFFECT OF INITIAL OXIDIZER MOLE FRACTION UPON IGNITION DELAY

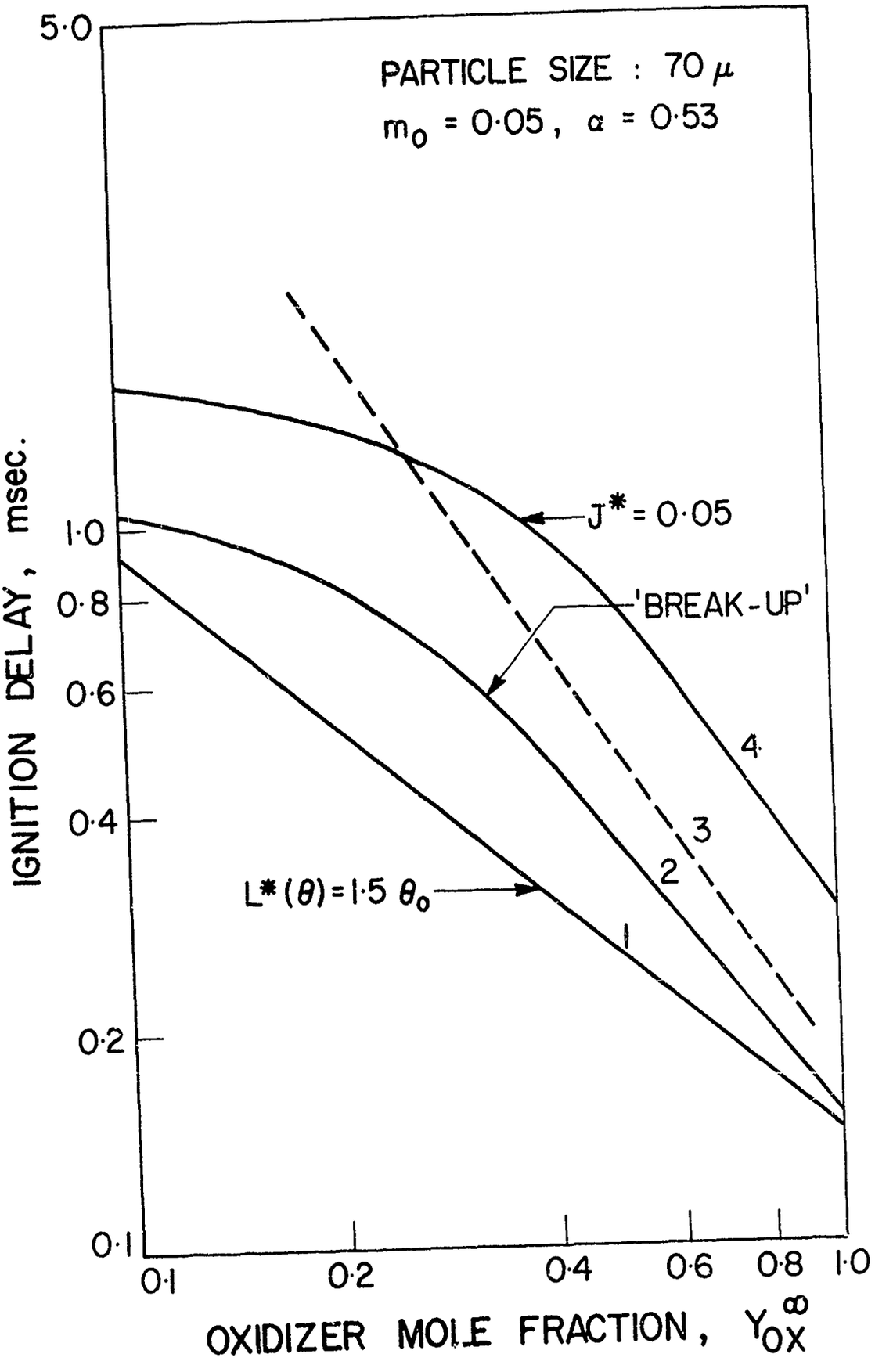

Figure 25

THEORETICAL "OSCILLOSCOPE" TRACES OF RELATIVE LIGHT EMISSION VERSUS TIME FOR HETEROGENOUS SOLID PROPELLANT

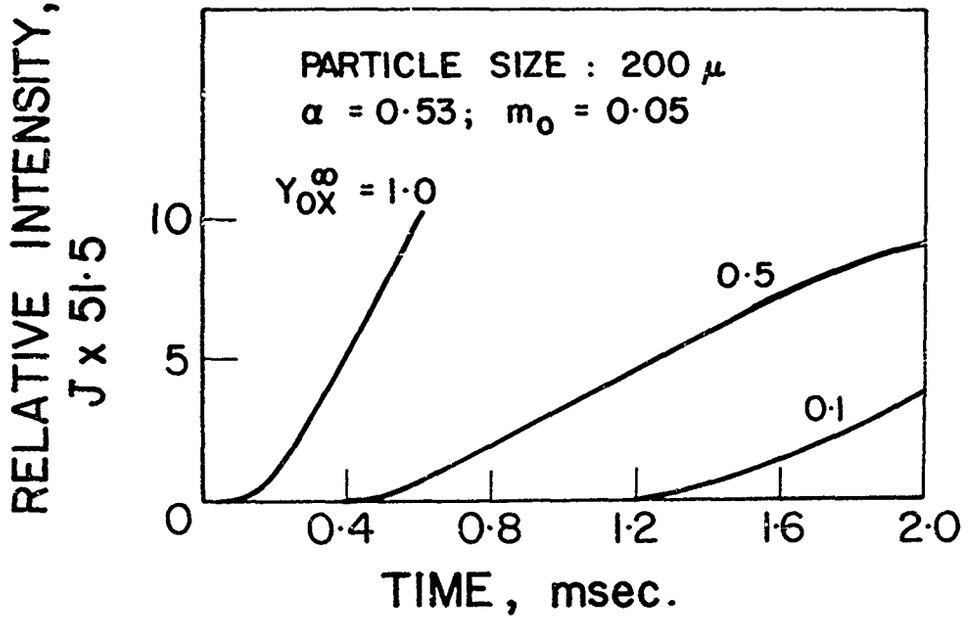

Figure 26

EFFECT OF INITIAL OXIDIZER MOLE FRACTION ON IGNITION DELAY (HETEROGENEOUS SOLID PROPELLANT)

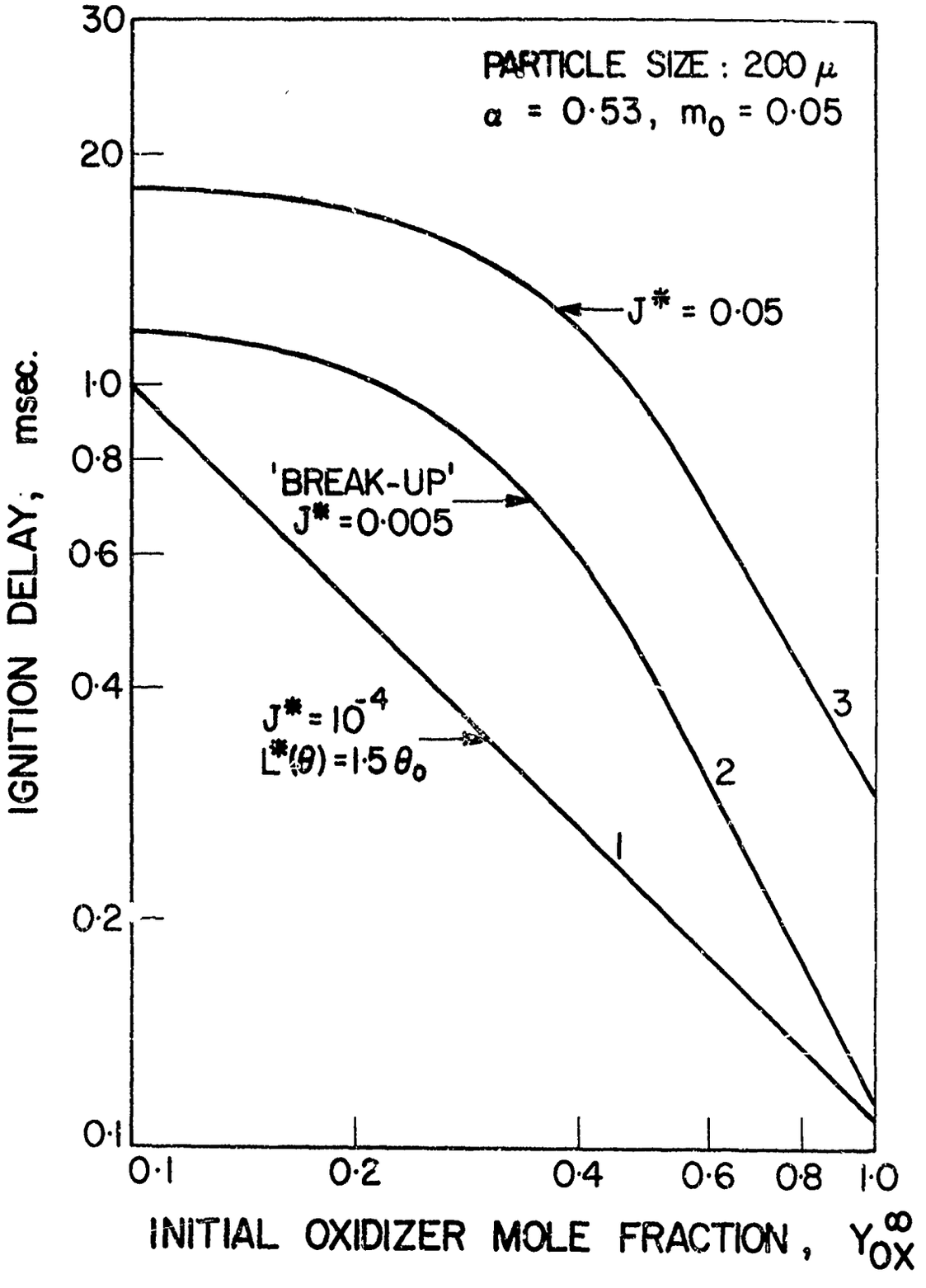

Figure 27

THEORETICAL OSCILLOSCOPE TRACES FOR A HETEROGENEOUS SOLID PROPELLANT

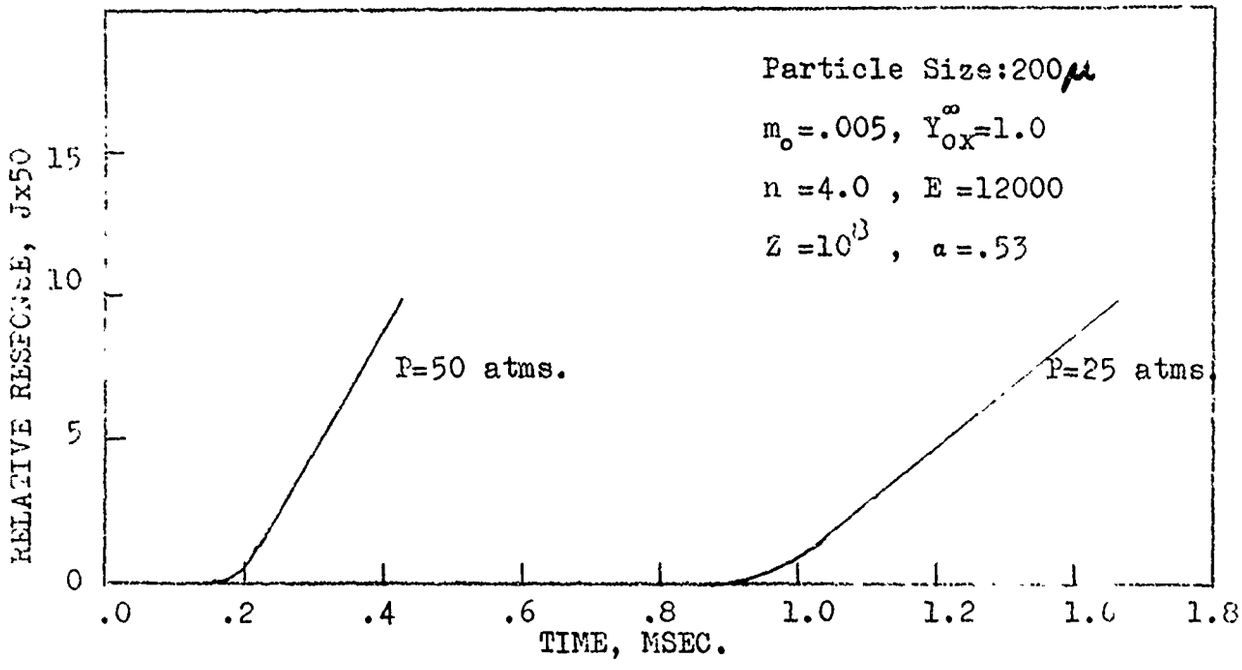

(b)

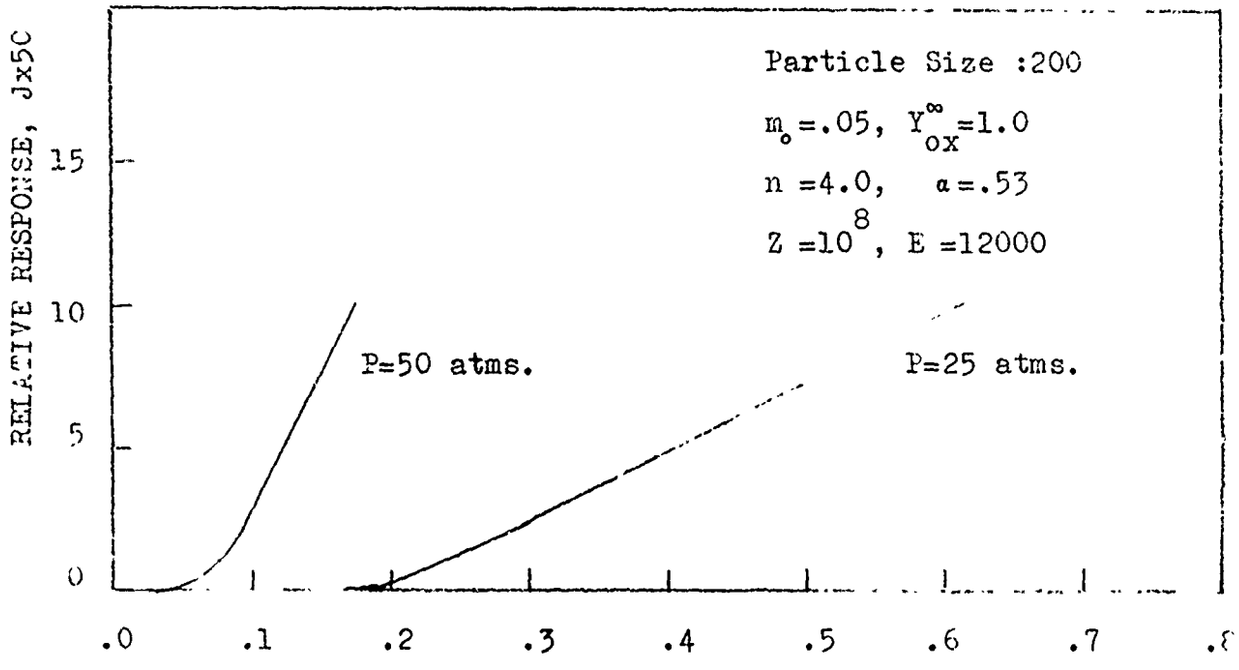

(a)

FIGURE 28

EFFECT OF GAS PHASE TOTAL PRESSURE ON IGNITION DELAY FOR A HETEROGENEOUS SOLID PROPELLANT

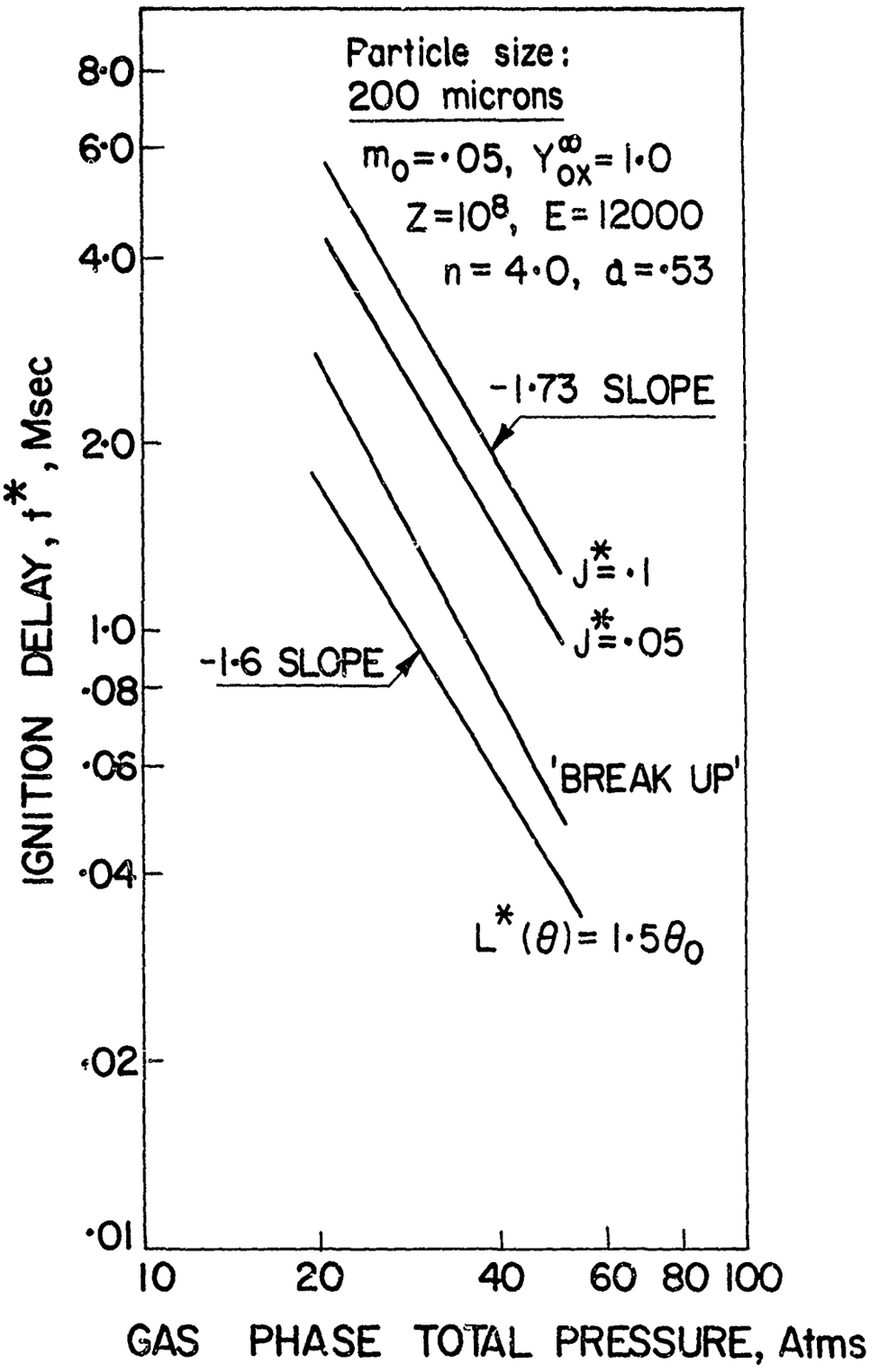

FIGURE 29

EFFECT OF GAS PHASE TOTAL PRESSURE ON IGNITION DELAY FOR A HETEROGENEOUS SOLID PROPELLANT

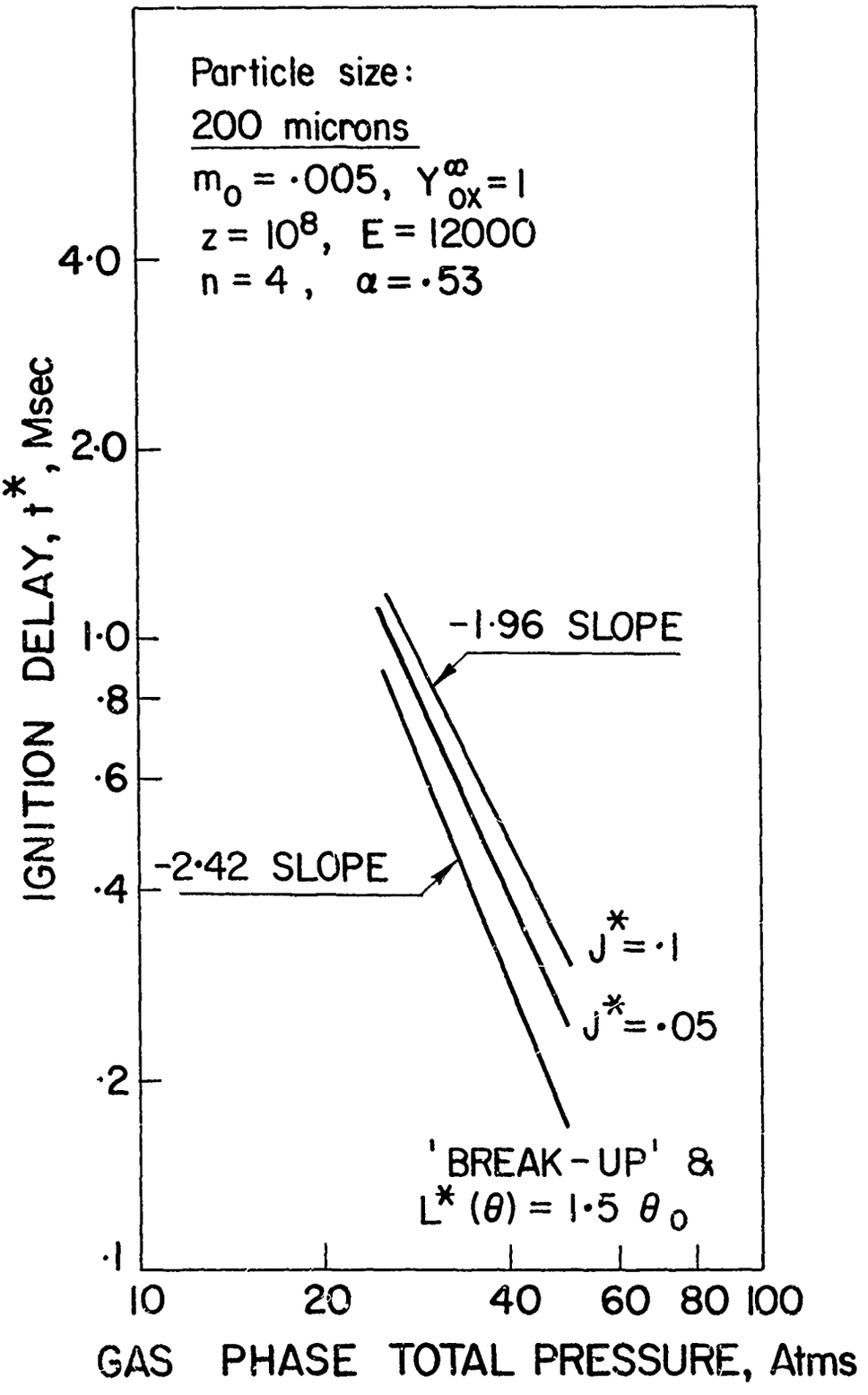

FIGURE 30

EFFECT OF Y_{ox}^{∞} UPON IGNITION DELAY OF A HETEROGENEOUS PROPELLANT

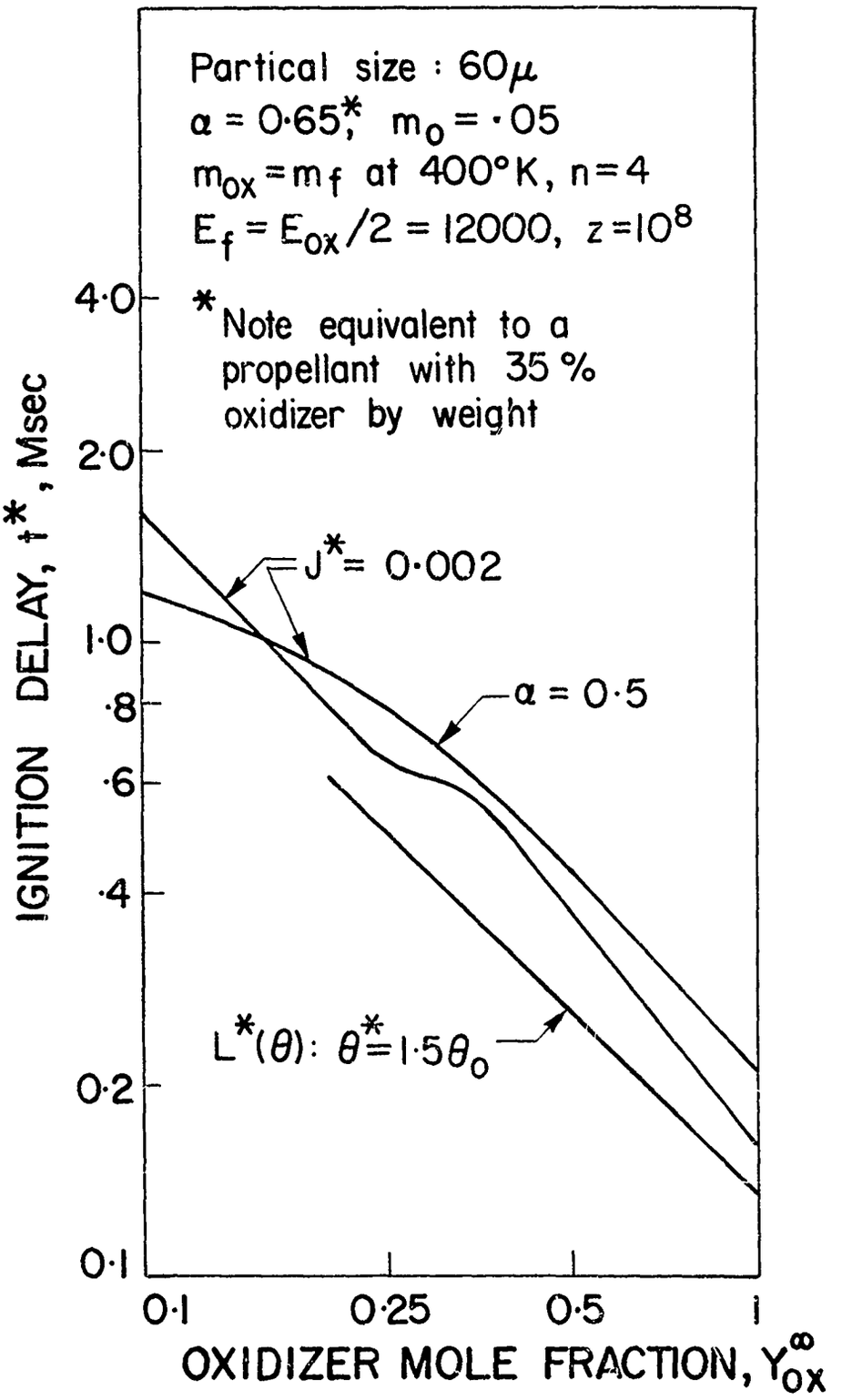

FIGURE 31

EFFECT OF RADIANT ENERGY FLUX UPON IGNITION DELAY OF A HOMOGENEOUS PROPELLANT

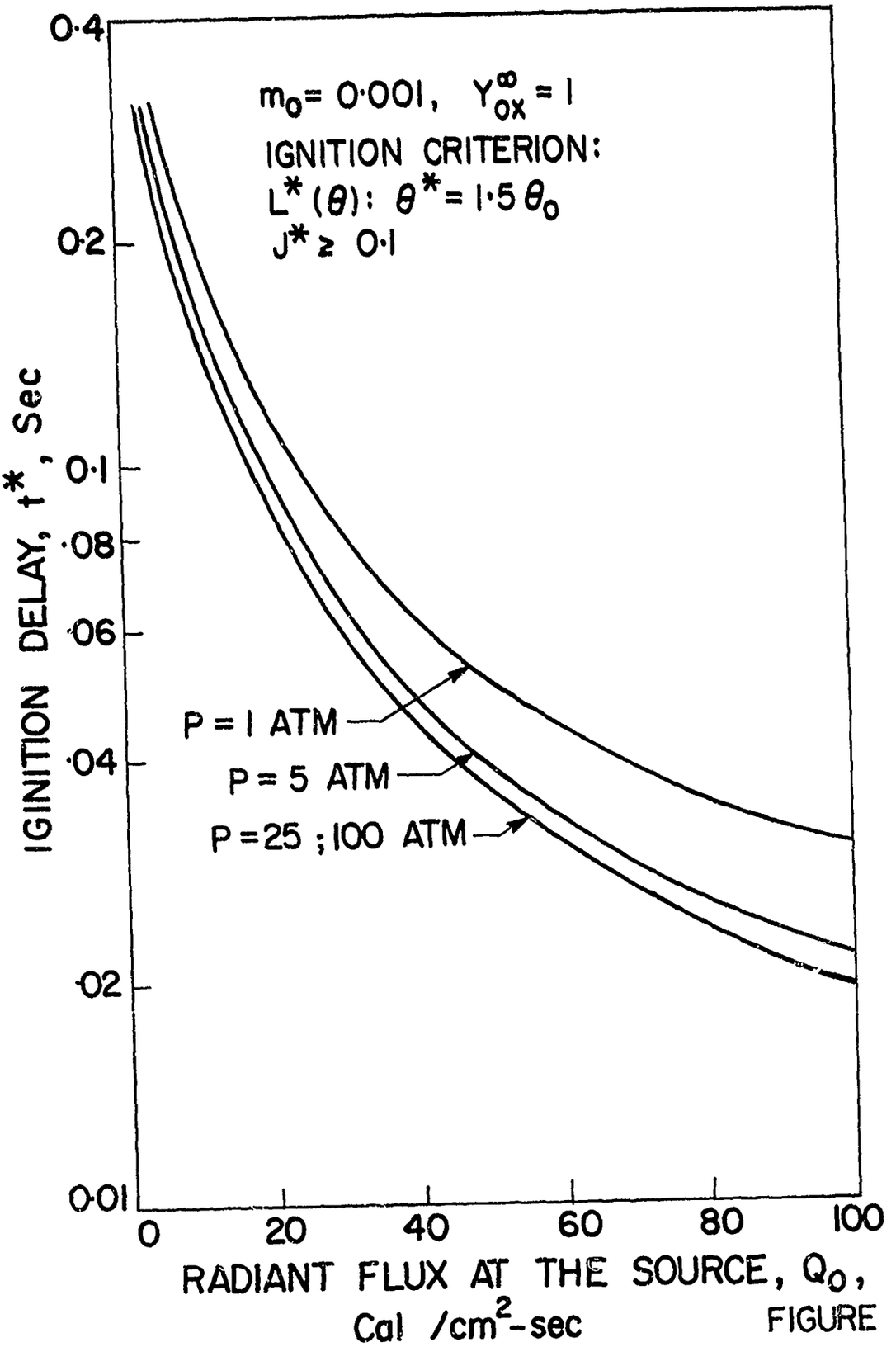

FIGURE 32

EFFECT OF RADIANT FLUX UPON GAS PHASE IGNITION DELAY OF A HOMOGENEOUS PROPELLANT

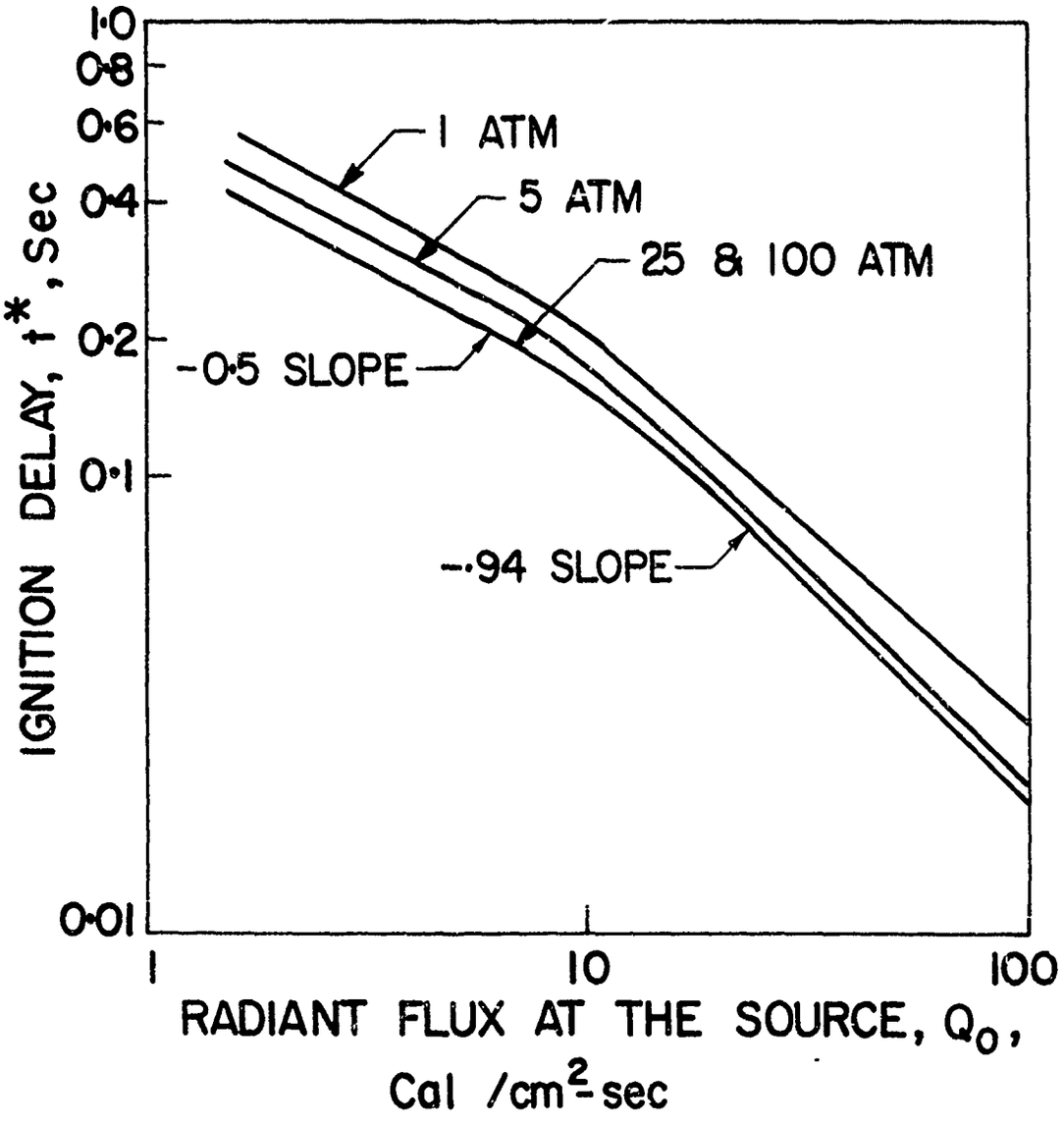

FIGURE 33

EFFECT OF GAS PHASE PRESSURE ON THE IGNITION DELAY OF HOMOGENEOUS PROPELLANTS DURING RADIANT IGNITION

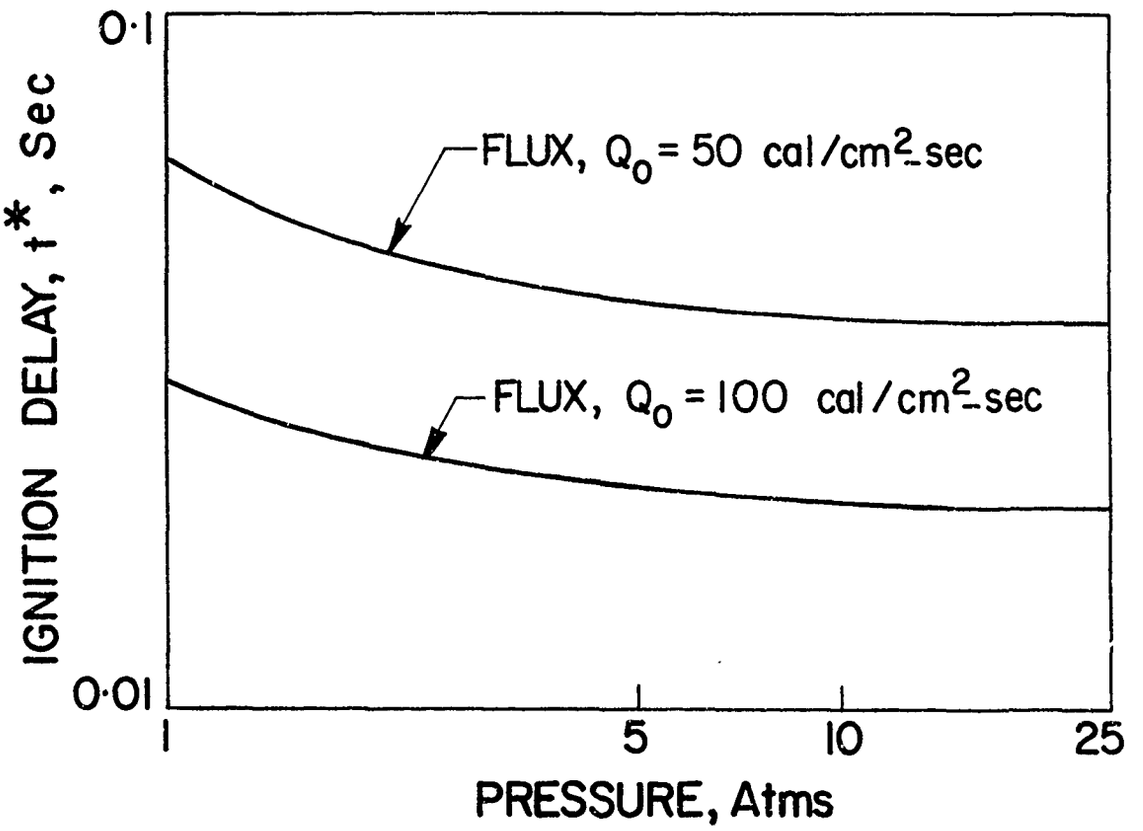

FIGURE 34